Understanding Additional Tier 1 CoCo Bond Prices using First-Passage Time Models

Berend Pieter Ritzema BSc (#:416123)

Master's Thesis Quantitative Finance

December 25, 2015

Abstract

Under new capital requirements, CoCo bonds can belong to the Additional Tier 1 (AT1) capital category under strict conditions. These conditions give rise to the risk of coupon cancellation and the risk of extension beyond call dates. This study proposes two first passage-time approaches to price AT1 conversion-to-equity CoCos: a structural model adapted to AT1 CoCo pricing, and a direct model for the triggering CET1 ratio. Both models include coupon cancel risk and extension risk by setting two extra thresholds for the CET1 ratio. This study contributes to the literature by being the first to include these risk factors to first passage-time models, and one of the few to calibrate its parameters to data not including market observed CoCo prices. We find that coupon cancel and extension risk have significant impact on a CoCo's risk profile, both driving its price down. Furthermore, we find that both models overprice CoCos for realistic values of the thresholds. This may be caused by: (i) the absence of extra downward pressure following coupon cancellation, extension, or conversion; and (ii) the absence of the risk of regulatory forced conversions. These factors provide interesting opportunities for further research.

Keywords: Contingent Convertibles, Additional Tier 1, first passage-time models, AT1P model, calibration, credit default swaps, extension risk, coupon cancel risk, Monte Carlo.

Academic supervisor: Dr. M. (Marcin) Jaskowski
Co-reader: Prof. dr. D.J.C. (Dick) van Dijk
Business supervisors: Michiel Hopman MSc and Gerdie Knijp MSc

Contents

Chapter 1

Introduction

Following the global financial crisis a vast set of new regulations, guidelines, and directives for banking businesses have emerged. These rules are designed to enhance the stability of the financial system and to create a level playing field in the financial industry. An important part of these regulations is constituted by the European Parliament (EP, 2014) in the Banking Recovery and Resolution Directive (BRRD). This Directive provides regulations designed to stimulate banks to be prepared for a future new crisis. It forces banks to increase their *bail-in* or *loss absorbing* capacity, where a banks' own creditors, instead of the government, recapitalize the firm in a crisis. Specifically, the Minimum Requirement for own funds and Eligible Liabilities (MREL, see European Banking Authority (2014)) sets out minimum bail-in capacity requirements. These requirements are elaborated in the Capital Requirement Regulations (CRR, see EP (2013b)), which set out specifically the minimum amounts of capital to be held in each capital category.

Following these new bail-in capital requirements, there has been an exponential rise in hybrid debt issuance by banks in the EU.[1] Contingent Convertible bonds (CoCos) are an example of such a hybrid security. CoCos are (callable) bonds, that are automatically converted into equity or suffer a (temporary) partial or complete write-down when a prespecified trigger event occurs. A CoCo is specified by the following main characteristics:

- Maturity, face value, coupon rate, coupon payment dates, and call dates. Just like a regular (callable) bond, a CoCo makes coupon payments and redeems the principal at maturity, when conversion is avoided. Furthermore, CoCos are often callable, with prespecified dates at which the issuer can call the bond at a predetermined price.

- The trigger event causing conversion. There exist three types of trigger events: (i) market triggers, based on a market driven quantity such as the issuer's stock price, reaching some threshold; (ii) regulatory triggers, based on the regulator judging that the bank is in need of recapitalization; and (iii) accounting triggers, based on a capital ratio such as the Common Equity Tier 1 (CET1) ratio falling below some threshold.[2] Combinations of

[1] The total amount of contingent debt outstanding at banks in the EU has risen up to over $200 billion as of September 2014, as estimated by Avdjiev, Bolton, Jiang, Kartasheva, and Bogdanova (2015) based on Bloomberg and Dealogic.

[2] The CET1 ratio equals the book value of common equity divided by the amount of risk-weighted assets. See Section 2.1 for more detail hereon.

different triggers also occur.

- The conversion mechanism, describing what happens upon occurrence of the trigger event. This can be conversion into a number of equity shares, or a (temporary) partial or complete write-down of the face value.[3] Furthermore, a distinction can be made between *dilutive* and *non-dilutive* CoCos.[4]

Hybrid instruments such as CoCos provide a cost-effective and efficient way of adding regulatory loss absorbing capital to the balance sheet.[5] Furthermore, when CoCos work as they are supposed to, they can reduce the bank's probability of default, and thereby the probability of the need for a new bail-out.

Depending on the specific structure of a CoCo, it is assigned to either the Additional Tier 1 (AT1) or the Tier 2 (T2) capital category.[6] As AT1 eligibility is very attractive for banks towards the capital requirements, this is currently the dominant style. However, to count as AT1 capital, a CoCo must be structured in a very specific way. The most important extra risk drivers originating from the AT1 restrictions are: (i) coupon cancel risk, as coupon payments on AT1 CoCos may be canceled on the discretion of the issuer or the regulator without consequences for the rest of the CoCo lifetime; and (ii) extension risk, as there may be no incentives to call an AT1 CoCo, and the regulator may prohibit a call.

Though there exists a range of literature on the pricing of various types of CoCos, little has been written on the impact of the AT1 requirements on a CoCo's risk profile. This is an important deficiency, as these extra requirements have significant impact on CoCo prices. Furthermore, few studies calibrate their pricing models without using actual market observed CoCo prices. Most studies present some theoretical model, and then either stick to guessed parameters, or use market observed CoCo prices to extract information on their model's parameters. However, to really understand what drives CoCo prices, we must explain them using only information from other markets.

This study aims to fill both these gaps. This study focuses on AT1 eligible CoCos with a CET1 ratio trigger and non-dilutive conversion to equity. This is an interesting and challenging type from a valuation perspective, as these CoCos contain both credit- and equity-like characteristics, and their triggering accounting ratio is non-tradable. AT1 CoCos with an accounting trigger and equity conversion make up about half of all CoCo issues in the EU over the past year.[7]

We model the CET1 ratio process and the stock price process, and approximate CoCo prices

[3] A partial write-down is defined as a part of the CoCo being written-down, and the remaining fraction being paid out to the holders in cash. CoCos with a temporary write-down feature can be written up again when the issuer's capital position has regained sufficient strength.

[4] In dilutive CoCos, the face value of the CoCo is converted into more shares than the equivalent amount of equity. Non-dilutive CoCos consist of CoCos with write-down features, or conversion to equity where the value of the claim after conversion would be the same or less than before conversion.

[5] Issuing a CoCo provides four benefits over issuing regular shares: (i) because CoCos are technically regarded as bonds, payments can be made from pretax earnings in the majority of EU countries, enhancing the firms' tax shield; (ii) CoCos allow banks to tap from a different pool of investors; (iii) issuing a CoCo does not dilute current shareholders when conversion is avoided; and (iv) the underwriting costs of issuing a CoCo are far lower than those of issuing equity for reasons concerning information and managerial agency problems (see e.g. Calomiris and Herring (2013)).

[6] The regulator dictates what types of liabilities are eligible for which capital category, and how much capital must be held in each of the categories. See Section 2.1 for more detail hereon.

[7] Estimated by Avdjiev et al. (2015).

using a Monte Carlo algorithm. We use two first passage-time approaches to do so: (i) an *Analytically Tractable First-Passage time* (AT1P) approach, based on Brigo and Tarenghi's 2004 extension of the Black-Cox structural model of default, adapted to AT1 CoCos; and (ii) a methodology to directly model the CET1 ratio and stock price as stochastic processes, based on the framework by Cheridito and Xu (2015). Both models are calibrated on Credit Default Swap (CDS), equity, and accounting data, i.e., without using CoCo prices. This enables us to examine their CoCo pricing strength, and investigate what impact each of the risk drivers has on the CoCo price. We assume coupon cancel risk and extension risk are driven by the CET1 ratio. That is, when the CET1 ratio is below a coupon cancel threshold at a payment date, the coupon payment is canceled. And when the CET1 ratio is below a call threshold at a call date, the CoCo is extended.

We test the models in a case study on AT1 CoCos issued by Banco Popular and ING in early 2015. We find that coupon cancel and extension risk have a significant impact on CoCo prices, both in the AT1P and in the direct CET1 model. A higher coupon cancel threshold significantly drives down CoCo prices. We find a similar effect for the extension risk, be it less strong. A higher call threshold implies less early redemptions, which results in a larger probability of conversion and stronger discounting of the potential principal. This effect is weakened by the value of potential extra coupon payments.

While both models yield comparable prices for equal levels of the thresholds, they show large differences in the relative contribution of the CoCo price components principal, coupons, and stocks. In the direct CET1 model the conversion rate is very high, but the average loss of value at conversion is low. In the AT1P model, the conversion rate is lower, but the average loss of value at conversion is much higher. The behavior of the AT1P model seems more realistic, as we expect conversion not to happen very often in reality, but with a large loss of value.

Furthermore, for both models, we need to set the call and coupon cancel thresholds unrealistically high to match market observed CoCo prices. In other words, when setting the thresholds at economically intuitive levels, both models overprice CoCos significantly. This may be caused by a number of reasons: (i) the lack of extra downward pressure or shocks following announcements of coupon cancellation, extension, or conversion; (ii) the lack of the uncertainty regarding the power of the regulator to force conversion; (iii) the absence of the Bond-CDS basis in the calibration procedure; and (iv) the lack of an extra CoCo illiquidity premium. These factors provide interesting opportunities for further research.

This study is structured as follows. Chapter 2 gives an overview of current CoCo literature and relevant valuation methods. Chapter 3 presents our AT1 CoCo valuation approaches, and elaborates on how their parameters can be calibrated using market data not consisting of CoCo prices. Furthermore, it introduces the Monte Carlo CoCo pricing algorithm. In Chapter 4 we apply the calibration methods from Chapter 3 on two AT1 CoCos. Chapter 5 analyzes the pricing behavior of both models, and compares model prices to market observed prices to examine their pricing strength and to understand what drives CoCo prices. It also conducts a sensitivity analysis on the input parameters. Chapter 6 concludes and provides recommendations for further research.

Chapter 2

Literature review

This chapter is divided into three parts. Section 2.1 introduces in detail the characteristics and risk drivers of Additional Tier 1 eligible CoCos. Section 2.2 then provides an overview of the current variety of CoCo pricing methods in the literature. We find that the class of first-passage time models is most suitable for our purpose, so Section 2.3 focuses on the most interesting studies on CoCo pricing using first-passage time models. It also outlines where the gaps in the current literature lie, which this study aims to fill.

2.1 AT1 CoCo bonds: a primer

The idea of hybrid securities that are a form of debt that converts to equity if the issuer gets in trouble was first offered by Flannery (2005). Later it was updated and specified as the currently known CoCo in Flannery (2009). Further extensions and specifications were provided among others by Kashyap, Rajan, and Stein (2008), who propose a systemic event to trigger conversion, instead of a firm-specific event. McDonald (2010) and Squam Lake Working Group (2009) propose a combined trigger that depends on both the issuer's individual health and the banking system as a whole.

As introduced in Chapter 1, there exist several different capital categories. The CRR (EP, 2013b) dictates what types of liabilities are eligible for which capital category, and how much capital must be held in each of the categories. The most general division of capital is into Tier 1 and Tier 2. Tier 1 is the most reliable category from the bank's perspective, and consists of instruments that can absorb losses without ceasing business operations. Tier 2 consists of supplementary capital instruments, that cannot be directly used to absorb losses without ceasing business operations.

The Tier 1 category constitutes the *core* capital, and is further divided into CET1 capital and AT1 capital. The CET1 capital is given by the book value of common stockholders' equity plus any share premium accounts related to these common stocks, retained earnings, accumulated other comprehensive income, and other reserves. The amount of CET1 capital on a bank's balance sheet forms the basis for the CET1 ratio. This ratio, as designed in EP (2013b) and EP

(2013a), is defined as the CET1 capital divided by the amount of risk-weighted assets (RWA). The amount of RWA is a function of the bank's assets and off-balance sheet exposures weighted according to their riskiness.

The AT1 category consists of instruments that are not CET1, but are still regarded as safe enough to be Tier 1 eligible. Almost all recent CoCo issues in Europe have been AT1 eligible. In order to qualify as AT1 capital CoCos need to oblige to some strict conditions. As these conditions have a large impact on a CoCo's risk profile and their value, we introduce the most important ones carefully. These conditions comprise:

1. The CoCo has to be subordinated to Tier 2 capital in event of insolvency (EP, 2013b, Article 52: 1d);

2. The CoCo needs to have fully discretionary non-cumulative coupon payments, meaning coupon payments can be canceled on the discretion of the issuer or the regulator (EP, 2013b, Article 52: 1l);

3. The CoCo must have a perpetual maturity, it may not have any incentives to redeem at its call dates, and the regulator may opt to prohibit a call (EP, 2013b, Article 52: 1g);

4. The first call date must be at least five years after issuance (EP, 2013b, Article 52: 1i);

5. The CET1 ratio should trigger the CoCo (accounting trigger), with a minimum conversion threshold at 5.125%, and the regulator may opt to force conversion as well (EP, 2013b, Article 54: 1a).

When a CoCo does not meet these requirements, it is qualified as Tier 2 capital. The most interesting requirements, especially from a valuation perspective, are (2) and (3). (2) implies that coupon payments may be canceled without any consequences for the further lifetime of the CoCo. This is in sharp contrast with the regular fixed income market. In a standard bond, canceling a coupon payment automatically results in bankruptcy. The fact that this does not hold for AT1 CoCo implies that we cannot speak of a *fixed* income product, and hence standard fixed income valuation approaches do not apply, even when conversion is avoided.

Restriction (3) implies that there may be no incentives for the issuer to redeem the CoCo as soon as possible. This is also in contrast with regular callable bonds, that traditionally contain a coupon step-up when a call date is skipped. That is, the coupon rate is contractually increased as a punishment when the issuer skips a call date. Moreover, markets traditionally consider skipping a call date to be a very serious sign of deteriorating credit-worthiness. This combination leads banks to almost always call their callable bonds at the first possible instant. However, for AT1 CoCos, this trend may very well be broken. As coupon step-ups or other incentives to call are prohibited, and regulators are likely to intervene when they feel that a call is inappropriate. More on this interesting characteristic in our determination of an expression for the AT1 CoCo price in Section 3.1.

In order to set up a CoCo valuation model, it is essential to have an exact understanding of all risks associated with holding an AT1 CoCo. A valid pricing model should incorporate all

these sources of risk. Below we provide a list of the risk drivers present in AT1 CoCos, partly driven by the AT1 characteristics set out above:

- *Interest rate risk*. Before conversion, a CoCo is similar to a fixed income product and its value is therefore sensitive to movements of the term structure of risk-free interest rates.
- *Conversion risk (loss absorption risk)*. This is risk originating from the probability the CoCo conversion is triggered. As this conversion generally entails a loss of value for the holder, investors demand to be compensated for this. This risk driver is present in every CoCo, and is treated in every study on CoCo valuation.
- *Equity risk*. Because of the potential conversion to equity, the CoCo holder is exposed to variations in the share price of the issuing bank, as this may influence the value of their claim when conversion occurs.
- *Coupon cancel risk*. The extra risk of coupon cancellation is born by the holder, and is reflected in the CoCo value. EP (2013a, Article 141) dictates that coupon payments may only take place when the bank has sufficient *Available Distributable Items* (ADI) and/or the payment does not exceed the Maximum Distributable Amount (MDA). The pricing of this risk is for example treated by Corcuera, De Spiegeleer, Fajardo, Jönsson, Schoutens, and Valdivia (2014) for CoCos with a market trigger.
- *Extension risk*. The absence of incentives to call results in an unknown, but possibly significant probability of extension. The issuer might opt not to call when the financing costs of issuing new debt are higher than those of keeping the CoCo in existence. Furthermore, the regulator may prohibit the issuer from redeeming its CoCo. De Spiegeleer and Schoutens (2014) quantify this extension risk in a reduced form framework.

2.2 Current variety in CoCo pricing models

The first problem that emerges when attempting to price a CoCo, is determining whether there exists a unique price in the first place. Sundaresan and Wang (2010) argue that CoCos with a market trigger can suffer from a *multiple equilibria problem* unless the trigger is designed in a way that avoids dilution of preexisting stock holders. They show that dilutive CoCo conversion leads to a situation where there can be more than one potential path for the stock price given a time path for the bank's asset value. This phenomenon would make it impossible to find a unique price for the CoCo. Moreover, it can disastrously destabilize the market, as a small change in market prices could lead the market to switch its belief to a different equilibrium (Calomiris and Herring, 2013).

These concerns about multiple equilibria have led to a shift towards using accounting triggers. Using a book value ratio rather than a market value ratio as conversion trigger removes the multiple equilibria problem. However, it does present some new valuation challenges. Calomiris and Herring (2013) argue that a book value trigger depends on the behavior of the management

and the regulator, which is not easily predictable and makes the probability of conversion difficult to quantify. Furthermore, CoCos with an accounting trigger contain derivative-like characteristics with a non-tradable underlying. When pricing such a derivative, special attention has to be paid to fundamental principals of derivative pricing, such as the existence of a replicating portfolio (see e.g. Cheridito and Xu (2015)).

There exist two main kinds of literature on CoCos: (i) literature on the effect of the introduction of CoCos on bank stability, risk taking, and optimal capital structure; and (ii) literature on the valuation of CoCos and the corresponding risk management. This study mainly belongs to the second category. For literature in the first category we refer to Pennacchi (2011); Bolton and Samana (2012); Koziol and Lawrenz (2012); Barucci and Del Viva (2013); Albul, Jaffee, and Tchistyi (2013); Zeng (2013); Calomiris and Herring (2013); Hilscher and Raviv (2014); Himmelberg and Tsyplakov (2014); Chan and Van Wijnbergen (2014); Berg and Kaserer (2015).

The valuation literature can in turn be decomposed in three distinct approaches: (i) the *first-passage time* approach, which models the conversion and/or default time as the first passage time of a stochastic process through a threshold barrier (e.g. in Pennacchi (2011); Glasserman and Nouri (2012); Buergi (2012); Brigo, Garcia, and Pede (2015); Albul et al. (2013); Metzler and Reesor (2015); Cheridito and Xu (2015)). The most widely used group of first-passage time models in the CoCo literature is the group of structural models, which model a company's asset value as a stochastic process and view default as the first time the asset value hits a certain barrier from above; (ii) the reduced-form approach, where the trigger time is modeled as the first arrival time of an intensity based model (e.g. in De Spiegeleer and Schoutens (2012); Jung (2012); Cheridito and Xu (2014, 2015)). This approach focuses on the credit characteristics of CoCos; and (iii) equity based models, which decompose the CoCo payoff as an ordinary bond and a set of equity derivatives (e.g. in De Spiegeleer and Schoutens (2012); Jung (2012); Corcuera, De Spiegeleer, Ferreiro-Castilla, Kyprianou, Madan, and Schoutens (2013)). This group of equity models is only appropriate for CoCo with a market trigger, and is hence omitted for the remainder of this study. For a critical assessment of some of the existing pricing approaches see also Wilkens and Bethke (2014).

The presence of these distinct approaches can be attributed to the hybrid nature of a conversion-to-equity CoCo. It contains credit like characteristics, namely in the periods where it acts as an ordinary bond.[8] This implies its value is driven by the interest rate and the issuers creditworthiness and probability of default. However, because of the lurking possibility of conversion to equity, its value is driven by the equity market as well. This results in the CoCo price reacting to movements in both the credit and in the equity market. It is hence essential for a valid valuation approach to inhabit both these characteristics.

As we want to build a model for AT1 CoCos with equity conversion, we need an approach that can include both the credit and equity components, and that provides enough flexibility to include coupon cancel and extension risk. Out of the three groups of valuation approaches, only first-passage time models have these characteristics. Furthermore, first-passage time models provide a clear connection with economic content, in linking a default or conversion barrier with

[8] We disregard here the possibility of coupon cancellation that is present in AT1 CoCos for a moment.

a set of economically interpretable stochastic processes (Brigo et al., 2015). This is in contrast to the reduced form (intensity) approach, which regards default and/or conversion as striking out of the blue (see e.g. Duffie and Singleton (1999)). Most pure credit approaches take the form of an intensity model. Pure credit approaches also lack the ability to include the CoCo's equity component.

In first passage time models, the model parameters can be calibrated to credit and equity markets simultaneously, thereby extracting market views from both markets. Furthermore, this approach allows us to hedge this hybrid instrument using both credit and equity securities. This is not possible when using a strictly credit or equity approach, but is essential when we want to set up a proper pricing method for AT1 CoCos with equity conversion under the risk-neutral measure. The reasons provided above lead us to select the first passage time approach as being most fit for AT1 CoCo valuation, and hence we focus on these models going forward.

2.3 The structural approach and other first-passage time models for CoCo valuation

Structural models for the firm value are build on a long line of research on capital structure that was pioneered by Merton (1974), Black and Cox (1976), and Leland (1994), and includes numerous subsequent papers. This approach is based on modeling a firm's assets, and prices debt and equity as claims on these assets. Merton assumes that the firm defaults when at maturity its (latent) actual asset value is less than the face value of debt. Black and Cox extend this approach by allowing default at any time, defining default as the first time the asset value drops to an exogenous reorganization barrier consisting of the debt of the firm and safety covenants. Leland adds strategic default timing to the framework. Numerous other extensions have been proposed, each with different specifications for the firm value process, the default barrier, and/or the default time. An inexhaustive list of such methods is provided in Bielecki and Rutkowski (2002) and the references therein. One interesting extension, especially in the context of AT1 CoCo valuation, is provided by Brigo and Tarenghi (2004).

Brigo and Tarenghi (2004) propose a more flexible extension to the Black and Cox-model, and call it the *Analytically Tractable First-Passage Time* (AT1P) model. They introduce a curved default barrier to enhance model flexibility. They also provide a way of calibrating the model parameters to the implied risk neutral survival probabilities extracted from CDS quotes, making use of analytical formulas for barrier options (Brigo et al., 2015). All structural models mentioned above are examples of the larger family of first-passage time models. This name originates from the fact that they deal with the first time a process hits a barrier.

There exists some literature on CoCo valuation using structural or other first passage time models. Pennacchi (2011) compares several CoCo structures by simulation with a jump diffusion model of the issuer's assets. Though his model is very complete and detailed, it lacks practical usefulness. This is because he skips the calibration step, and limits his study to using guessed benchmark parameters. Albul et al. (2013) construct closed form pricing expressions under the

assumption that the conversion trigger is defined as a threshold level for the issuer's assets and that all debt has infinite maturity. They provide elegant formulas, but use a conversion trigger that is not used in any actual CoCo issues. Glasserman and Nouri (2012) consider a GBM model for the assets, an equity over assets conversion trigger and partial and on-going conversion in amounts just sufficient to meet the minimum capital ratio. They overjump the fact that the CET1 ratio triggering the CoCo is unequal to the market value of equity-over-assets ratio. Hilscher and Raviv (2014) obtain closed-form expressions for finite maturity debt and an asset level trigger, where the contingent capital converts to a fixed proportion of total capital.

Brigo et al. (2015) use the AT1P model to price fixed maturity Tier 2 CoCos. They find a link between the assets-over-equity ratio and CET1 ratio by cross-sectional regression analysis. Buergi (2012) takes a similar approach, adding the assumption that the actual asset value is equal to its book value in times of financial distress. Cheridito and Xu (2015) take a shortcut, and instead of assuming a structural model for the firm, they directly specify a first-passage time model on the CET1 ratio triggering the CoCo. They calibrate the model to CDS rates by assuming that default is driven purely by the CET1 ratio falling below a critical threshold. The latter three studies are the only ones to our knowledge that calibrate their model parameters to market data not consisting of CoCo prices, and use these calibrated models to price CoCos.

None of the studies listed above take into account the two important extra risk factors present in AT1 CoCos: coupon cancel and extension risk. However, in reality these factors are likely to have significant impact on AT1 CoCo prices. This study aims to add these factors to the valuation approach. Furthermore, it aims to calibrate the model parameters without using market observed CoCo prices. This way, we can actually test the model's ability to price CoCos, and determine how the different risk factors contribute to this price. This combination is not yet present in the literature.

We investigate two first-passage time approaches: the structural AT1P model suggested by Brigo et al. (2015), adapted to AT1 CoCos, and a direct CET1 model designed specifically for AT1 CoCo valuation, based on the framework by Cheridito and Xu (2015). We select the AT1P model for its flexibility and possibilities to be calibrated to a full term structure of CDS rates and equity data. Furthermore, the AT1P model provides options to translate the structural model to the AT1 CoCo risk drivers. We select the direct CET1 model for its direct applicability to the CET1 ratio and its elegant simplicity. It models just those processes needed for AT1 CoCo valuation, and not any other superfluous information. Furthermore, the direct CET1 model offers a nice alternative approach for its calibration, directly linking default to the CET1 ratio falling below some barrier.

Chapter 3

Model specification and methods

This chapter introduces the models and methods we propose for AT1 CoCo valuation. Section 3.1 introduces an expression for the price of an AT1 CoCo with conversion to equity and a CET1 ratio trigger. From this expression we then deduce which processes need to be modeled to approximate this price. Section 3.2 specifies how CDS spreads can be written as a function of risk-neutral survival probabilities. These probabilities play an important role in the calibration of our model parameters. Section 3.3 introduces the structural firm value model and specifically the AT1P model, and discusses the assumptions and techniques for the calibration of the model to observed credit and equity data. This includes finding expressions for the risk-neutral survival probabilities in the AT1P setting. Furthermore, it introduces how the AT1P model can be translated to the processes relevant for AT1 CoCo pricing. Section 3.4 introduces a method to directly model the CET1 ratio, and to derive an expression for the risk-neutral survival probabilities in terms of this model's parameters. Combining the expressions for the risk-neutral survival probabilities from both models with the expressions for the CDS rates derived in Section 3.2 allows us to calibrate the model parameters. Section 3.5 introduces the Monte Carlo algorithm to approximate CoCo prices, and proposes techniques to include the relevant risk drivers for AT1 CoCos in this approach.

3.1 AT1 CoCo pricing

We consider a financial institution with an outstanding AT1 CoCo with non-dilutive equity conversion. We assume that there exist three relevant state variables, combined in the 3-dimensional stochastic process (X_t). Here $(X_t^1)_{t\geq 0} = (S_t)_{t\geq 0}$ denotes the stock price process, $(X_t^2)_{t\geq 0} = (C_t)_{t\geq 0}$ denotes the CET1 ratio process, and $(X_t^3)_{t\geq 0} = (r_t)_{t\geq 0}$ denotes the interest rate process. The filtration formed by all observable events is denoted by $(\mathcal{F}_t)_{t\geq 0}$, and discounted prices of future cash-flows are martingales under the risk neutral measure $\mathbb{Q}$. In this framework, the default time τ and the conversion time ϑ are modeled as first passage times in

both the AT1P and the direct CET1 model:

$$\text{AT1P model: } \tau = \inf\{t \in [0,T] : A_t \leq \widehat{H}_t\}, \quad \vartheta = \inf\{t \in [0,T] : C_t \leq c_\vartheta\}, \tag{3.1.1}$$

$$\text{CET1 model: } \tau = \inf\{t \in [0,T] : C_t \leq c_\tau\}, \quad \vartheta = \inf\{t \in [0,T] : C_t \leq c_\vartheta\}, \tag{3.1.2}$$

where A_t and $\widehat{H}_t$ are the firm value and default barrier in the AT1P model (see Section 3.3), and c_τ, c_ϑ are constants. For tractability, we take the process C_t to be continuous and observable. Furthermore, we must always make the following assumption:

$$\text{Assumption: } \mathbb{Q}(\vartheta < \tau) = 1. \tag{3.1.3}$$

That is, we assume that conversion always happens before default. This assumption, though certainly debatable, is essential to justify the remainder of this analysis. Namely, we are calibrating the state variable processes to market observed CDS spreads. Consequently, we use CDS contracts to form the CoCo hedging portfolios, which is an essential step to justify our risk-neutral pricing approaches. If default would be possible before conversion, CDS contracts could not be used to perfectly hedge CoCos.

Note that in reality default is in fact possible before conversion. Some bank defaults over the past decade have been driven more by liquidity issues than by capital issues.[9] For this reason, as put forward by Whittall (2014), CoCo investors still remain indecisive as to how to efficiently hedge their CoCo exposure. There are several fixed income specialists who claim there should be a separate instrument in addition to subordinated CDS contracts, specially designed to hedge CoCos. However, for the time being, we are restricted to regular subordinated CDS contracts to calibrate and hedge CoCos, thus making the assumption $\vartheta < \tau$ necessary.

3.1.1 Quantifying the AT1 restrictions

An AT1 CoCo with equity conversion and a CET1 ratio trigger can be viewed as the sum of a perpetual, callable, defaultable bond for which the coupon payments can be canceled, and an option paying out a variable number of equity shares upon conversion. The perpetual nature of the bond proposes clear difficulties when attempting to develop a Monte Carlo based pricing approach. However, as introduced in Section 2.1, perpetual callable Tier 1 bonds issued by banks have historically always been expected to be called at the first opportunity, no matter whether economic conditions would suggest differently. Consequently, these securities are usually valued on that basis as well.

The widely believed rationale behind this assumption is as follows. If the bank does not call the bond, it would damage investor confidence to such an extent, that it could never come back to the market to raise Tier 1 or other capital again. Furthermore, when the bond is not called and hence becomes perpetual, the only real difference compared to equity is the certain (higher)

[9] We do make a note here on liquidity as driver of default. While liquidity is often the direct cause of a bank default, liquidity issues are likely to be caused by capitalization problems. When deposit holders believe that a bank's creditworthiness is strongly deteriorating, they may opt to withdraw their deposits, which in turn can lead to a 'liquidity-driven' default.

coupon rate on the bond versus an uncertain dividend on equity. These reasons, supported by the fact that only very few occurrences of a non-call on a Tier 1 perpetual have taken place, have supported for a long time the market's view of pricing these bonds under the assumptions that maturity equals the first call date.

However, some non-calls following the global financial crisis have exposed weaknesses in the above reasoning. Notable non-calls include a $650 mn. Deutsche Bank Tier 1 in January 2009, a $1 bn. Deutsche bank Subordinated Tier 2 in December 2008, and a $430 mn. Monte dei Paschi di Siena (BMPS) Tier 1 in February 2011. These non-calls were based on the, seemingly rational, decision that as a *flight-to-quality* was taking place during these crisis times, refinancing the debt would cost the banks much more than just the extra cost of the coupon step-up associated with extending the bond (see also De Spiegeleer and Schoutens (2014)). These occurrences (temporarily) scared off subordinated bond investors, with declining prices en inflating CDS spreads as a result.

AT1 CoCo bonds contain an additional reason to seriously consider the risk of extension. Namely, as put forward in Section 2.1, in order to qualify as AT1 capital, it is prohibited for a CoCo to inherit any incentive to be redeemed at its call dates. Where regular perpetuals, including the non-calls mentioned above, all faced an increase in coupon once a call date was surpassed, AT1 CoCos do not. Furthermore, as put forward in EP (2013b, Article 78(1)), the regulator will only permit the issuer to call the CoCo when the CET1 ratio remains sufficiently high after redemption. This is another argument increasing the possibility of extension. On the other hand, the CoCo bond market is expected to be a lot more mature some years from now. This gives the CoCo issuer an incentive to call, as it is likely that it can then directly issue a new CoCo under better conditions. Once the issuer can directly issue a new CoCo, the regulator will be more lenient in allowing redemption.

Combining the reasons above we conclude that for the CoCos we consider we indeed have to include some risk of extension in our pricing model. We do this as follows. We choose our CoCo 'maturity' T to be 10 years after issuance. For AT1 CoCos this implies that there occur potential call dates t_c, $c = 1, 2, \ldots, D$, before T. At these call dates, we assume that the issuer calls the CoCo, unless the regulator prohibits it from doing so. The regulator prohibits a call if the CET1 ratio is not high enough. This fits our model nicely, as it allows us to determine a CoCo call threshold c_φ. When C_t is above the call threshold at a call date, the CoCo is called. When $C_{t_c} < c_\varphi$ however, the regulator prohibits a call, and the CoCo is extended up to at least the next call date. We believe that we can safely assume that up to 10 years after issuance, there will be at least one call date on which the CoCo is called, or a CoCo conversion date. For this reason, the model's pricing error due to possible value stemming from over 10 years after issuance is likely to be very small. The appropriateness of this assumption is assessed in Section 5.4.

Furthermore, the option of discretionary coupon cancellation must be included in the pricing model as well. As put forward in Section 2.1, the regulator prohibits the issuer from paying out a coupon when the issuer has insufficient ADI and/or the payment exceeds the MDA. ADI and MDA, while both impossible to model directly in our framework, are notions that can be related

directly to the amount of CET1 capital on the bank's balance sheet. Both are functions of free capital reserves, retained earnings, and equity, and thus are in close relation with CET1 capital. This leads us to introduce a certain coupon cancel level c_{cc} as well: if the CET1 ratio is below this level on a distribution payment date, this payment is canceled in full.

3.1.2 Expression for the price of an AT1 CoCo

If we consider an AT1 CoCo with non-dilutive conversion to equity, and we assume the product can be hedged with liquid instruments, and has not been converted or called yet by time $t < T$, its unique arbitrage-free price is:

$$\begin{aligned} CoCo_t(S_t, C_t, r_t, T) = \sum_{t_i > t} d_i P \mathbb{E}_t^{\mathbb{Q}} \left[e^{-\int_t^{t_i} r_u \mathrm{d}u} \mathbb{I}_{\{C_{t_i} > c_{cc}, \vartheta > t_i, \varphi \geq t_i\}} \right] + P \mathbb{E}_t^{\mathbb{Q}} \left[e^{-\int_t^T r_u \mathrm{d}u} \mathbb{I}_{\{\vartheta > T, \varphi > T\}} \right] \\ + P \mathbb{E}_t^{\mathbb{Q}} \left[e^{-\int_t^{\varphi} r_u \mathrm{d}u} \mathbb{I}_{\{\varphi \leq T, \varphi < \vartheta\}} \right] + \mathbb{E}_t^{\mathbb{Q}} \left[\left| \frac{P}{\max\{S_\vartheta, F\}} \right| e^{-\int_t^{\vartheta} r_u \mathrm{d}u} S_\vartheta \mathbb{I}_{\{\vartheta \leq T, \vartheta \leq \varphi\}} \right]. \end{aligned} \tag{3.1.4}$$

The intuition behind this expression is as follows: (i) the first term represents the discounted sum of future coupon payments, contingent on the CET1 ratio C_t being larger than the coupon cancel trigger c_{cc} at the coupon payment date t_i, and both conversion time ϑ and redemption time φ not having occurred yet. The coupon rate at t_i is denoted by d_i for $i = 1, \ldots, M$, with M the total number of coupon payment dates up to 'maturity' T; (ii) the second term is the discounted value of the principal P, contingent on both conversion and redemption not to occur before 'maturity' T; (iii) the third term denotes the discounted value of the principal when the CoCo is called at its issue price. This is logically contingent on redemption occurring before maturity and before conversion; and (iv) the fourth term denotes the value of the possible conversion into equity. This term depends on the stock price at conversion, the floor price F, and the amount of stocks obtained, and is contingent on the conversion occurring before maturity and before redemption.[10]

Some further implications of (3.1.4) are that when conversion coincides with a coupon payment date, no coupon payment takes place. And that when two or more of the events 'conversion', 'redemption', or 'maturity' happen simultaneously, conversion goes before redemption and maturity, and redemption goes before maturity. This is all in line with the details provided in the prospectuses of relevant CoCo issues.

Judging from (3.1.4), we can find the CoCo price if we can specify under the $\mathbb{Q}$-measure the processes r_t, C_t, S_t, and the processes underlying the stopping times ϑ and φ. These stopping times, as specified earlier in this section, are all driven by the process C_t. Hence specifying the parameters in the 3-dimensional stochastic process X_t under the $\mathbb{Q}$-measure suffices to construct a Monte Carlo approach to approximate expression (3.1.4).

[10] The non-dilutive conversion to equity mechanism works as follows. At conversion, the CoCo holder must buy stocks for a price of $\max\{S_\vartheta, F\}$. That is, when the stock price is higher than the floor price at conversion, CoCo conversion does not result in a significant loss of value. When however the stock price at conversion is lower than the floor price, the CoCo holder must buy stocks for the floor price, which results in a significant loss of value.

3.2 Credit Default Swap pricing

In this section we specify the Credit Default Swap (CDS) rate in terms of risk-neutral survival probabilities. This way we can use market observed CDS spreads to calibrate the parameters of the relevant processes. The buyer of a Credit Default Swap (CDS) acquires protection against the default event of a reference entity. The seller thus pays the buyer when the reference entity defaults. In exchange, the buyer of the CDS periodically pays a premium to the seller.

Consider a CDS contract on a reference entity with recovery rate R starting at T_0, with premium times T_i, $i = 1, \ldots, N$, and maturity T_N. Furthermore, the time t prices of zero coupon bonds with maturity m are observed in the market and given by $P(t,m) = \mathbb{E}_t^{\mathbb{Q}}\left[e^{-\int_t^m r_u \mathrm{d}u}\right]$. Then the time $t < T_N$ discounted pay-off of the CDS for the buyer is given by the difference between the default leg DL_t and the premium leg PL_t:

$$DL_t = (1-R)\sum_{i:T_i>t}\left(P(t,\tau)\mathbb{I}_{\{T_{i-1}<\tau\leq T_i\}}\right) \tag{3.2.1}$$

$$PL_t = \sum_{i:T_i>t}\left(\delta\left[P(t,T_i)\alpha\mathbb{I}_{\{\tau>T_i\}} + P(t,\tau)(\tau - T_{i-1})\mathbb{I}_{\{T_{i-1}<\tau\leq T_i\}}\right]\right), \tag{3.2.2}$$

where α denotes the time between premium payments in years. This is typically $1/4$. δ is the CDS rate specified in the contract. Equation (3.2.2) gives the discounted premium payments, including the accrued premium in the period where default occurs.

The price of the CDS at time t is now given by the expected value of $DL_t - PL_t$ evaluated under the $\mathbb{Q}$-measure and conditional on $\mathcal{F}_t$. Brigo et al. (2015) propose two assumptions to make this expectation more tractable. Firstly, we approximate the accrual term by half the full premium to be paid at the end of each period. Secondly, with respect to the default leg, we use the premium leg time-grid as discretization for the resulting integral. The latter assumption proves to work well. The error resulting from it is very small while it reduces computation time considerably. The former assumption cannot be tested explicitly, but its resulting error is at most half a premium payment. Combined with the fact that default is not likely to occur very often, makes the total error of this assumption small. The benefits it provides in terms of making evaluation of the expression a lot more tractable mathematically outweigh this error.

Under these assumptions we obtain as price $CDS_{T_0,T_N}(t)$:

$$\begin{aligned} CDS_{T_0,T_N}(t) &= (1-R)\sum_{i:T_i>t} P(t,T_i)\left(\mathbb{Q}_t(\tau>T_{i-1}) - \mathbb{Q}_t(\tau>T_i)\right) \\ &-\delta\sum_{i:T_i>t} P(t,T_i)\alpha\left(\mathbb{Q}_t(\tau>T_i) + \frac{1}{2}\left[\mathbb{Q}_t(\tau>T_{i-1}) - \mathbb{Q}_t(\tau>T_i)\right]\right), \end{aligned} \tag{3.2.3}$$

where $\mathbb{Q}_t(\cdot)$ denotes the probability under the risk-neutral measure $\mathbb{Q}$ at time t. Now in practice, CDSs are quoted in terms of the rate that would make its current price equal to zero. We hence

obtain as CDS rate at time $t = T_0$ for maturity T_N:

$$\delta_{t,T_N} = \frac{(1-R)\sum_{i:T_i>t} P(t,T_i)\left(\mathbb{Q}_t(\tau > T_{i-1}) - \mathbb{Q}_t(\tau > T_i)\right)}{\sum_{i:T_i>t} P(t,T_i)\alpha\left(\mathbb{Q}_t(\tau > T_i) + \frac{1}{2}\left[\mathbb{Q}_t(\tau > T_{i-1}) - \mathbb{Q}_t(\tau > T_i)\right]\right)}. \tag{3.2.4}$$

In this setting, we only need to express the risk-neutral survival probability $\mathbb{Q}_t(\tau > t)$, for any $T_0 \leq t \leq T_N$ in terms of the model parameters. When we achieve this, we are able to calibrate the parameters to a term structure of CDS rates and zero coupon bond prices.

3.3 The AT1P model

In the structural approach, we aim to model the banks' asset value using a stochastic process, viewing its debt and equity as claims on these assets. As introduced in Section 2.3, Merton (1974) models the value of the firm (or asset value) A as a Geometric Brownian Motion. Under the risk neutral measure this entails:

$$\mathrm{d}A_t = (r-q)A_t\mathrm{d}t + \sigma_A A_t \mathrm{d}W_t, \tag{3.3.1}$$

where r is the risk free rate, q the pay-out rate, and σ_A the asset volatility. All these parameters are assumed constant in the original Merton model. W_t denotes a Brownian Motion under the risk neutral measure $\mathbb{Q}$ defined in the probability space $(\Omega, \mathcal{F}, \mathbb{Q})$. This implies lognormal dynamics for the asset value. When the firm considered is a bank, this asset value comprises of a portfolio of loans, securities, and off-balance sheet positions. Under the risk-neutral measure, the instantaneous rate of return of these assets is equal to the instantaneous risk-free rate. Crouhy, Galai, and Mark (2000) note that this assumption of lognormality is quite robust in practice and, according to KMVs empirical studies, actual data conform quite well to these dynamics.[11] However, we note that the assumption of constant parameters is quite restrictive, and it gives the model very little flexibility to fit a term structure of CDS rates. This implies it may not be able to generate accurate probabilities of default.

This criticism on using GBM with constant parameters to describe the evolution of the assets is mainly formalized by the observation that lognormal dynamics cannot match high short-term CDS spreads observed in the market (see e.g. Lando (2004)). The reason for this is that under GBM the instantaneous probability of default of a sound firm is close to zero. A single constant volatility is simply not able to provide realistic default probabilities for varying maturities. There are several ways to account for this anomaly. Firstly, the structural model can be extended to incorporate jumps in the asset value (see e.g. Zhou (2001); Hilberink and Rogers (2002)). These jumps have a natural interpretation in the setting of a bank, as a bank's assets are known to suffer from sudden shocks in value, e.g. when important information about their creditworthiness is disclosed. An asset process including jumps however poses large complications

[11] KMV stands for the famous quantitative credit analysis company founded by Kealhofer, McQuown and Vasicek.

when attempting calibration to market quotes of CDS spreads. A more practical method to circumvent the model's disability to fit short maturity CDS spreads, is to omit the shortest maturities from the calibration procedure.

Though omitting the shortest maturities from the calibration procedure does not actually improve the model's very short term performance, it does make sure that the calibration results are not strongly distorted by this anomaly. That is, including very short term maturities would cause the parameters (especially the volatility) to be adapted strongly towards fitting the short maturities, thereby significantly deteriorating the model performance for longer maturities. However, in the context of CoCo pricing, having a generally accurate fit on the short, medium, and long end of the CDS curve is more important for the pricing accuracy than having an exact fit for very short maturities.[12]

Now firm value A is at any time composed out of an equity part E and a debt part D:

$$A_t = E_t + D_t.$$

Merton (1974) assumes simple zero coupon debt with maturity T and face value F. For a bank, this assumption is too restrictive, as a banks' debt exists among other things of customer deposits, senior bonds, subordinated bonds, and (contingent) convertible bonds. All these forms of debt have distinctly different maturities and associated costs. In the Merton-model, default is linked to the ability of the firm to pay back all its issued debt. If at maturity T, the firm value A is larger than the face value of debt F, all debt is repaid and the firm survives. If however A_T is smaller than F, the firm defaults. This implies that firm default can be viewed as a stopping time, which in this case is defined as: $\tau = T\mathbb{I}_{\{A_T<F\}} + \infty\mathbb{I}_{\{A_T\geq F\}}$, where $\mathbb{I}_Y$ denotes an indicator function which equals 1 if Y holds, and 0 otherwise.

Now in a Black-Scholes economy where A_t is the only risky asset and there exists a bank account B whose value grows deterministically and is given by:

$$B_t = B_0 e^{rt},$$

we can use the Black-Scholes results for option pricing to price the equity and debt. The value of debt at maturity is $D_T = \min(A_T, F) = F - (F - A_T)^+$, which gives for $t < T$:

$$\begin{aligned} D_t &= Fe^{-r(T-t)} - \left(Fe^{-r(T-t)}\Phi(-d_2) - A_t\Phi(-d_1)\right), \text{ where} \\ d_1 &= \frac{\ln(A_t/F) + \left(r - q + \sigma_A^2/2\right)(T-t)}{\sigma_A\sqrt{T-t}} \\ d_2 &= d_1 - \sigma_A\sqrt{T-t}, \end{aligned} \tag{3.3.2}$$

where $\Phi(\cdot)$ denotes the CDF of the standard Gaussian distribution. The second term in (3.3.2) comes from the fact that $(F - A_T)^+$ is the pay-off of a standard European put option on the

[12] It does not influence the CoCo price that much when the model is a bit off in determining when exactly during the first two years default or conversion may take place. It does matter a lot that the model gives a generally accurate distribution of conversions/defaults over its full maturity.

asset value with strike F. Combining this with the asset dynamics from (3.3.1) gives the familiar expression for the put price.

The equity value at maturity is given by the remaining asset value after all debt is repaid, and is hence given by $E_T = (A_T - F)^+$, yielding for $t < T$:

$$E_t = A_t \Phi(d_1) - F e^{-r(T-t)} \Phi(d_2), \tag{3.3.3}$$

with d_1 and d_2 defined above. Again this result follows from standard option pricing noting that the equity pay-off equals that of a call option on the asset value with strike F. An important limitation of this model, apart from the restrictive assumption on the debt structure, is the fact that default can only occur at maturity. Black and Cox (1976) were the first to introduce the possibility of early default, resulting from the breaching of a safety covenants barrier. They assume this barrier to be exponential. As noted by Glasserman and Nouri (2012), this boundary, in the case of a regulated bank, can be interpreted as the minimum capital requirement the bank must maintain. This capital requirement will set the liquidation boundary higher than the actual default boundary: the bank is seized by the regulator before bankruptcy if the capital requirement is not maintained. For more intuition about the interpretation of the default barrier in our model, see Section 4.3.

In the Black-Cox framework the default time τ is defined as: $\tau = \inf\{t \in [0,T] : A_t \leq H_t\}$, where $\inf\{\emptyset\} = \infty$, and the dynamics of the default barrier H are given by:

$$H_t = \begin{cases} F & t = T \\ K e^{-\gamma(T-t)} & t < T, \end{cases}$$

where γ and K are positive constants. When attempting to calibrate this model to CDS market quotes, this model gives analytical formulas for CDS quotes using results from barrier option pricing. However, the model shows to lack flexibility: its four free parameters σ_A, K, F, and γ do not provide enough degrees of freedom to properly fit a term structure of CDS spreads.

This problem is addressed by Brigo and Tarenghi (2004), who propose a more flexible model, that still yields analytical formulas for CDS quotes. Their model is based on work by Lo, Lee, and Hui (2003) and Rapisarda (2005). They show that it is possible to find analytical barrier option prices for models with time-dependent parameters, when the barrier has a particular curved shape, partly dependent on the time dependent volatility. The resulting AT1P model is designed as:

$$\text{Firm value: } \mathrm{d}A_t = (r_t - q)A_t \mathrm{d}t + \sigma_A(t) A_t \mathrm{d}W_t \tag{3.3.4}$$

$$\overset{\text{Itô}}{\Rightarrow} A_t = A_0 \exp\left\{ \int_0^t \left(r_u - q - \frac{1}{2}\sigma_A^2(u) \right) \mathrm{d}u + \int_0^t \sigma_A(u) \mathrm{d}W_u \right\} \tag{3.3.5}$$

$$\text{Default barrier: } \widehat{H}_t = H \exp\left(\int_0^t \left(r_u - q - L\sigma_A^2(u) \right) \mathrm{d}u \right), \tag{3.3.6}$$

where $H > 0$ and L are free parameters that can be used to shape the barrier. $\sigma_A(t)$ denotes

a time-dependent deterministic function of volatilities. The model can be made as flexible as desired by varying the amount of parameters in this function. We note that the AT1P model allows for a time dependent risk free rate, pay-out ratio, and asset volatility. Default time τ is again defined as the first time A hits $\widehat{H}$ from above, starting with $A_0 > H$.

The equity value in this framework is somewhat more involved than the regular European call option from the Merton model, due to the possibility of early default and the time-dependent default barrier. This equity value can be seen as a European down-and-out call option on an underlying with time-dependent parameters. That is, the pay-off is $(A_T - \widehat{H}_T)^+$ if the underlying stays above the barrier level up to maturity (survival) and pay-off is zero when the underlying hits the barrier at any time before or at maturity (default). The equity value is thus given by:

$$E_t = \mathbb{E}_t^{\mathbb{Q}} \left[e^{-\int_t^T r_u \mathrm{d}u} (A_T - \widehat{H}_T)^+ \mathbb{I}_{\{\tau > T\}} \right]. \tag{3.3.7}$$

There exists an analytical solution to this expression, which is further elaborated in Section 4.3. In this setting the risk-neutral survival probability $\mathbb{Q}\{\tau > T\}$ can be derived analytically as well. This probability can in turn be used to calibrate the model to market CDS quotes.

3.3.1 Translating the structural model to the CoCo risk drivers

In order to price a CoCo using the AT1P framework, we need to find a link between (3.3.4), (3.3.6), (3.3.7), and the CoCo value driving processes S_t and C_t. For the link between E_t and S_t, we simply note that the market value of equity E_t is equal to the firm's market capitalization $MC_t = O_t \cdot S_t$, where O_t denotes the number of shares outstanding at time t. Throughout this study we assume O_t to be constant over time. The stock price at time $t < T$ is hence given by $S_t = E_t / O$.

To find a link with the CET1 ratio C_t, we again take a look at the definition of this ratio, introduced in Section 2.1. We have that the CET1 ratio is at any time $t < \tau$ defined as $C_t = CET1_t / RWA_t$, where $CET1_t$ denotes the amount of CET1 capital on the bank's balance sheet, and RWA_t denotes the amount of risk-weighted assets.

As noted in Section 2.1, CET1 capital is an accounting (or book) quantity, which clearly differs from the *market* value E_t coming from our model. However, we do expect there to be a clear relationship between these two quantities. The amount of RWA is a function of the bank's assets and off-balance sheet exposures weighted according to their riskiness. It is hence of the general form: $RWA_t = \sum_j w_{j,t} Y_{j,t}$, where the weights $w_{j,t}$ are set by the regulator, and $Y_{j,t}$ is the exposure to asset class j at time t. The sum is over all possible asset classes j. We thus expect that there is a clear relationship between the total asset value and the RWA.

Next to incorporating the dependencies defined above, we need to make sure that the necessary condition $\varphi < \tau$, as set out in Section 3.1, is satisfied in our definition of C_t. Brigo et al. (2015) propose a way achieve all this, by performing cross-sectional regressions of banks' capital ratios on their respective book value of assets over book value of equity ratios. The weakness of their approach however, is that they establish a relationship based on book values, which

they use in their market-value based pricing approach. Attempting to establish the relationship directly on market values poses problems as well, as total asset value is not observed in the market. To cope with this problem we use a solution as proposed by Calomiris and Herring (2013). That is, we use the *quasi* market value of the assets (QMVA), rather than the true one. The QMVA is calculated as $QMVA_t = MC_t + F_t$, where F_t denotes the face (book) value of liabilities at time t. Using the face value of debt rather than the market value is necessary, as the marking to market of bank debt, especially on ongoing basis, proposes great practical difficulties. The assumption is also sensible, as it is likely that the market and face value of debt remain close to each other.[13]

We estimate the relationship between the CET1 ratio and the market values of assets and equity hence as follows:

$$C_i = \beta_0 + \beta_1 \left(\frac{QMVA_i}{MC_i} \right) + \varepsilon_i, \quad \text{for } i = 1, \ldots, W, \tag{3.3.8}$$

where W denotes the number of banks considered for the cross-sectional analysis. Now, within the AT1P model, the total asset value at time t is denoted by A_t. Brigo et al. (2015) then assume the total liabilities to be given by $\widehat{H}_t$ within the model. This is again a sloppy assumption, as this implicitly assumes that the equity value E_t is equal to the difference between A_t and default barrier $\widehat{H}_t$. This is however, for $L \neq 0$, untrue in the AT1P model.[14] For this reason, we make use of the market value of equity E_t within our model instead. That is, letting $\hat{\beta}_0$ and $\hat{\beta}_1$ denote the estimated parameters from the regression (3.3.8), we express the proxy for C_t as:

$$\widehat{C}_t = \begin{cases} \hat{\beta}_0 + \hat{\beta}_1 \left(\frac{A_t}{E_t} \right), & E_t > E_{\min}, \\ 0, & E_t \leq E_{\min}, \end{cases} \tag{3.3.9}$$

where

$$E_{\min} = \left| \min \left\{ \hat{\beta}_1 / \hat{\beta}_0, 0 \right\} \right| \cdot A_t.$$

This last condition is necessary to ensure a nonnegative CET1 ratio. Now, similar to Brigo et al. (2015), but adapted to our definitions, we need two conditions to ensure that (3.1.3) always holds in this model. Firstly, we clearly need that the initial value of A_t/E_t is such that C_t is above the conversion threshold c_ϑ. This condition is assured by adding the model approximation of the CET1 ratio, together with the market observed ratio, to the objective function of the calibration, as set out in Section 4.3. Secondly, we need $\hat{\beta}_1 < 0$. We expect this to hold, as a higher asset-on-equity ratio implies higher assets and/or lower equity. Higher assets in turn implies higher risk-weighted assets, and lower equity implies lower CET1 capital. These factors both drive the CET1 ratio down.

The proof that these two conditions imply (3.1.3) is as follows. We clearly have that $A_t/E_t \to \infty$ as $E_t \to 0$. Now from (3.3.7) we see that $E_t \to 0$ when $A_t \to \widehat{H}_t$ from above. Now from $\hat{\beta}_1 < 0$

[13] Except when a major interest rate shock occurs. However, as our model only contains continuous stochastic factors, this is unlikely to happen.

[14] See Appendix E for elaboration hereon.

and (3.3.9) we have that $C_t \to 0$ as $A_t/E_t \to \infty$. This mean that in the limit of $E_t \to 0$ and thus $A_t \to \widehat{H}_t$ (bank approaching default), C_t goes to zero. Now observing from (3.3.9) we see that C_t is continuous for $E_t > E_{\min}$. Combining this with the starting value for C_t being above the conversion threshold, we conclude that C_t would have to pass through the conversion threshold before the bank reaches the default barrier.

Now, as (3.3.8) is a cross-sectional regression, it makes no sense to use the error distribution from this regression to decorrelate the CET1 ratio from the assets-on-equity value in the simulation paths. Brigo et al. (2015) propose a solution to this issue. It entails introducing a new random shock $\varkappa_t \sim \mathcal{N}(0,1)$, independent of the Brownian motion underlying the asset value. The CET1 capital in the simulation paths is then given by:

$$C_t = \hat{\beta}_0 + \hat{\beta}_1 \cdot \text{std}(A_t/E_t)\left(\varrho \frac{A_t/E_t}{\text{std}(A_t/E_t)} + \sqrt{1-\varrho^2}\varkappa_t\right), \tag{3.3.10}$$

where 'correlation' parameter $\varrho \in [0,1]$. Correlation is written between quotation marks here as we have $\text{corr}(C_t, A_t/E_t) = \varrho \cdot \text{sign}(\beta_1)$.

In terms of our overall state process X_t we hence have the following settings: $X_t^1 = S_t = E_t/O$, for O constant.[15] Furthermore, $X_t^2 = C_t$ as defined above, and $X_t^3 = r_t$.

3.3.2 Hedging CoCos in the AT1P model

To prove there exists a CoCo hedging strategy in the AT1P framework, we follow the approach of Cheridito and Xu (2015), adapted to our specification of the state process X_t. We assume there exists a bank account with return r_t, such that a unit of currency in the bank account evolves as $\Pi_t^0 = e^{\int_0^t r_u \mathrm{d}u}$. Next to the bank account, we use three liquid hedging instruments. The prices of the hedging instruments are given by Π_t^j, $j = 1,2,3$. Now as the state variables are Markov processes, the values of the CoCo and the hedging instruments at time $t < \vartheta$ can be written as $\Pi(t, X_t)$ and $\Pi^j(t, X_t)$, for deterministic functions Π, Π^j: $[0,T] \times \mathbb{R}^3 \to \mathbb{R}$.

Now the dynamic hedging strategy ξ_t^j, $j = 0,1,2,3$, for $t < \vartheta$, has to satisfy two properties: (i) the value of the hedging portfolio should at any time be equal to the value of the CoCo; and (ii) the sensitivity of the hedging portfolio with respect to the different risk factors should always be equal to the sensitivity of the CoCo value to the risk factors. From Itô's lemma we obtain that these properties can be formalized as:

$$\frac{\partial \Pi}{\partial x^i}(t, X_t) = \sum_{j=1}^{3} \xi_t^j \frac{\partial \Pi^j}{\partial x^i}(t, X_t), \quad i = 1,2,3, \quad \text{and} \quad \Pi(t, X_t) = \xi_t^0 \Pi_t^0 + \sum_{j=1}^{3} \xi_t^j \Pi^j(t, X_t). \tag{3.3.11}$$

We need three hedging instruments that can account for the equity risk (X^1), conversion, coupon cancel, and extension risk (X^2), and interest rate risk (X^3). We note that we assume conversion, coupon cancellation, and extension are all driven by the CET1 ratio. Now we observe that the CET1 ratio is a function of the assets-on-equity ratio in the AT1P model, and the assets

[15] As the equity E_t is valued using a Martingale pricing approach with the asset value A_t as underlying, its discounted version is a Martingale by definition. Furthermore, noting that a Martingale multiplied by a constant remains a Martingale, we conclude that the necessary condition set out in the beginning of Section 3.1 is satisfied.

and equity (through the assets and default barrier) processes are calibrated to market observed CDS rates. Furthermore, conversion always happens before default in our model. This implies that the CET1 ratio is a function of the CDS rates in the AT1P model, and we can use a CDS contract to hedge the conversion, coupon cancel, and extension risk factors. Furthermore, we can use stock shares to hedge the equity risk factor, and interest rate swaps to hedge the interest rate risk factor. We combine these observations with the fact that the coefficients of the expression for C_t do not depend on the value of $S_t = E_t/O$, the coefficients of the SDE for r_t do not depend on S_t, and C_t is independent of r_t. This allows us to let Π^1 be the stock S, Π^2 a CDS contract, and Π^3 an interest rate swap. Then for $t < \vartheta$ we can rewrite (3.3.11) to become:

$$\begin{aligned}
\frac{\partial \Pi}{\partial x^1}(t, X_t) &= \xi_t^1 \\
\frac{\partial \Pi}{\partial x^2}(t, X_t) &= \xi_t^2 \frac{\partial \Pi^2}{\partial x^2}(t, X_t) \\
\frac{\partial \Pi}{\partial x^3}(t, X_t) &= \xi_t^3 \frac{\partial \Pi^3}{\partial x^3}(t, X_t) \\
\Pi(t, X_t) &= \xi_t^0 \Pi_t^0 + \sum_{j=1}^{3} \xi_t^j \Pi^j(t, X_t).
\end{aligned}$$

We see that we have here, for any $t < \vartheta$, a system of four equations with four unknowns (ξ_t^j, $j = 0, 1, 2, 3$). This system can hence be solved, proving that the CoCo can be perfectly hedged in this AT1P model, and that we can price the CoCo under the risk-neutral measure $\mathbb{Q}$ using expression (3.1.4) in the AT1P model.

3.4 The direct CET1 model

Another possibility is to model the CET1 ratio directly as a diffusion process, as suggested by Cheridito and Xu (2015). We assume again that all noise is generated by a 3-dimensional diffusion process (X_t), with the definitions and assumptions from Section 3.1. The default time τ and the conversion time ϑ are thus modeled as first passage times:

$$\tau = \inf\{t \in [0, T_i] : C_t \leq c_\tau\}, \quad \vartheta = \inf\{t \in [0, T_i] : C_t \leq c_\vartheta\}, \tag{3.4.1}$$

where $c_\vartheta > c_\tau$ are constants, and C_t is the CET1 ratio process, which is of the form $C_t = f(X_t)$ for a continuous function $f : \mathbb{R}^3 \to \mathbb{R}$ defined below.

Furthermore, the instantaneous risk-free interest rate r_t is of the form $r_t = g(X_t)$ for a continuous function $g : \mathbb{R}^3 \to \mathbb{R}$. As will become clear later, we do not need to specify explicitly this short rate process for calibration of the model.

The first element of (X_t) is the stock price process, which we assume to follow a GBM with dividend payout rate d:

$$\mathrm{d}X_t^1 = \mathrm{d}S_t = (r_t - d)S_t \mathrm{d}t + \sigma S_t \left(\sqrt{1-\rho^2}\mathrm{d}W_t^1 + \rho \mathrm{d}W_t^2\right), \tag{3.4.2}$$

where W_t^1 and W_t^2 are Brownian motions under the risk neutral measure $\mathbb{Q}$, and σ and ρ are constants. Furthermore, the dividend pay-out rate d is assumed constant as well. The last term results from Choleski decomposition of two independent $\mathbb{Q}$-Brownian motions W_t^1 and W_t^2, and is a $\mathbb{Q}$-Brownian motion itself as well. We do this to get correlation ρ between the Brownian motions of the stock price and the CET1 ratio processes. We can verify by Itô that the corresponding functional form is given by:

$$S_t = S_0 \exp\left\{ \int_0^t r_u \mathrm{d}u - \left(d + \frac{1}{2}\sigma^2 \right) t + \sigma \left(\sqrt{1-\rho^2} W_t^1 + \rho W_t^2 \right) \right\}. \tag{3.4.3}$$

Now the discounted stock price process is given by:

$$\tilde{S}_t = e^{-\int_0^t r_u \mathrm{d}u} e^{dt} S_t = S_0 \exp\left\{ -\frac{1}{2}\sigma^2 t + \sigma \left(\sqrt{1-\rho^2} W_t^1 + \rho W_t^2 \right) \right\}.$$

And by Itô the corresponding SDE is given by:

$$\mathrm{d}\tilde{S}_t = \left\{ \sigma \left(\sqrt{1-\rho^2} \mathrm{d}W_t^1 + \rho \mathrm{d}W_t^2 \right) \right\},$$

which is a $\mathbb{Q}$-martingale. Furthermore, the time t prices of risk-free zero coupon bonds with maturity m are given by $P(t,m) = \mathbb{E}_t^{\mathbb{Q}} \left[e^{-\int_t^m r_u \mathrm{d}u} \right]$.

As introduced above, we assume default is driven by the CET1 ratio falling below some threshold. This is a very practical assumptions, as this allows us to calibrate the model to market observed CDS spreads. Now we let the second element of (X_t) be the process governing the CET1 ratio. We choose the CET1 ratio to follow an Exponential Ornstein-Uhlenbeck (EOU) process. We find that this is both an economically intuitive choice, and that it yields better calibration results than for example GBM dynamics. The economic intuition is that banks always have a target CET1 ratio, represented as the long-run mean of the EOU process. The CET1 ratio generally roams around this long run mean, as banks adjust their strategy as to let the CET1 ratio move towards their target. We take the exponential variant of the OU process as the CET1 ratio cannot become negative.

The SDE for the logarithm of the CET1 ratio is hence given by:

$$\mathrm{d}\left(\log\left(X_t^2 \right) \right) = \mathrm{d}\left(\log\left(C_t \right) \right) = \mathrm{d}H_t = \kappa(\bar{h} - H_t)\mathrm{d}t + \eta \mathrm{d}W_t^2, \tag{3.4.4}$$

where $\bar{h}$ denotes the long-run mean, κ the speed of mean reversion, and η the variance of the process. That is, we define the process $H_t = \log(C_t)$. Note that we can thus also state that $H_t = h(X_t)$ for a continuous function $h : \mathbb{R}^3 \to \mathbb{R}$.

3.4.1 Calibration to CDS spreads using PDEs

In order to calibrate the model to CDS rates, we need to express the implied risk-neutral survival probabilities in terms of the parameters.

In order to do so, we define the domain $D := \{h \in \mathbb{R} : h > \log(c_\tau)\}$ and denote for all

$(t,h) \in [0,T_i] \times D$ by $\mathbb{Q}_{t,h}$ the risk-neutral probability conditioned on $H_t = h$ and $t < \tau$. The corresponding conditional expectation is denoted by $\mathbb{E}^{\mathbb{Q}}_{t,h}$. That is, the domain is given by the settings for which the CET1 ratio is above the default threshold, and hence the company is not in default. Now we employ a Feynman-Kac type result, which is suggested by Cheridito and Xu (2015), to obtain a partial differential equation (PDE) for $\mathbb{Q}^{CET1}_{t,h}(\tau > T_i)$, $i = 1,\dots,N$. That is, the risk-neutral survival probabilities within the direct CET1 model for several maturities.

Let $i = 1,\dots,N$, and assume there exists a bounded function $g : [0,T_i] \times \bar{D} \to \mathbb{R}$ satisfying the following PDE:

$$\frac{\partial g}{\partial t}(t,h) + [\kappa(\bar{h} - h)]\frac{\partial g}{\partial h}(t,h) + \frac{1}{2}\eta^2 \frac{\partial^2 g}{\partial h^2}(t,h) = 0, \tag{3.4.5}$$

with boundary conditions

$$g(t,h) = 0 \text{ for } h \in \partial D, \quad g(T_i,h) = \mathbb{I}_{\{h \in D\}}, \tag{3.4.6}$$

where the stochastic process H on the interval $[0,T_i]$ is defined as in (3.4.4) with $H_t = h$. Now applying Itô to the process $g(t,H_t)$ gives us:

$$\mathrm{d}g = \left\{ \frac{\partial g}{\partial t}(t,H_t) + [\kappa(\bar{h} - H_t)]\frac{\partial g}{\partial h}(t,H_t) + \frac{1}{2}\eta^2 \frac{\partial^2 g}{\partial h^2}(t,H_t) \right\} \mathrm{d}t + \eta \frac{\partial g}{\partial h}(t,H_t)\mathrm{d}W^2_t.$$

Rewriting this expression to integral form we obtain:

$$g(T_i,H_{T_i}) - g(t,H_t) = \int_t^{T_i} \left\{ \frac{\partial g}{\partial t}(u,H_u) + [\kappa(\bar{h} - H_u)]\frac{\partial g}{\partial h}(u,H_u) + \frac{1}{2}\eta^2 \frac{\partial^2 g}{\partial h^2}(u,H_u) \right\} \mathrm{d}u + \int_t^{T_i} \eta \frac{\partial g}{\partial h}(u,H_u)\mathrm{d}W^2_u.$$

Taking expectations conditional on $\mathcal{F}_t$, we see that the first term of the right-hand side is zero by (3.4.5) and the second term is zero by definition of stochastic integrals. We hence obtain:

$$\begin{aligned} \mathbb{E}^{\mathbb{Q}}_{t,H_t}\left[g(T_i,H_{T_i}) - g(t,H_t)|\mathcal{F}_t\right] &= 0 \\ \Rightarrow g(t,H_t) &= \mathbb{E}^{\mathbb{Q}}_{t,H_t}\left[\mathbb{I}_{\{H_{T_i} \in D\}}\right] \quad \text{for all} \quad (t,H_t) \in [0,T_i] \times D \\ \Rightarrow g(t,H_t) &= \mathbb{Q}^{CET1}_{t,H_t}(\tau > T_i) \quad \text{for all} \quad (t,H_t) \in [0,T_i] \times D, \end{aligned} \tag{3.4.7}$$

where the second step follows from (3.4.6) and the fact that $g(t,H_t)$ is $\mathcal{F}_t$-measurable.

We have proved here that the solution of (3.4.5) with boundary conditions (3.4.6), gives us the value for the risk-neutral survival probability in terms of the model parameters. This allows us to calibrate the direct CET1 model parameters to a term structure of CDS rates.

3.4.2 Hedging CoCos in the direct CET1 model

To prove there exists a CoCo hedging strategy in the CET1 model, we again follow the approach of Cheridito and Xu (2015), adapted to our specification of the state process X_t. We assume there

exists a bank account with return r_t, such that a unit of currency in the back account evolves as $\Pi_t^0 = e^{\int_0^t r_u \mathrm{d}u}$. Next to the bank account, we use three liquid hedging instruments. The prices of the hedging instruments are given by Π_t^j, $j = 1, 2, 3$. Now as the state variables are Markov processes, the values of the CoCo and the hedging instruments at time $t < \vartheta$ can be written as $\Pi(t, X_t)$ and $\Pi^j(t, X_t)$, for deterministic functions Π, Π^j: $[0, T] \times \mathbb{R}^3 \to \mathbb{R}$.

Now the dynamic hedging strategy ξ_t^j, $j = 0, 1, 2, 3$, for $t < \vartheta$, has to satisfy two properties: (i) the value of the hedging portfolio should at any time be equal to the value of the CoCo; and (ii) the sensitivity of the hedging portfolio with respect to the different risk factors should always be equal to the sensitivity of the CoCo value to the risk factors. From Itô's lemma we obtain that these properties can be formalized as:

$$\frac{\partial \Pi}{\partial x^i}(t, X_t) = \sum_{j=1}^{3} \xi_t^j \frac{\partial \Pi^j}{\partial x^i}(t, X_t), \quad i = 1, 2, 3, \quad \text{and} \quad \Pi(t, X_t) = \xi_t^0 \Pi_t^0 + \sum_{j=1}^{3} \xi_t^j \Pi^j(t, X_t). \tag{3.4.8}$$

We need three hedging instruments that can account for the equity risk (X^1), conversion, coupon cancel, and extension risk (X^2), and interest rate risk (X^3). We note that conversion, coupon cancellation, and extension are all driven by the CET1 ratio. As the CET1 ratio is calibrated to (and hence is a function of) CDS rates, and conversion always happens before default in our model, we can use a CDS contract to hedge the conversion, coupon cancel, and extension risk factors. Furthermore, we can use stock shares to hedge the equity risk factor, and interest rate swaps to hedge the interest rate risk factor. We combine these observations with the fact that the coefficients of the SDE for C_t do not depend on S_t, the coefficients of the SDE for r_t do not depend on S_t, and C_t is independent of r_t. This allows us to let Π^1 be the stock S, Π^2 a CDS contract, and Π^3 an interest rate swap. Then for $t < \vartheta$ we can rewrite (3.4.8) to become:

$$\begin{aligned}
\frac{\partial \Pi}{\partial x^1}(t, X_t) &= \xi_t^1 \\
\frac{\partial \Pi}{\partial x^2}(t, X_t) &= \xi_t^2 \frac{\partial \Pi^2}{\partial x^2}(t, X_t) \\
\frac{\partial \Pi}{\partial x^3}(t, X_t) &= \xi_t^3 \frac{\partial \Pi^3}{\partial x^3}(t, X_t) \\
\Pi(t, X_t) &= \xi_t^0 \Pi_t^0 + \sum_{j=1}^{3} \xi_t^j \Pi^j(t, X_t).
\end{aligned}$$

We see that we have here, for any $t < \vartheta$, a system of four equations with four unknowns (ξ_t^j, $j = 0, 1, 2, 3$). This system can hence be solved, proving that the CoCo can be perfectly hedged in this CET1 model, and that we can price the CoCo under the risk-neutral measure $\mathbb{Q}$ using expression (3.1.4) in the direct CET1 model.

3.5 Monte Carlo pricing algorithm

Once the parameters of the models from Section 3.3 and Section 3.4 are calibrated, we can build simulation paths. The general idea is that at each path of the simulation, the discounted pay-off of the CoCo is calculated. Once these pay-offs are averaged over a large number of paths, we obtain an accurate estimate of the value (price) of the CoCo at the pricing date. We simulate G paths for the state variables S_t, C_t, and r_t.

We outline here how we simulate one path for the AT1P and the direct CET1 model. At the starting date $t = 0$, all variables are known and given by:

AT1P model: $A_0 = 1, \widehat{H}_0 = H, E_0 = MC_0/QMVA_0$, where MC_0 and $QMVA_0$ are observed from the market and financial statements, $C_0 = CET1_0/RWA_0$, where $CET1_0$ and RWA_0 are observed from financial statements.

CET1 model: S_0 observed from market, and H_0 (and thus C_0) from calibration.

Furthermore we note that at each next step t, the variable values at the previous steps are known. Moreover, in the AT1P model, the values for $\widehat{H}_t$ and $\sigma_A(t)$ are deterministic and thus known for every $0 \leq t \leq T$. We divide T into M equally spaced intervals of length $\Delta t = 1$ day $= T/M$. Then for $t = 1, \ldots, M$, we perform the following steps iteratively:

AT1P model

1. We draw A_t from the Euler-discretization of (3.3.5), that is:

$$A_t = A_{t-1} \exp\left\{\left(r_{t-1} - q - \frac{1}{2}\sigma_A^2(t-1)\right)\Delta t + \sigma_A(t-1)\sqrt{\Delta t}\varepsilon_t\right\},$$

   where $\Delta t = 1$ day $= T/M$, and $\varepsilon_t \sim \mathcal{N}(0,1)$.

2. We determine E_t as the solution of (3.3.7), calculated using the Crank-Nicolson method as put forward in Appendix B and Appendix E.

3. We draw C_t using (3.3.10), where we use the draws for A_t and E_t computed above.

4. We determine S_t by using $S_t = E_t/O$.

Direct CET1 model

1. We draw S_t from the Euler-discretization of (3.4.3), that is:

$$S_t = S_{t-1} \exp\left\{\left(r_{t-1} - d - \frac{1}{2}\sigma^2\right)\Delta t + \sigma\sqrt{\Delta t}\left(\sqrt{1-\rho^2}\varsigma_t^1 + \rho\varsigma_t^2\right)\right\},$$

   where $\Delta t = 1$ day $= T/M$, and $\varsigma_t^1, \varsigma_t^2 \sim$ i.i.d. $\mathcal{N}(0,1)$.

2. We draw H_t from the Euler-discretization of (3.4.4), that is:

$$H_t = H_{t-1} + \kappa(\bar{h} - H_{t-1})\Delta t + \eta\sqrt{\Delta t}\varsigma_t^2,$$

where Δt and ς_t^2 as above.

3. We determine C_t by using $C_t = e^{H_t}$.

Within each of these simulation paths for C_t and S_t, we can now evaluate the pay-off of the CoCo. The CoCo price is given by the sum of the different components from the expression for the CoCo price (3.1.4). We evaluate these components as follows:

- On every coupon payment date t_i, when $C_{t_i} \geq c_{cc}$ and conversion or redemption has not occurred, the present value of the coupon payment is given by $d_i P e^{-\int_0^{t_i} r_u \mathrm{d}u}$. When $C_{t_i} < c_{cc}$, $\vartheta < t_i$, or $\varphi < t_i$, the present value of the i-th coupon payment is zero.
- When C_t falls below c_ϑ for the first time, and this occurs before maturity T or redemption date φ, we have $t = \vartheta$. At this point the conversion to equity occurs, and the present value of the received equity shares is given by $\left\lfloor \frac{P}{\max\{S_\vartheta, F\}} \right\rfloor S_\vartheta e^{-\int_0^{\vartheta} r_u \mathrm{d}u}$.
- When at a call date t_c we have $C_{t_c} > c_\varphi$, and conversion has not occurred yet, the CoCo is called, and thus $t_c = \varphi$. The CoCo holder then receives his principal P, which has a present value given by $P e^{-\int_0^{\varphi} r_u \mathrm{d}u}$.
- When at maturity T, conversion time ϑ and redemption time φ have not occurred yet, the CoCo holder receives his principal P. This has present value given by $P e^{-\int_0^{T} r_u \mathrm{d}u}$.

Chapter 4

Calibration case studies

In this chapter we apply the methods set out in Chapter 3 to real world examples of AT1 CoCos. To do so we need data on a number of variables. Section 4.1 introduces this data. It starts with giving details on the CoCo contracts we investigate. Then, in Section 4.1.1, we introduce the data used for calibration of the model parameters for both the AT1P and the direct CET1 model. Section 4.1.2 introduces the extra data we use in the AT1P model to translate the structural model to the relevant processes for AT1 CoCos. Section 4.2 provides the results of the calibration procedure for the direct CET1 model. Section 4.3 does the same for the AT1P model.

4.1 Data description

For application of our calibration and valuation approaches, we select two banks that have recently issued a non-dilutive equity conversion AT1 CoCo with a CET1 ratio trigger. We choose ING Group, parent company of ING Bank, the largest banking institution in the Netherlands, and Banco Popular Group, parent company of Banco Popular Espanol, the fourth largest banking group in Spain. We select banks with different credit-worthiness, to evaluate how this affects the calibration and valuation results. ING Group has issued a dollar-denominated AT1 CoCo security on April 16, 2015. Banco Popular Group has issued a euro-denominated AT1 CoCo security on February 6, 2015. See Table 4.1 for details on these issues. Both have a 7.0% CET1 ratio trigger level, and full conversion into equity upon occurrence of the trigger event. Note that both CoCos satisfy the restrictions for AT1 as set out in Section 2.1.

4.1.1 Model calibration

To calibrate the models, we make use of mid CDS curves on subordinated debt of ING and Banco Popular (BP). The CDS quotes are extracted from Bloomberg with maturities $T_N = 2, 3, 4, 5, 7,$ and 10 years. There are shorter maturities available as well, but for the reasons put forward in Section 3.3 we choose to omit these from the calibration procedure. These quotes denote so-called *CDS-spreads*. These spreads are determined by Bloomberg based the following set of

TABLE 4.1: This table shows the details of the CoCo issues by ING Group and Banco Popular Group that form the main research candidates of this study.

	ING Group
Issue date:	April 16, 2015
Name securities:	Perpetual Additional Tier 1 Contingent Convertible Capital Securities
ISIN ID:	US456837AE31
Face value:	$1 bn. in minimum denominations of $200 k.
Maturity:	Perpetual, no fixed maturity or redemption date.
Coupons:	6.000% per annum, payable semi-annually in arrear, for the first 5 years, and the sum of 4.445% and the 5-year Fixed vs. 6M Libor Mid-Market Swap Rate afterwards. Payments occur on April 16 and October 16 in each year.
Day count convention:	30/360.
Coupon cancel options:	Coupon payments can be canceled at sole discretion of the issuer and the regulator.
Callable?	Callable every 5 years on the discretion of the issuer and the regulator, commencing 5 years after issue.
Trigger:	Group CET1 ratio, calculated by the issuer, falling below 7.0% at any time. The regulator can also force conversion.
Conversion mechanism:	Converts into $\lfloor P/(\max\{S_\vartheta, \$9.00, N_\vartheta\})\rfloor$ ordinary equity shares, where P denotes the principal amount, S_ϑ the market price per share on conversion date ϑ, N_ϑ the nominal value per share on the conversion date ϑ, $ 9.00 the floor price, and $\lfloor\cdot\rfloor$ denotes the floor function.*
Seniority:	Unsecured, subordinated AT1.

	Banco Popular Group
Issue date:	February 6, 2015
Name securities:	Additional Tier 1 High Trigger Contingent Convertible Perpetual Preferred Securities
ISIN ID:	XS1189104356
Face value:	$750 mn.
Maturity:	Perpetual, no fixed maturity or redemption date.
Coupons:	8.250% per annum, payable quarterly in arrear, for the first 5 years, and the sum of 8.179% and the 5-year Fixed vs. 6M Euribor Mid-Swap Rate afterwards. Payments occur on January 10, April 10, July 10, and October 10 in each year.
Day count convention:	Actual/Actual.
Coupon cancel options:	Coupon payments can be canceled at sole discretion of the issuer and the regulator.
Callable?	Callable at the discretion of the issuer and the regulator on every coupon payment date, commencing 5 years after issue.
Trigger:	Group CET1 ratio, calculated by the issuer, falling below 7.0% at any time. The regulator can also force conversion.
Conversion mechanism:	Converts into $\lfloor P/(\max\{S_\vartheta, €1.889, N_\vartheta\})\rfloor$ ordinary equity shares, where P denotes the principal amount, S_ϑ the market price per share on conversion date ϑ, N_ϑ the nominal value per share on the conversion date ϑ, €1.889 the floor price, and $\lfloor\cdot\rfloor$ denotes the floor function.**
Seniority:	Unsecured, subordinated AT1.

Notes: * When at conversion the stock is not traded on the stock exchange, S_ϑ drops from the maximum function. The amount of shares received is then solely determined by the nominal value per share and the floor price. The nominal value is expected to always be less than the floor price, and hence will not affect the number of shares received. Furthermore, the floor price is subject to adjustments following events that directly affect or could potentially affect the number of ordinary shares. Such events include consolidation, reclassification, subdivision, issuance, extraordinary (non-cash) dividends, and rights to convert, exchange, subscribe, purchase or otherwise acquire, ordinary shares. These so-called *anti-dilution* adjustments are outside the scope of this study: we always assume that the floor price and the number of ordinary shares remain constant up to conversion, and that the stock is traded on the exchange at conversion.

** Subject to the same conditions as given above for the ING CoCo.

assumptions: (i) the recovery rate is 20%;[16] (ii) the ISDA CDS Fixing Swap Curve is used for discounting the cash flows;[17] and (iii) premium payments occur quarterly. The spread then denotes the per annum percentage of the principal the CDS buyer pays that makes the initial value of the contract zero. We use a monthly dataset, consisting of end-of-month observations. For ING we pick a sample of 103 observed CDS curves from April 2007 until October 2015. This period cannot be taken longer, as short term CDS spreads are not available for ING for earlier dates. For BP we pick a sample of 87 observed CDS curves, from August 2008 until October 2015. Again a longer period is not possible due to lack of data. We purposefully select sample periods that contain different economic circumstances, including recessions. This allows us to examine our models' calibration performance for various types of CDS curves, both including volatile and less volatile times, and higher and lower CDS rates.

Figure 4.1 displays the time series of CDS curves for ING and BP. Figure 4.2 shows benchmark estimates of the corresponding risk-neutral (or $\mathbb{Q}$-) survival probabilities, calculated using a piecewise linear hazard rate function as defined in (4.2.2). These denote the risk neutral probabilities that the firm does not default within the specified maturity. Note that the maturity axis is inverted to ease visual inspection. We find for both banks that during the end of 2011 and halfway 2012 the CDS spreads were the highest, likely as a result of the European sovereign debt crisis. For BP the curve was even inverted at some points. This indicates that the market was very negative about the bank's short-term outlook. However, the market did think that when the bank would survive the first period, it would become more likely that it would survive for a longer period. This is also indicated by the hyperbolic downward shape of the $\mathbb{Q}$-survival probabilities in these periods. However, at most points, we see that the CDS curve is upward sloping and curved, and the $\mathbb{Q}$-survival curve is downward sloping and close to a straight line. Finally, we see that in general BP's CDS spreads are significantly higher than those of ING, indicating that ING overall has a higher credit-worthiness.

For the calibration procedures, we need the ISDA CDS Fixing Swap Curves as well, as Bloomberg uses this curve to discount CDS payments in their quoted spreads. This data is available from Bloomberg at a daily frequency. We obtain monthly end-of-month data for these rates for April 2007 until October 2015. The CDS curves, along with the swap curves, and assumptions on the recovery rate, coupon frequency, and a specification of the risk-neutral survival probabilities for different maturities, allow us to calibrate the parameters of our models.

4.1.2 Link to CET1 ratio in the AT1P model

To construct the link to the CET1 ratio in the structural model, we make use of a cross-sectional set of data on European banks at a single point in time: June 30, 2015. The reasons we pick a single date to perform this analysis are set out in Section 4.3.1. We do realize that picking a single date may make the results sensitive to what date we choose. For this reason, we perform a sensitivity analysis on the regression results in Section 5.4. The variables we consider for

[16] This is a widespread market assumption on the recovery rate on subordinated debt.

[17] This curve represents euro-denominated interest rate swaps. The short end of the curve are Euribor rates, and the long end of the curve is based fixed-versus-6M Euribor swaps.

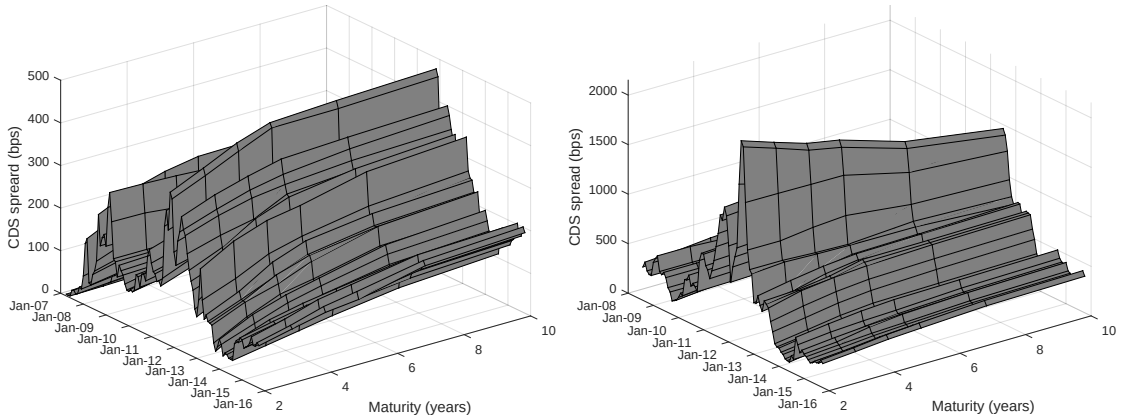

(a) *ING Group* (b) *Banco Popular Group*

FIGURE 4.1: Market observed CDS spreads for different maturities using end-of-month data. For ING (a) the period is April 2007 until October 2015. For Banco Popular (b) the period is August 2008 until October 2015.

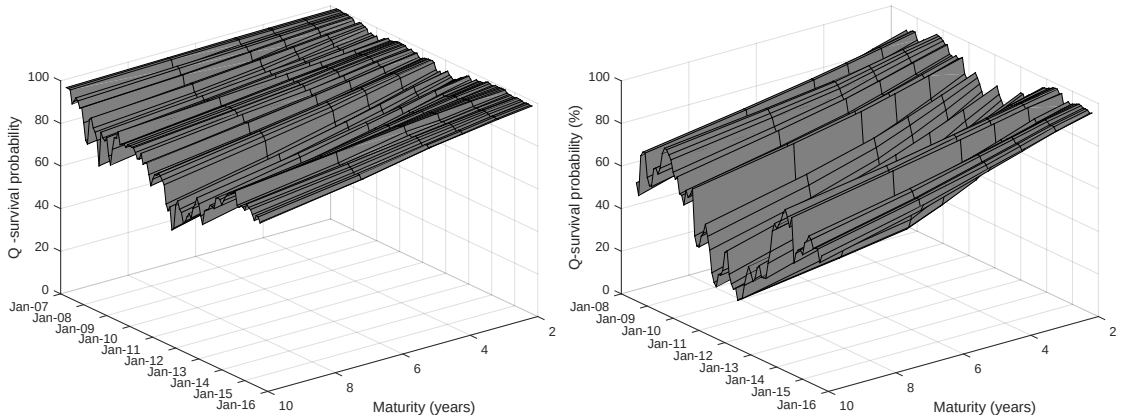

(a) *ING Group* (b) *Banco Popular Group*

FIGURE 4.2: Estimates for the risk-neutral survival probabilities, calculated using the method of O'Kane and Turnbull, as set out in (4.2.2). Calculation is done for different maturities using end-of-month data. For ING (a) the period is April 2007 until October 2015. For Banco Popular (b) the period is August 2008 until October 2015. Note: maturity axis is inverted to ease visual inspection.

the regression analysis are: risk-weighted assets, CET1 capital, market capitalization, and book value of liabilities. The data on risk-weighted assets and CET1 capital is extracted from half-year interim reports. The data on market capitalization is extracted from interim reports and Bloomberg. See Table A.1 in Appendix A for a full list of the 57 banks we use to perform the cross-sectional analysis. These banks are selected both on availability of accurate data, and for having similar exposures to retail and corporate clients. That is, banks with risk profiles comparable to ING and BP.

4.2 Calibration direct CET1 model

In order to calibrate the CET1 ratio model from Section 3.4, we need to solve the PDE from (3.4.5). This is a linear PDE with Dirichlet boundary conditions, which we can solve efficiently using the Crank-Nicolson finite difference method.[18] See Appendix B for elaboration on this method in this context. The default barrier level c_τ is set equal to the minimum CET1 ratio required by the Basel III regulations, i.e. 4.5%. That is, we assume that default occurs when C_t drops to 4.5% before or at maturity, or equivalently when H_t drops to $\log(4.5\%)$. This is a valid assumption, as e.g. EP (2013b) dictates that banks will be forced to enter resolution when their CET1 ratio drops below 4.5%. This assumption also automatically ensures that (3.1.3) holds, as the CoCo conversion threshold is always higher than 4.5%, and C_t is a continuous process.

As for the recovery rate R, present in the expression for the CDS rate given in (3.2.4), we use the 20% assumed in the CDS rates extracted from Bloomberg. Furthermore, the parameter α is given by $1/4$ for the CDS contracts considered. In this setting, we aim to optimize the parameters κ, $\bar{h}$, η, and H_t, to match the term structure of CDS rates as closely as possible. We define an error function, which we minimize using the calibration parameters. However, this minimization poses some problems, as the error function constructed from only CDS rates is nearly flat in certain regions, which causes problems for gradient-based minimization algorithms. This problem is caused by combinations of the model parameters having a similar, or opposite effect on the model outcomes. For example, increasing η drives model CDS rates up, while increasing κ drives model CDS rates down. This implies that there may be multiple combinations of η and κ that result in similar error function value. These interactions and the corresponding stability concerns are assessed in detail in Section 4.2.1 and Section 4.2.2.

Cheridito and Xu (2015) propose a technique to make the parameters better identified. They suggest computing the $\mathbb{Q}$-survival probabilities inferred from the CDS rates using the reduced form method of O'Kane and Turnbull (2003), and add those to the error function as well. That is, as 'actual' risk-neutral survival probabilities are not observed in the market, we use the method of O'Kane and Turnbull as benchmark. This results in the following objective function, which yields more stable minimization results:

$$\min_{\kappa,\bar{h},\eta,H_t} EF_t^{CET1} = \sum_{T_N=2,3,4,5,7,10} \left[\left(\frac{\delta_{t,T_N}^{CET1} - \delta_{t,T_N}^{market}}{\delta_{t,T_N}^{market}} \right)^2 + \left(\frac{\mathbb{Q}_t^{CET1}(\tau > T_N) - \mathbb{Q}_t^{OKT}(\tau > T_N)}{\mathbb{Q}_t^{OKT}(\tau > T_N)} \right)^2 \right], \tag{4.2.1}$$

$$\text{subject to: } \kappa, \bar{h}, \eta, H_t > 0,$$

where the superscripts $CET1$, $market$, and OKT, denote quantities derived using the model from Section 3.4, obtained from the market, and derived using the method of O'Kane and Turnbull, respectively.

For the model quantities, we plug in the expression for the CDS rate from (3.2.4), and for

[18] As noted by Cheridito and Xu (2015), Göing-Jaeschke and Yor (2003) and Alili, Patie, and Pedersen (2005) derive analytical formulas for the hitting time distributions of Ornstein-Uhlenbeck processes. However, due to the cumbersomeness of these expressions, solving numerically is more practical.

the Q-survival probabilities the numerical solutions to the PDEs from (3.4.5), for all relevant maturities T_i. For the market quantities, we plug in the market quotes for the CDS rates for the relevant maturities, as well as the observed zero coupon bond prices $P(t, T_i)$, which occur in (3.2.4). For the O'Kane and Turnbull values, we compute the risk-neutral survival probabilities by calibrating by forward induction a piecewise linear hazard rate function $\lambda(t)$ to the term structure of CDS rates, that is:

$$\mathbb{Q}_t^{OKT}(\tau > t+n) = \begin{cases} \exp\left(-\lambda_{0,2} n\right) & \text{if } 0 < n \leq 2 \\ \exp\left(-2\lambda_{0,2} - \lambda_{2,3}(n-2)\right) & \text{if } 2 < n \leq 3 \\ \exp\left(-2\lambda_{0,2} - \lambda_{2,3} - \lambda_{3,4}(n-3)\right) & \text{if } 3 < n \leq 4 \\ \exp\left(-2\lambda_{0,2} - \lambda_{2,3} - \lambda_{3,4} - \lambda_{4,5}(n-4)\right) & \text{if } 4 < n \leq 5 \\ \exp\left(-2\lambda_{0,2} - \lambda_{2,3} - \lambda_{3,4} - \lambda_{4,5} - \lambda_{5,7}(n-5)\right) & \text{if } 5 < n \leq 7 \\ \exp\left(-2\lambda_{0,2} - \lambda_{2,3} - \lambda_{3,4} - \lambda_{4,5} - 2\lambda_{5,7} - \lambda_{7,10}(n-7)\right) & \text{if } n > 7, \end{cases} \tag{4.2.2}$$

where the λ's are fitted one by one using a root searching algorithm on (3.2.4) minus the relevant CDS market quote. For details on this method see O'Kane and Turnbull (2003).

We minimize (4.2.1) using the `fmincon` function in `MATLAB R2015a`.

4.2.1 Results

Figure 4.3 shows the results of the calibration at every point in our dataset for ING, as well as the fit of the model at the pricing date June 30, 2015. Figure 4.4 shows the same results for BP.

Some observations from Figure 4.3 and Figure 4.4 are the following. The highest point for the CDS spreads and correspondingly the lowest point for the Q-survival probabilities is reached in July 2012 (see also Figure 4.1 and Figure 4.2). This is reflected in low values for H_t and $\bar{h}$, especially for BP. BP shows here a starting CET1 ratio of $C_t = e^{H_t} = e^{2.06} = 7.85\%$, which is only barely above the conversion threshold of 7%. The long run mean estimate at that moment was even below the default threshold at $e^{1.10} = 3.0\%$. However, the speed of mean reversion for BP at this point is very low, implying that the model does not move quickly towards this long run mean. Surprisingly, we find that the variance has a dip at this point as well. This is somewhat counterintuitive as we would expect there to be a lot of uncertainty (and thus volatility) in times where the company is close to default. It can however be explained by a combination of two observations. Firstly, we have that a low volatility parameter is necessary to achieve an inverted CDS curve in this model. This is due to a high volatility parameter drastically increasing the probability of default, especially over longer horizons.

Secondly, we note that the variance of C_t is given by $\frac{\eta^2}{2\kappa}\left(1 - e^{-2\kappa t}\right)$, which goes to $\eta^2/2\kappa$ when t gets large.[19] In general the variance of C_t increases in η and decreases in κ. In Figure 4.4a we

[19] It can be easily shown that the solution of the SDE (3.4.4) for any $t > 0$ is given by $H_t = H_0 e^{-\kappa t} + \bar{h}(1 - e^{-\kappa t}) + e^{-\kappa t}\int_0^t \eta e^{\kappa u} \mathrm{d}W_u^2$, which is normally distributed. Now using the property $\mathrm{Var}\left[\int_0^t e^{au}\mathrm{d}W_u\right] = \int_0^t e^{2au}\mathrm{d}u$, we see that the variance of H_t is given by $e^{-2\kappa t}\eta^2 \int_0^t e^{2\kappa u}\mathrm{d}u = \frac{\eta^2}{2\kappa}\left(1 - e^{-2\kappa t}\right)$. This clearly goes to $\eta^2/2\kappa$ when t gets large.

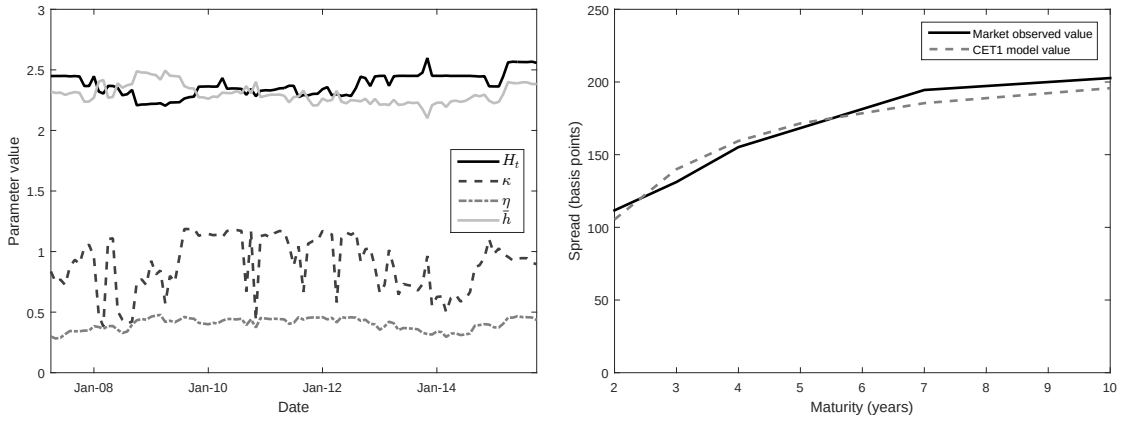

(a) *Optimal parameter values.* (b) *Model implied versus market observed spreads on June 30, 2015.*

FIGURE 4.3: Results of the calibration of the CET1 model for **ING**. Calibration is performed monthly using end-of-month data and the objective function (4.2.1), for the period April 2007 until October 2015. (a) displays the optimal parameter values at every point, and (b) shows the model implied CDS curve versus the market observed curve on the CoCo pricing date June 30, 2015.

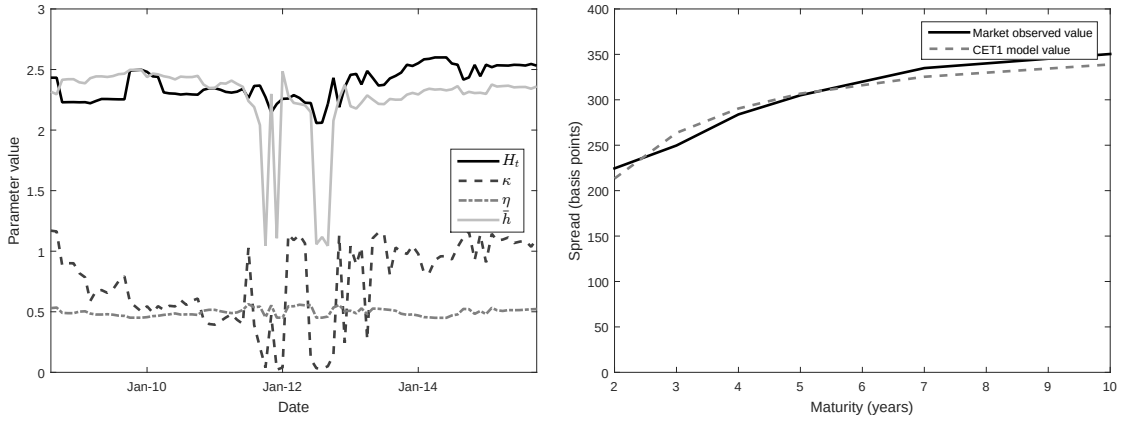

(a) *Optimal parameter values.* (b) *Model implied versus market observed spreads on June 30, 2015.*

FIGURE 4.4: Results of the calibration of the CET1 model for **Banco Popular**. Calibration is performed monthly using end-of-month data and the objective function (4.2.1), for the period August 2008 until October 2015. (a) displays the optimal parameter values at every point, and (b) shows the model implied CDS curve versus the market observed curve on the CoCo pricing date June 30, 2015.

see that during the periods of very high CDS spreads, we have $\eta > \kappa$, while at the majority of the other periods $\kappa > \eta$. This implies that while η is lower in the periods with high spreads, the actual variance of the CET1 ratio is higher here than in other periods.

For ING we observe that higher CDS spreads are reflected in the model parameters mostly through low values for κ. This can be explained, similarly to above, by noting that a lower κ implies a higher volatility for the CET1 ratio, which results in lower probabilities of survival and thus higher CDS spreads. The other parameters remain relatively constant over the sample.

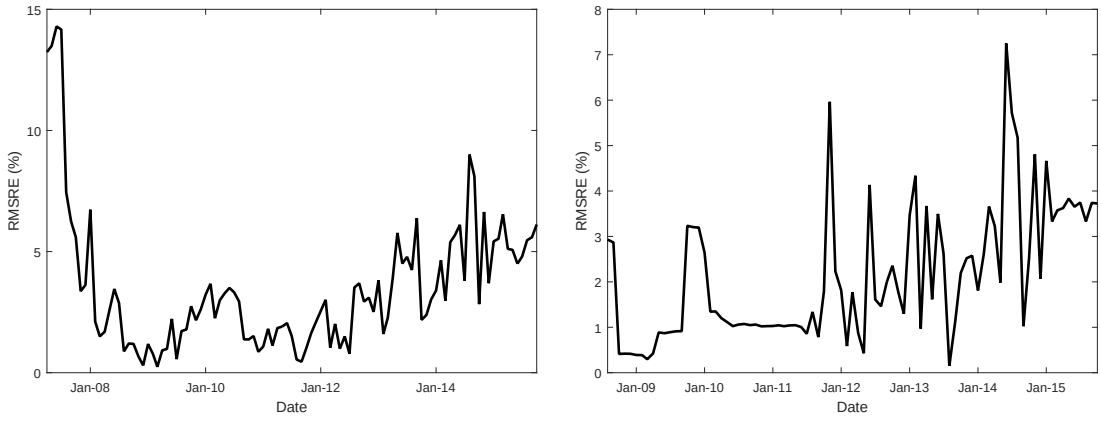

(a) *ING Group* (b) *Banco Popular Group*

FIGURE 4.5: Root Mean Squared Relative Errors, calculated by (4.2.3), of calibrations of the CET1 model performed monthly using end-of-month data and the objective function (4.2.1), for the period April 2007 until October 2015 for ING, and August 2008 until October 2015 for BP. (a) displays the RMSREs for ING Group, and (b) shows the RMSREs for Banco Popular Group.

4.2.2 Evaluation

To evaluate how well the model is able to fit the term structure of CDS spreads, we make use of the Root Mean Squared Relative Error (RMSRE) of the calibrations, which is calculated by:

$$RMSRE = \sqrt{\frac{1}{6} \sum_{N=2,3,4,5,7,10} \left(\frac{\delta^{CET1}_{t,T_N} - \delta^{market}_{t,T_N}}{\delta^{market}_{t,T_N}} \right)^2}. \tag{4.2.3}$$

Figure 4.5 shows how well the CET1 model is able to fit the CDS curves of both banks in terms of the RMSREs.

From Figure 4.5 we see that the fit for BP is better at almost every point in time. In general, we find that the model has a better fit for higher CDS spreads. For the first periods for ING, when the CDS spreads were extremely low, the model fit is bad. At the periods of very high CDS spreads however, the model fits the data fairly accurately. Furthermore, we see that the fit is better for upward sloping, curved CDS term structures. For inverted or flat curves the fit is less accurate, as we can see when comparing Figure 4.1b and Figure 4.5b.

To further assess the calibration behavior of the direct CET1 model, we conduct autocorrelation tests on the calibration error series from Figure 4.5. Presence of autocorrelation in the calibration error series is undesirable, as this would imply that the errors are not independently distributed. Ideally, we want the errors to behave like white noise. This would signal that the calibration captures trends in credit-worthiness, but omits any independent idiosyncratic noise in the CDS rates.

We test the presence of serial correlation with the Ljung-Box test (Ljung and Box, 1978). This test evaluates the null hypothesis H_0 : the data are independently distributed, against the alternative of serial correlation for a specified number of lags. It is a *portmanteau* test. That is, its alternative hypothesis H_a is loosely specified as H_a: the data are not independently distributed;

TABLE 4.2: P-values for the Ljung-Box serial correlation tests for the series of relative calibration errors from Figure 4.5 for ING and Banco Popular. For ING this entails 103 observations in the full sample, from April 2007 until October 2015. For Banco Popular it entails 87 observations in the full sample, from August 2008 until October 2015. The number of lags is set at $l = 10$ in the full sample, and $l = 6$ in the short sample.

	Full sample	Short sample (final 36 months)
ING	2.2×10^{-16}	0.4298
Banco Popular	1.7×10^{-14}	0.5123

Notes: lag selection for the Ljung-Box test based on the rule of thumb from Hyndman and Athanasopoulos (2013).

there exists serial correlation. It does not specify at with lag(s) there is autocorrelation. The Ljung-Box test does require us to pick the number of lags to test. We use the rule of thumb as proposed by Hyndman and Athanasopoulos (2013) for non-seasonal data to determine the number of lags to include. That is, number of lags l is given by $l = \min\{10, \lfloor K/5 \rfloor\}$, where K is the number of observations. In our case this reduces to $l = 10$ for both the ING and the BP error series.

Table 4.2 presents the autocorrelation test results. We observe that both for ING and for BP there is clear evidence of autocorrelation in the calibration error series. This autocorrelation is visible in Figure 4.5 as well, where we observe trends in the error series. These trends are caused, as explained above, by the fact that the direct CET1 model gives a better fit for high CDS rates and upward sloping, curved term structures. This proposes a problem when we want to use these direct CET1 model calibrations to price CoCos over long horizons. This is true as model CoCo prices will clearly be less accurate in periods of low and/or flat/inverted CDS curves. However, as we introduce in Chapter 5, we only price CoCos in the final 7 (for ING) or 9 (for BP) months of the sample. In these small subsamples we find the levels and slopes of the CDS curves to be rather similar, and we thus expect the calibration errors to be much closer to white noise. This implies that the problem of serial correlation is not relevant for the scope of our pricing study.

To verify this, we also perform Ljung-Box tests for smaller subsamples, consisting of the final 2.5 years (36 months) of our original samples. We pick this range as the CDS curves of ING and BP are of comparable level and slope over this range. Following the rule of thumb, we set the number of lags for this analysis at $l = 7$. Table 4.2 provides the results of this analysis. We see that indeed there is no significant evidence to reject the hypothesis of independently distributed errors over this smaller sample. This implies that the direct CET1 model calibration results can safely be used for CoCo pricing over the small sample we consider in Chapter 5. In Section 6.1 we provide a suggestion on how the calibration procedure in the direct CET1 model can be adapted to be more suitable for CoCo pricing over a longer horizon.

On the pricing date June 30, 2015, the parameter estimates are given by:

$$\text{For ING: } C_t = e^{H_t} = 13.0\%, \quad \bar{c} = e^{\bar{h}} = 10.9\%, \quad \kappa = 0.9430, \quad \eta = 0.4666. \tag{4.2.4}$$

$$\text{For BP: } \quad C_t = e^{H_t} = 12.7\%, \quad \bar{c} = e^{\bar{h}} = 10.6\%, \quad \kappa = 1.0674, \quad \eta = 0.5132. \tag{4.2.5}$$

The last reported CET1 ratios stem from the 2015 Q2 report and are given by 12.8% and 12.8% for ING and Banco Popular, respectively. Hence, the calibrated values for H_t lie very close to the actual reported CET1 ratios. This is nice, as this ensures that the simulation paths start at a realistic point. Furthermore, the long run means of around 10-11% agree with what is advised by the regulator as target CET1 ratio.[20] It is hence logical that banks will steer on this target as well.

To analyze the stability of the calibration results of the CET1 model, we look at the value of the objective function (4.2.1) for different combinations of the parameters. We analyze the stability of pairs of two parameters, keeping the other two parameters fixed at their optimal value. Figure C.1 and Figure C.2 in Appendix C show the results of this analysis. Figure C.1a shows that, keeping H_t and $\bar{h}$ fixed, there is a curve of combinations of κ and η that produce a similar value of the objective function. The actual optimal solution is only slightly better than some other combinations. Logically, these combination lie in an increasing line in the $\eta - \kappa$ plane. This can be explained by the argument introduced in Section 4.2: the variance of C_t is $\frac{\eta^2}{2\kappa}\left(1 - e^{-2\kappa t}\right)$, so increasing both η and κ can keep the variance more or less constant. The curved shape of the trend in the $\eta - \kappa$ plane in Figure C.1a is explained by the fact that η is squared in the expression for the variance.

From Figure C.1b we see that the optimal solution in the $H_t - \bar{h}$ plan, keeping κ and η constant, is a lot more stable. There is one combination that clearly yields the lowest objective function. It is logical that we do not see a similar trend here, as H_t and $\bar{h}$ both 'work in the same direction', i.e. increasing both results in lower CDS rates, while decreasing both results in higher rates.

The same holds for H_t and κ, as Figure C.2b displays. These also work in the same direction, which explains the declining line in the $H_t - \kappa$ plane. However, setting both H_t and κ somewhat higher or lower can result in nearly the same objective function value. This also explains the simultaneous kinks in Figure 4.3a for H_t and κ: a slight change in CDS rates can result in the optimal solution to shift upwards for both H_t and κ.

4.3 Calibration AT1P model

As introduced in Section 3.3, we need to derive an expression for the risk-neutral survival probabilities implied by the model of (3.3.4) and (3.3.6), in order to calibrate the parameters to a term structure of CDS rates. See Appendix D for details on the derivation of this expression. The risk-neutral survival probability for any maturity $T > t$ is given by:

$$\mathbb{Q}_t(\tau > T) = \Phi\left(\frac{\log\left(\frac{V_t}{H}\right) + \frac{2L-1}{2}\int_t^T \sigma_A^2(u)\mathrm{d}u}{\sqrt{\int_t^T \sigma_A^2(u)\mathrm{d}u}}\right) - \left(\frac{H}{V_t}\right)^{2L-1}\Phi\left(\frac{\log\left(\frac{H}{V_t}\right) + \frac{2L-1}{2}\int_t^{T_i} \sigma_A^2(u)\mathrm{d}u}{\sqrt{\int_t^T \sigma_A^2(u)\mathrm{d}u}}\right), \tag{4.3.1}$$

where $\Phi(\cdot)$ denotes the cumulative distribution function of the standard Gaussian distribution.

[20] According to the latest Basel publications, the regulators are aiming at a target CET1 ratio of 10-12.5%.

We notice from (4.3.1), that H and V_t only occur as ratio, and never alone. This property allows us to rescale the initial value of the firm to $V_t = 1$, and express H as a fraction of it (Brigo, Morini, and Pallavicini, 2013, Chapter 3). This is practical, as it implies we do not need to know the real initial value of the firm, or its real debt situation, in order to calibrate to CDS rates. It also allows us to rewrite the barrier as in Brigo et al. (2013, Chapter 3), as to provide some more economical intuition behind this barrier:

$$\widehat{H}_t = \frac{H}{A_0}\mathbb{E}_0^{\mathbb{Q}}[A_t]\exp\left(-L\int_0^t \sigma_A^2(u)\mathrm{d}u\right).$$

The basis of this default barrier is the proportion of the expected value of the asset value at time t, controlled by parameter H. This parameters may depend among others on the liability structure, safety covenants, capital regulations, and more general on the characteristics of the capital structure. The benefit of the calibration scheme we employ here, is that we do not have to specify explicitly the derivation of the parameter H. We include it in the calibration procedure, as to extract the market information on this parameter from the CDS rates. The structure of the default barrier is in line with Giesecke (2004), who observes that the fallacies when implementing the simpler Black-Cox model in empirical settings can be explained by the assumption that the total debt grows at a positive rate, similar to the firm value, or that firms have some target leverage ratio (see Collin-Dufresne and Goldstein (2001)). This feature is present in the AT1P model.

Thereby, through the shaping parameter L, it is possible that this basis default barrier is modified to account for the asset volatility (see e.g. Brigo, Morini, and Tarenghi (2010)). $L > 0$ has the interpretation that when volatility increases, which can happen independent from credit quality, the barrier is lowered somewhat, to give the company some more space before entering default.

Furthermore, we need an expression for the value of equity within the model E_t^{AT1P}. See Appendix E for details on the derivation of this expression. Finally, we use the proxy for the CET1 ratio from (3.3.9). Adding this to the objective function ensures that the model produces a starting value for the CET1 ratio that is very close to the actual CET1 ratio, and thus well above the conversion threshold. As for the recovery rate R, present in the expression for the CDS rate given in (3.2.4), we use the 20% assumed in the CDS rates extracted from Bloomberg. Furthermore, the parameter α is given by $1/4$ for the CDS contracts considered.

For the volatilities $\sigma_A(t)$, we use a piecewise constant function consisting of 6 volatility parameters, corresponding to the 6 CDS maturities we are calibrating on. Similar to the O'Kane and Turnbull method from (4.2.2), the first volatility $\sigma_{A,1}$ corresponds to $0 < t \leq 2$, the second $\sigma_{A,2}$ corresponds to $2 < t \leq 3$, and so on. In this setting, we aim to find values for the parameters H, L, and $\sigma_{A,1}, \ldots, \sigma_{A,6}$ which produce a term structure of CDS rates, market value of equity E_t, and CET1 ratio C_t, as close as possible to those observed in the market.

Analogous to the calibration of the direct CET1 model, we add the Q-survival probabilities inferred from the CDS rates using the reduced form method of O'Kane and Turnbull (2003)

to the calibration as well.[21] We hence define an error function, which we minimize using the calibration parameters. The minimization problem is defined as follows:

$$\min_{H,L,\sigma_{A,1},\ldots,\sigma_{A,6}} EF_t^{AT1P} = \sum_{N=2,3,4,5,7,10} \left(\frac{\delta_{t,T_N}^{AT1P} - \delta_{t,T_N}^{market}}{\delta_{t,T_N}^{market}} \right)^2 + \left(\frac{E_t^{AT1P} - E_t^{market}}{E_t^{market}} \right)^2 + \left(\frac{C_t^{AT1P} - C_t^{market}}{C_t^{market}} \right)^2 + \sum_{N=2,3,4,5,7,10} \left(\frac{\mathbb{Q}_t^{AT1P}(\tau > T_N) - \mathbb{Q}_t^{OKT}(\tau > T_N)}{\mathbb{Q}_t^{OKT}(\tau > T_N)} \right)^2, \tag{4.3.2}$$

$$\text{subject to: } 0 < H \leq 1, \text{ and}$$

$$\sigma_{A,1}, \ldots, \sigma_{A,6} > 0,$$

where the superscripts $AT1P$, $market$, and OKT, denote quantities derived using the model from Section 3.3, obtained from the market, and derived using the method of O'Kane and Turnbull, respectively.

For the model quantities, we plug in the expression for the CDS rate from (3.2.4), and for the $\mathbb{Q}$-survival probabilities the expression from (4.3.1), for all relevant maturities T_i. Furthermore, for the equity value we plug in the expression derived in Appendix E. For the CET1 ratio C_t we plug in the proxy from (3.3.9). As for the market quantities, we plug in the market quotes for the CDS rates for the relevant maturities, as well as the observed zero coupon bond prices $P(t, T_i)$, which occur in (3.2.4), the market value of equity as a fraction of the *quasi* firm value, and the reported CET1 ratio.[22] For the O'Kane and Turnbull values, we compute the risk-neutral survival probabilities by calibrating by forward induction a piecewise linear hazard rate function $\lambda(t)$ to the term structure of CDS rates (see Section 4.2).

The calibration procedure outlined above is justified for reasons set out e.g. in Brigo and Tarenghi (2004). We are not interested in estimating the real process of the firm value. We only want to reproduce risk-neutral survival probabilities with a model that is also justifiable economically. While we appreciate the economic interpretation of the model, we are not seeking to sharply estimate the firm value process or its capital structure. We use the structural set-up as a tool for assessing the realism of the calibrations, and to check their economic consequences.

We minimize (4.3.2) using the `fmincon` function in `MATLAB R2015a`.

4.3.1 Results

Before we can initiate the optimization algorithm on (4.3.2), we need to estimate regression (3.3.8). We need the estimated regression parameters to calculate C_t^{AT1P} in (4.3.2). We estimate (3.3.8) using OLS on the dataset of European banks introduced in Table A.1 on June 30, 2015. We choose to investigate this relationship on this single date. This is in contrary to e.g. Brigo et al. (2015), who estimate their model on a number of dates spanning over ten years, and take the average of the parameters of each date to use in their calibration and simulation model. We believe there are some important reasons why their method yields unreliable results.

[21] See Section 4.2 for elaboration hereon.

[22] As we do not know the actual firm value, we use here an approximation given by the sum of the market value of equity and the book value of debt. See Section 3.3.

Firstly, the definition of the CET1 ratio has changed heavily over the recent years. Both the definition of CET1 capital, and the calculation method for the RWA, have changed fundamentally. Therefore, what banks calculated to be their Common Tier 1 ratio ten years ago, is something very different from what is reported recently as CET1 ratio. Secondly, following the global financial crisis, capital requirements have gone up immensely, and subsequently CET1 ratios have increased significantly for banks across Europe. For these reasons we believe we get more reliable results when estimating (3.3.8) at the most recent available data point: June 30, 2015. The results of the OLS estimation are as follows, with t-statistics between parentheses.

$$C_i = \underset{(21.36)}{15.20} - \underset{(-3.490)}{0.1173} \cdot \left(\frac{QMVA_i}{MC_i} \right) + \varepsilon_i, \quad \text{for } i = 1, \ldots, W, \tag{4.3.3}$$

where W denotes the number of banks in the dataset. The R^2 of this regression is 30%.

We hence see that, even though our dataset is not very large, the regression coefficient is strongly significant. Thereby, as expected, we have a negative value for $\hat{\beta}_1$. An important observation on this model is that the value of $QMVA/MC$ will always be larger than one, as $QMVA/MC = 1$ would imply that the bank has zero debt on its balance sheet. This implies, from (3.3.10), that in the AT1P model the CET1 ratio never stays consistently larger than $15.20 - 0.1173 = 15.08\%$. This in contrast to the CET1 model, where the CET1 ratio can grow unrestrained.

Now the fact that we only pick one recent date to estimate the regression model poses problems when attempting to calibrate the AT1P model parameters over the full horizon of CDS data using (4.3.2). The observed CET1 ratios for both ING and BP were very low in the beginning of our samples, and show a consistent upward trend over the sample. The corresponding assets-over-equity values, however, do not show an upward trend. They follow more the trends of the varying credit-worthiness and the economic cycle, also reflected in the CDS curves. This is again explained by noting that the CET1 ratio is an accounting quantity, which has been subject to the vagaries of the changing regulatory landscape over the past decade. Adding both the market value of equity and the CET1 ratio, calculated through (4.3.3), to the objective function, hence yield unreliable and uninterpretable results for periods too long ago.[23]

For this reason, we choose to limit the range on which we calibrate the AT1P model to the periods for which the definition of the CET1 ratio was constant, and the strong upward trend in the reported CET1 ratios was stagnating. This is for both ING and BP around the end of 2012.

Figure 4.6 shows the results of the calibration at every point starting October 2012 for ING. Figure 4.7 shows the same results for BP.

Some observations from Figure 4.6 and Figure 4.7 are the following. From Figure 4.6b we see that $\sigma_{A,1}$ is often the highest. This is necessary to obtain sufficiently high short term CDS spreads. Furthermore, we surprisingly see the volatilities increasing over time, and H decreasing

[23] Note that the problems described here are not directly relevant for the calibration of the direct CET1 model, described in Section 4.2. The calibrated starting CET1 ratios from Section 4.2.1 are indeed not very close to the actual reported CET1 ratios in the beginning of the calibration samples. However, since the actual CET1 ratio and market value of equity are not part of the objective function of the calibration procedure for the direct CET1 model, the calibration results for the direct CET1 model are not distorted by the problems described in this section.

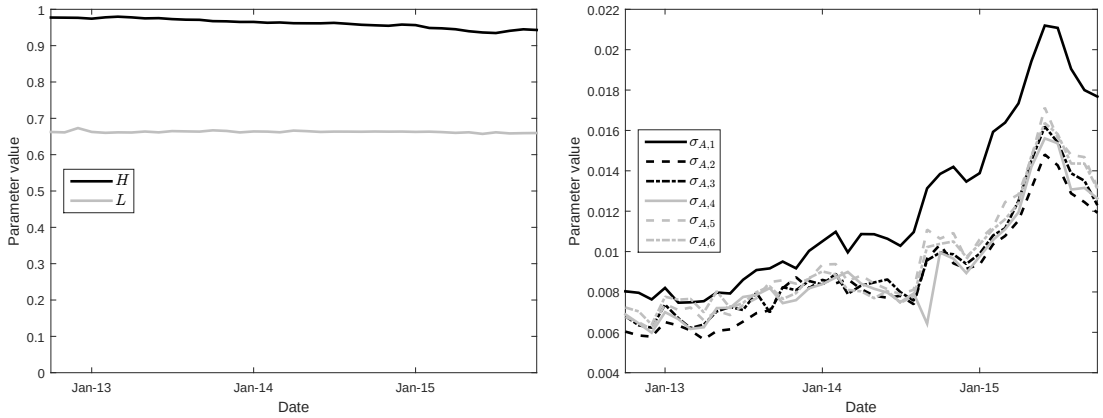

(a) *Optimal parameter values for H and L.* (b) *Optimal parameter values for $\sigma_{A,1}, \ldots, \sigma_{A,6}$.*

FIGURE 4.6: Results of the calibration of the AT1P model for **ING**. Calibration is performed monthly using end-of-month data and the objective function (4.3.2), for the period October 2012 until October 2015. (a) displays the optimal parameter values for the parameters H and L, and (b) shows the optimal parameter values for parameters $\sigma_{A,1}, \ldots, \sigma_{A,6}$.

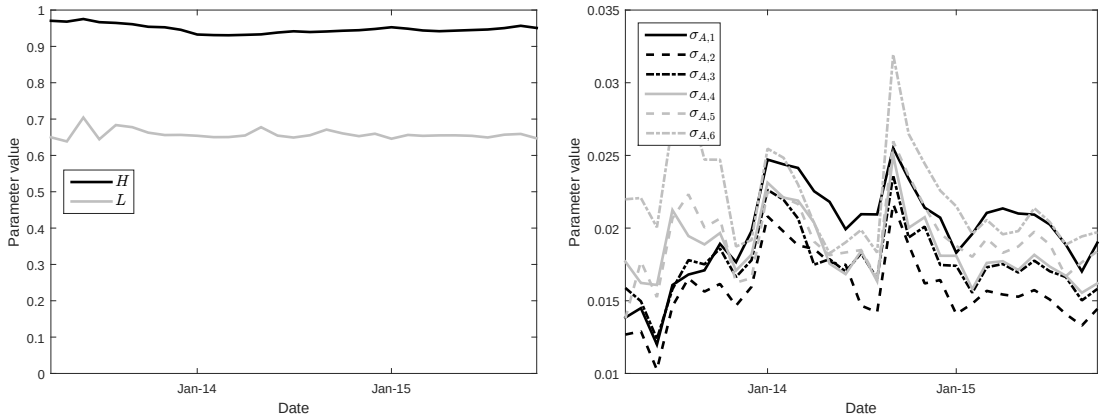

(a) *Optimal parameter values for H and L.* (b) *Optimal parameter values for $\sigma_{A,1}, \ldots, \sigma_{A,6}$.*

FIGURE 4.7: Results of the calibration of the AT1P model for **Banco Popular**. Calibration is performed monthly using end-of-month data and the objective function (4.3.2), for the period October 2012 until October 2015. (a) displays the optimal parameter values for the parameters H and L, and (b) shows the optimal parameter values for parameters $\sigma_{A,1}, \ldots, \sigma_{A,6}$.

over time for ING. This is caused by the presence of the market value of equity as fraction of the total firm value in the objective function. This market value of equity has increased almost monotonically over the past two years. For the model to fit this trend, the parameter H must decrease, as that results in a lower default barrier and consequently a higher market value of equity. However, keeping the volatilities constant, lowering H would result in sharply decreasing CDS spreads, as lowering H drives down the probability of default. In reality, while the trend in CDS spreads was generally decreasing as well over the last years, this effect was less strong, and so the volatilities must increase to achieve the correct CDS rates.

As for the parameter L for ING, we see that this is quite constant at just under 0.7. This

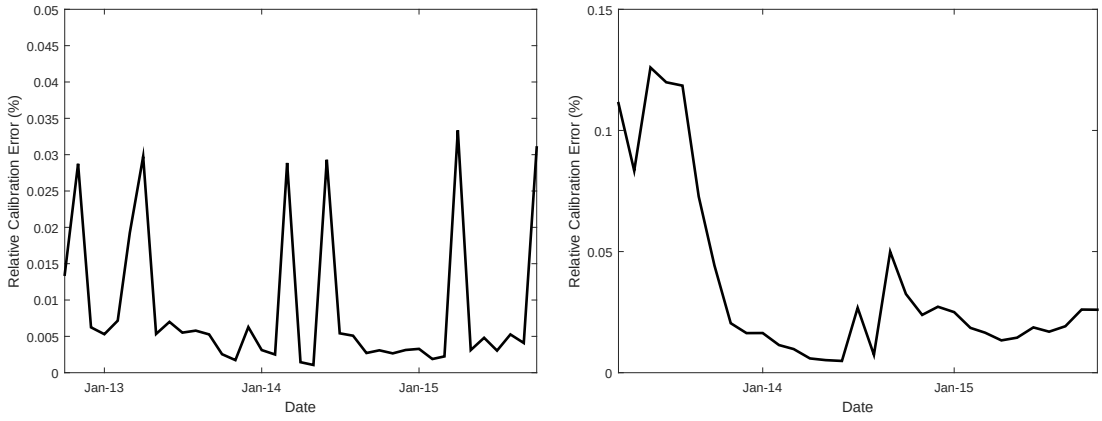

(a) *ING Group* (b) *Banco Popular Group*

FIGURE 4.8: Root Mean Squared Relative Errors, calculated by (4.2.3), of calibrations of the AT1P model performed monthly using end-of-month data and the objective function (4.3.2), for the period October 2012 until October 2015. (a) displays the RMSREs for ING Group, and (b) shows the RMSREs for Banco Popular Group.

implies that the model adjusts to changes in the CDS rates, CET1 ratio, and market value of equity more easily through the volatility parameters, keeping the adjustment parameter L relatively constant. Furthermore, from (3.3.5) and (3.3.6), we note that as $L > 0.5$, the drift of the default barrier is smaller than the drift of the firm value. This feature helps the model in obtaining the curved shape of the CDS curves.

From Figure 4.7 we can make similar observations for BP. The market value of equity saw an increase from begin 2013 up to begin 2014, and a decrease afterwards. This is reflected in the calibrated values of H. Then given these values for H, the CDS curves are replicated by tweaking the volatility parameters. The shaping parameter L is again relatively steady, signaling that the model tweaks its outcomes more easily through the volatility parameters, while L assists in obtaining the correct shape of the CDS curves. Logically, we see that the volatilities for BP are higher than those of ING, as BP's CDS rates are higher as well.

4.3.2 Evaluation

To evaluate how well the model is able to fit the term structure of CDS spreads, we again make use of the RMSRE of the calibrations. RMSREs are calculated equivalently using (4.2.3), replacing the direct CET1 implied CDS spreads by the AT1P implied CDS spreads.

Figure 4.8 shows how well the AT1P model is able to fit the CDS curves of both banks in terms of the RMSREs.

Observing Figure 4.8 we see that the calibration errors are far lower than those of the direct CET1 model. This is simply explained by the fact that the AT1P model has 8 free fitting parameters, while the direct CET1 model has only 4. This larger overfit of the AT1P model yields a better in sample fit by definition. It does not make sense to analyze the time series of RMSREs for the AT1P model in much detail, as the differences are driven mostly by discrepancies in the minimization algorithm. The algorithm stops when the objective function values of consecutive

steps are less than 1^{-4} apart. That is, the differences in RMSREs lie in the region where the algorithm hits its tolerance. They are thus not driven by the calibration behavior of the AT1P model, but by the termination conditions of the minimization algorithm.

Basically, the AT1P model can perfectly fit a term structure of CDS spreads through its six volatility parameters, while H and L are used to obtain a fit on E_t and C_t as well. Equivalently to the O'Kane and Turnbull procedure from (4.2.2), the AT1P model can fit the first maturity CDS rate using $\sigma_{A,1}$, then the second maturity using $\sigma_{A,2}$, and so on. While the AT1P model thus obtains a better in sample fit than the direct CET1 model, this does not imply it produces more accurate CoCo prices as well. The AT1P model could be fitting a lot of noise, impeding its CoCo pricing strength. Whether this is the case is investigated in Chapter 5.

Chapter 5

Pricing case studies

To examine the strength of the two pricing models introduced and calibrated before, we use them to price the CoCos from Table 4.1 at different points in time. Comparing the model-implied CoCo values with market observed prices serves as an out-of-sample test of our pricing models. It examines how well the models translate relevant market views from CDS and equity markets into CoCo values. Note that both models, and especially the AT1P model, are largely overfitted, as they contain a lot of parameters compared to the amount of market observed quantities they are calibrated on. This would pose big problems when we would want to use the models to forecast prices. However, our out-of-sample test does not include forecasting a future CoCo price, but just examining whether the models can translate the information from the credit and equity market into the CoCo price at the same instant. For this purpose, the overfit is not a problem.

Furthermore, we analyze how the price is affected by the coupon cancel and call thresholds, and how this price can be contributed to the different CoCo components. As the Banco Popular CoCo was issued in February 2015 and we use end-of-month data, we price this CoCo on nine dates: February 27 up to October 30, on every last day of the month. The ING CoCo was issued in April 2015, and hence we price it on seven moments: April 30, 2015 up to October 30, 2015, on every last day of the month.

Before we can initiate the CoCo pricing algorithm as put forward in Section 3.5, we first have to determine parameter values for the parameters that are not calibrated in Chapter 4. For the AT1P model, this parameter is the 'correlation' parameter ϱ between the CET1 ratio and the assets-over-equity ratio. For the CET1 model, these parameters are the correlation between the Brownian motions governing the variability in the stock price and the CET1 ratio, ρ, and stock volatility σ.

So far, we have ignored the pay-out rate parameters q in AT1P model, and d in the direct CET1 model. As there exist no apparent methods to estimate these parameters in a robust way, we opt to set it equal to zero in the initial pricing analysis in this section. In Section 5.4 we analyze the sensitivity of the CoCo price for the pay-out rate by running scenarios on it.

As for the coupon cancel threshold c_{cc} and the CoCo call threshold c_{φ}, we examine consis-

tency conditions among the different pricing dates. That is, we investigate what combination of market views of c_{cc} and c_{φ}, consistent over time, are implied by each model. Then we evaluate these combinations on their economic interpretation and realism, to compare the relative strength of both models.

As for the risk-free rate process r_t, we opt use a fixed value at each pricing date. For the sake of tractability of the study we do not fit a stochastic model for the short rate. At each pricing date, we use the 10 year maturity point of the Overnight Indexed Swap (OIS) curve as relevant risk-free rate.[24]

We choose to use $G = 10,000$ paths for obtaining the approximated CoCo price in each setting. We find that for this relatively small number, the CoCo price is already stable, and confidence intervals are sufficiently small. While more paths obviously yields more accurate results, computation time limits us from doing so. We need to evaluate CoCo prices for a lot of different settings. Hence, setting the amount of paths per price higher, vastly increases the total computation time up to infeasible levels.

Section 5.1 describes the execution of the steps introduced above for the CET1 model. Section 5.2 does the same for the AT1P model.

5.1 Pricing in the direct CET1 model

Before we can examine the CoCo pricing strength of the CET1 model, we need to specify the stock volatility parameter σ, the (constant) annualized volatility of the stock return. We use the 10-year Bloomberg implied volatility for this extent. That is, the volatility implied from at-the-money call options on the stock. Bloomberg uses a series of different techniques to obtain this implied volatility. For elaboration on these techniques see Bloomberg (2014). As there is no liquid market for options of a maturity of 10 years, Bloomberg uses an extrapolation technique, also described in aforementioned document.

As for the correlation ρ between the Brownian motions W_t^1 and W_t^2 from (3.4.2) and (3.4.4), we are forced to make use of an intuitive argument. Estimating the correlation is not possible due to the very low frequency of available CET1 ratio data. Therefore we argue as follows. Firstly, the correlation must clearly be positive. When the bank's capital ratio deteriorates, and thus the bank moves towards conversion, this will have a negative impact on the stock price. This is true since a declining CET1 ratio signals a declining credit-worthiness, which drives the stock price down. Thereby, both the market and CoCo issuers clearly assume that any conversion will entail a significant loss in value for the investor, judging from the high coupon rates on CoCos. Conversion only entails a significant loss in value when the stock price at conversion S_ϑ is below the floor price F, which is already significantly below the actual stock price at the issue date for both CoCos considered. This implies that a declining CET1 ratio will always be accompanied by a declining stock price. Moreover, the actual announcement of a CoCo conversion is likely to

[24] The OIS curves denote the fixed rates for fixed-versus-floating swap contracts where the floating leg is the overnight rate. We use the Libor variant for the dollar-denominated ING CoCo, and the Euribor variant for the euro-denominated Banco Popular CoCo. The data is extracted from Bloomberg. These curves are market standards to use as risk-free term structures.

TABLE 5.1: This table shows the prices (as percentage of the principal) of the CoCos from Table 4.1, issued by ING Group on April 16, 2015, and by Banco Popular Group on February 2, 2015, on a number of end-of-month pricing dates. Thereby, it shows the calibrated parameter values H_t, $\bar{h}$, κ, and η, the stock volatility σ, stock price S_t, and risk-free rate r, to be used in the pricing algorithm. These are all values used for pricing the CoCo in the CET1 model.

					ING Group			
t	$CoCo_t^{market}$	S_t (\$)	r (%)	σ (%)	H_t	$\bar{h}$	κ	η
October 30, 2015	100.350	14.582	1.985	30.41	2.5576	2.3832	0.8948	0.4346
September 30, 2015	97.250	14.145	1.743	31.66	2.5678	2.3834	0.9091	0.4557
August 31, 2015	98.500	15.288	1.985	31.16	2.5642	2.3969	0.9446	0.4582
July 31, 2015	100.625	17.044	2.046	28.78	2.5647	2.3972	0.9459	0.4588
June 30, 2015	100.250	16.518	2.185	28.37	2.5657	2.3893	0.9430	0.4666
May 29, 2015	100.300	16.432	2.057	27.40	2.5673	2.3915	0.9268	0.4547
April 30, 2015	99.950	15.470	1.928	27.70	2.5619	2.3993	0.9566	0.4551

					Banco Popular Group			
t	$CoCo_t^{market}$	S_t (€)	r (%)	σ (%)	H_t	$\bar{h}$	κ	η
October 30, 2015	98.661	3.741	0.6580	34.95	2.5318	2.3602	1.1027	0.5223
September 30, 2015	96.532	3.259	0.7050	36.00	2.5457	2.3415	1.0364	0.5203
August 31, 2015	99.729	3.804	0.8570	36.01	2.5328	2.3558	1.0861	0.5172
July 31, 2015	101.897	4.160	0.7480	35.82	2.5375	2.3554	1.0787	0.5138
June 30, 2015	99.486	4.326	0.8875	35.80	2.5389	2.3528	1.0674	0.5132
May 29, 2015	101.634	4.490	0.5950	35.07	2.5324	2.3663	1.1135	0.5140
April 30, 2015	102.255	4.668	0.4250	35.62	2.5336	2.3634	1.0959	0.5067
March 31, 2015	103.944	4.541	0.2910	35.48	2.5349	2.3595	1.0887	0.5126
February 27, 2015	103.178	4.098	0.4330	36.01	2.5192	2.3759	1.1436	0.5324

Notes: In February and March the ING CoCo was not yet listed. Therefore there are only seven pricing dates for the ING CoCo, whereas the Banco Popular CoCo has nine pricing dates. As for the risk-free rates r, we use the 10 year maturity points from Overnight Indexed Swap (OIS) curves. These curves denote the fixed rates for fixed-versus-floating swap contracts where the floating leg is the overnight rate. We use the Libor variant for the dollar-denominated ING CoCo, and the Euribor variant for the euro-denominated Banco Popular CoCo.

entail an extra downward shock to the stock price.

Another argument for the above assumption lies in CoCo hedging strategies. CoCo investors may opt to hedge their positions, especially when conversion comes closer, by taking a short position in the bank's stock. This way they are protected against the fact that they may be forced to buy stock at a relatively high price at conversion. These short position however may in turn drive the stock price further down. All arguments presented here advocate a strong positive correlation between movements in the CET1 ratio and movements in the stock price. Therefore we set this parameter at $\rho = 0.9$. Section 5.4 investigates the sensitivity of this choice on model CoCo prices.

Table 5.1 displays the CoCo prices (as percentage of the principal) of the CoCos from Table 4.1, at the different pricing dates. Furthermore, it summarizes the values we use for each relevant parameter in the CoCo pricing approach under the direct CET1 model.

5.1.1 Pricing behavior

Figure 5.1 and Table 5.2 display some charts and tables to get a feeling of the CoCo pricing behavior of the CET1 model. It shows the CET1 model CoCo price for different combinations of c_{cc} and c_{φ}. Furthermore, it shows how the different components (stocks, principal, and coupons) contribute to this price. For each combination of c_{cc} (x-axis) and c_{φ} (y-axis) the color gives the corresponding price (in Figure 5.1a) or relative contribution (in Figure 5.1b, Figure 5.1c, and Figure 5.1d). The legends on the right side of the charts give the values corresponding to the colors.

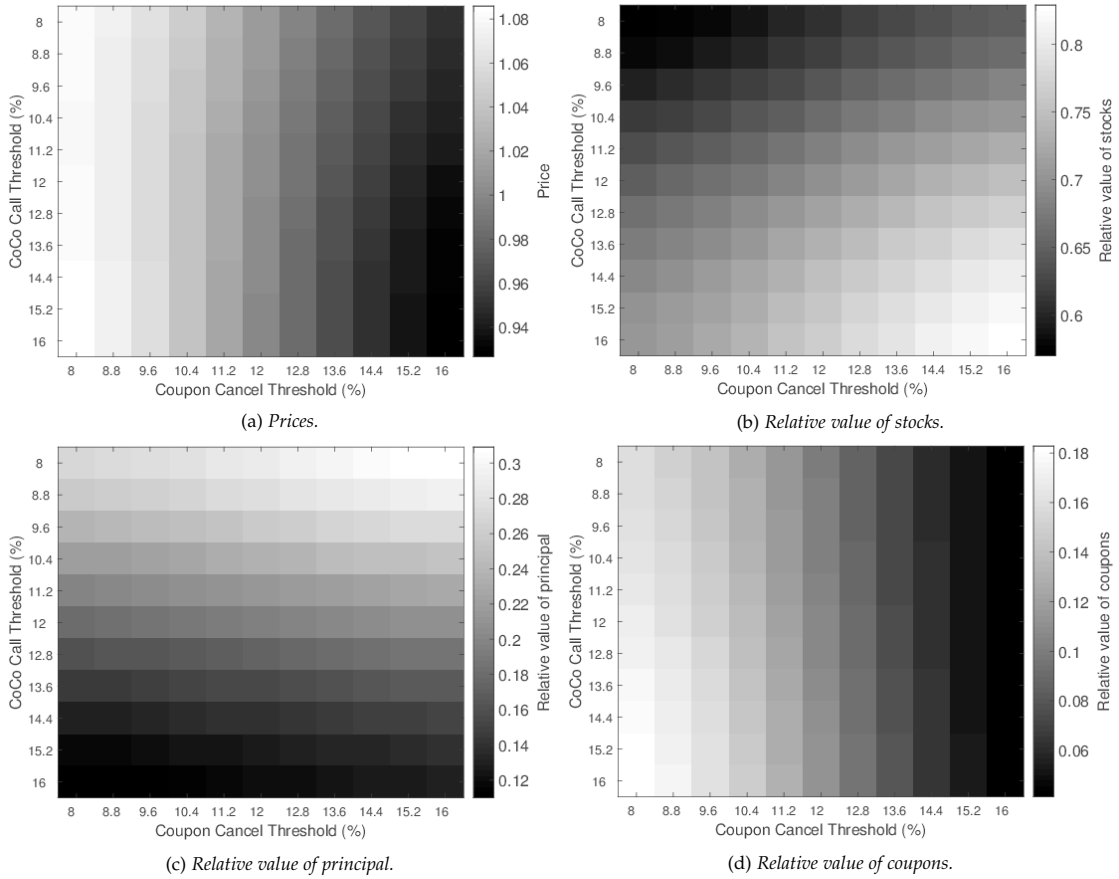

(a) *Prices.*

(b) *Relative value of stocks.*

(c) *Relative value of principal.*

(d) *Relative value of coupons.*

FIGURE 5.1: Results of the CoCo pricing procedure for the ING CoCo on June 30, 2015, using the parameter values for the CET1 model from Table 5.1 and $G = 10,000$ simulation paths per combination of c_{cc} and c_{φ}. Pricing is done using a range of different values for the coupon cancel threshold c_{cc} and the CoCo call threshold c_{φ}. Panel (a) shows the resulting CoCo prices. Panel (b), (c), and (d) show the proportion of this price that can be attributed to the potential value of stocks received, principal received, and coupon payments, respectively.

Figure 5.1a and Table 5.2 show that, as we would expect, the CoCo price decreases in c_{cc}. Logically, when more coupon payments are canceled, the CoCo price decreases. Furthermore, the price decreases in c_{φ} as well, be it more gradual. This is the so-called extension risk introduced in Section 2.1 and in De Spiegeleer and Schoutens (2014). When the CoCo call threshold is higher, the CoCo is redeemed less often. This implies that there is more often a longer period

TABLE 5.2: Price variation of the ING CoCo for different values of the coupon cancel and call thresholds in the CET1 model. Pricing done on June 30, 2015, where we recall that the market price of the CoCo was 1.0025 per unit of notional.

c_{cc} (%)	c_{φ} (%)	Estimated price	95% confidence interval
9	9	1.0690	[1.0668; 1.0712]
	10	1.0679	[1.0657; 1.0702]
	11	1.0675	[1.0651; 1.0698]
	12	1.0673	[1.0659; 1.0697]
10	9	1.0513	[1.0490; 1.0535]
	10	1.0498	[1.0475; 1.0521]
	11	1.0488	[1.0464; 1.0512]
	12	1.0479	[1.0455; 1.0504]
11	9	1.0312	[1.0290; 1.0335]
	10	1.0293	[1.0270; 1.0316]
	11	1.0277	[1.0253; 1.0301]
	12	1.0260	[1.0236; 1.0285]
12	9	1.0100	[1.0078; 1.0122]
	10	1.0076	[1.0054; 1.0099]
	11	1.0055	[1.0031; 1.0078]
	12	1.0030	[1.0006; 1.0054]

of possible conversion to equity, and that the present value of the potential principal payment decreases due to time-value of money. Both are factors that drive down the CoCo price. We do notice that this effect is weaker for low values of the coupon cancel threshold. When this threshold is low, extension implies more coupons being payed out, counteracting the previously mentioned effects.

Figure 5.1b shows that the relative contribution of stocks grows in c_{cc} and in c_{φ}. This is logical, as a higher c_{cc} implies more coupons are canceled and thus coupon payments contribute less to the CoCo value. A higher c_{φ} implies the CoCo is extended more often, giving more time and thus a higher probability of conversion to stocks. Furthermore, we notice the extremely high relative contribution of stocks, ranging from 60-80% of the CoCo value. This implies that in the CET1 model CoCo conversion occurs very often.

Figure 5.1c is straightforward. More canceled coupons drive up the relative value of the principal. When the coupon is extended more often, the probability that the principal is returned, as well as the present value of the principal when returned goes down, both decreasing the relative contribution of the principal.

Figure 5.1d is straightforward as well. More canceled coupons drive down the relative contribution of coupon payments. And more extensions increases the average amount of coupons received, driving up the relative contribution of coupon payments.

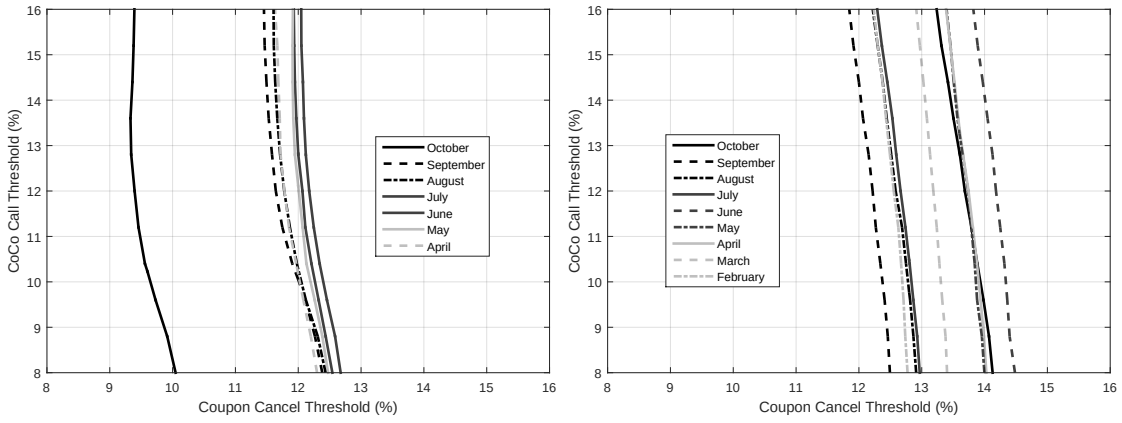

(a) *ING Group* (b) *Banco Popular Group*

FIGURE 5.2: Combinations of the coupon cancel threshold c_{cc} and the CoCo call threshold c_{φ} that make the CET1 model implied CoCo price equal to the market observed price. For the model parameters and the market observed prices we use the values from Table 5.1. The pricing dates are the last days of the months mentioned in the legends.

5.1.2 Comparison to observed market prices

Now we move on to comparing the results from our pricing algorithm to the market observed prices on the different pricing dates. Using the settings from Table 5.1, we again evaluate the CoCo price for different combinations of the CoCo call threshold c_{φ} and the coupon cancel threshold c_{cc}. Instead of displaying the whole range, we now determine which combinations of c_{φ} and c_{cc} make the CET1 model implied CoCo price equal to the market observed price on each of the pricing dates. Figure 5.2 shows the results of this analysis for both the ING and the Banco Popular CoCo.

In a perfect pricing model, the contour lines for the different pricing dates would all intersect in one unique point: the point that gives the actual values (or what the market believes the actual values are) for the CoCo call threshold and the coupon cancel threshold. Furthermore, we note that there is no clear reason to believe that the market has shifted it views on the values of c_{cc} and c_{φ} over the course of 2015. Therefore we assume that any deviation from the 'perfect intersection' is caused by inconsistency of the pricing model in translating the information from the credit and equity market into the CoCo price. Or, broader, the incapability of models based solely on credit and equity markets to explain CoCo prices.

From Figure 5.2a we see that the CET1 model is quite consistent for the ING CoCo. The contour lines, except one, lie very close to each other. Furthermore, it again shows that the CoCo price is not very sensitive to the amount of extension risk. When comparing e.g. $c_{\varphi} = 16\%$ and $c_{\varphi} = 8\%$ (or their difference Δ_{φ}=8%), the difference in the corresponding values for c_{cc} making the model price equal to the market price is way smaller (around 12%-12.5%, or $\Delta_{cc} = 0.5\%$, on average). Furthermore we note that the values for c_{cc} making the model price equal to the market price are very high. It seems unrealistic that coupon payments will be canceled when the CET1 ratio is 12%. This observation leads us to believe that the market prices are driven down by some other factor(s), not included in the CET1 model.

Figure 5.2b strengthens this idea. It shows, firstly, that the CET1 model is not very consistent for the Banco Popular CoCo. The contour lines show quite some dispersion, and do not have a lot of common intersections. Thereby, the values for the coupon cancel threshold need to be even higher than for the ING CoCo, to make the model price equal to the market price. As it is unrealistic that coupons will be canceled at a CET1 ratio of over 13%, this gives us strong evidence that there exists some factor, not included in the CET1 model, that the market considers that drives down CoCo prices.

5.2 Pricing in the AT1P model

To price CoCos in the AT1P model, we first need to specify the 'correlation' parameter $\varrho \in [0,1]$ between the CET1 ratio and the assets-over-equity ratio. Note that as we have $\hat{\beta}_1 < 0$, the actual correlation between the CET1 ratio and the assets-on-equity ratio is $-\varrho$. It is logical that this is a negative value, as we expect both the CET1 capital to have a strong positive correlation with the equity value, and the RWA to have a strong positive correlation with the asset value. This would imply a negative relation between the CET1 ratio and the assets-on-equity ratio. Thereby, an increasing assets-over-equity ratio clearly indicates deterioration of the bank's credit-worthiness: the bank moves towards default. This will be accompanied by a decreasing CET1 ratio. For these reasons, we set this parameter at $\varrho = 0.9$. Section 5.4 investigates the sensitivity of this choice on model CoCo prices.

Table 5.3 displays the CoCo prices (as percentage of the principal) of the CoCos from Table 4.1, at the different pricing dates. Furthermore, it summarizes the values we use for each relevant parameter in the CoCo pricing approach under the AT1P model.

At every pricing date we assume the number of shares outstanding to remain equal to its initial value over the remaining term. We need this number of shares, combined with the initial QMVA, to calculate the stock price at conversion through $S_\vartheta = (E_\vartheta \cdot QMVA_t)/O_t$. Here we note that E_ϑ is a ratio over the initial QMVA.

5.2.1 Pricing behavior

Figure 5.3 and Table 5.4 display some charts and tables to get a feeling of the CoCo pricing behavior of the AT1P model. It shows the AT1P model CoCo price for different combinations of c_{cc} and c_φ. Furthermore, it shows how the different components (stocks, principal, and coupons) contribute to this price. The interpretation of the graphs is as explained in Section 5.1.1.

Starting at the graphs for the relative contribution of the components, Figure 5.3b, Figure 5.3c, and Figure 5.3d, we can make the same observations as in Section 5.1.1. However, in the AT1P model the changes are a lot sharper and less gradual, and there is almost no variability in the extreme cases for c_{cc} and c_φ. This difference is caused by the fact that there is a lot less variability in the CET1 ratio in the AT1P model, compared to the direct CET1 model. The fact that the relative contribution of stocks is a lot lower in the AT1P model, and thus conversion occurs a lot less often, confirms this observation.

TABLE 5.3: This table shows the prices (as percentage of the principal) of the CoCos from Table 4.1, issued by ING Group on April 16, 2015, and by Banco Popular Group on February 2, 2015, on a number of end-of-month pricing dates. Thereby, it shows the calibrated parameter values H, L, and $\sigma_{A,1}, \ldots, \sigma_{A,6}$, and equity E_t as ratio of the initial QMVA, the quasi-market value of assets $QMVA_t$ (in mn.), CET1 ratio C_t, number of shares outstanding O_t (in mn.), and risk-free rate r, to be used in the pricing algorithm. These are all values used for pricing the CoCos in the AT1P model.

	ING Group								
t	$CoCo_t^{market}$	E_t (%)	C_t (%)	O_t	$QMVA_t$ ($)	r (%)	H	L	$[\sigma_{A,1}, \ldots, \sigma_{A,6}]$
October 30, 2015	100.350	5.823	12.60	3870	968,892	1.7430	0.9431	0.6596	[0.0177, 0.0119, 0.0123, 0.0126, 0.0132, 0.0131]
September 30, 2015	97.250	5.661	12.60	3870	967,228	1.7430	0.9450	0.6592	[0.0180, 0.0124, 0.0135, 0.0132, 0.0147, 0.0144]
August 31, 2015	98.500	6.089	12.67	3869	971,635	1.9850	0.9408	0.6585	[0.0191, 0.0129, 0.0139, 0.0131, 0.0148, 0.0144]
July 31, 2015	100.625	6.738	12.73	3869	978,400	2.0460	0.9347	0.6615	[0.0211, 0.0143, 0.0154, 0.0154, 0.0156, 0.0158]
June 30, 2015	100.250	6.581	12.80	3868	967,770	2.1850	0.9363	0.6572	[0.0212, 0.0148, 0.0162, 0.0156, 0.0171, 0.0164]
May 29, 2015	100.300	6.171	13.20	3866	1,029,400	2.0570	0.9397	0.6616	[0.0194, 0.0131, 0.0145, 0.0142, 0.0146, 0.0148]
April 30, 2015	99.950	5.540	13.60	3864	1,079,055	1.9280	0.9452	0.6600	[0.0173, 0.0115, 0.0125, 0.0119, 0.0128, 0.0124]

	Banco Popular Group								
t	$CoCo_t^{market}$	E_t (%)	C_t (%)	O_t	$QMVA_t$ ($)	r (%)	H	L	$[\sigma_{A,1}, \ldots, \sigma_{A,6}]$
October 30, 2015	98.661	5.093	12.65	2119	155,676	0.6580	0.9507	0.6470	[0.0190, 0.0144, 0.0158, 0.0162, 0.0184, 0.0197]
September 30, 2015	96.532	4.466	12.65	2119	154,655	0.7050	0.9567	0.6591	[0.0170, 0.0133, 0.0150, 0.0156, 0.0177, 0.0194]
August 31, 2015	99.729	5.148	12.58	2119	156,616	0.8570	0.9503	0.6570	[0.0189, 0.0141, 0.0166, 0.0167, 0.0167, 0.0189]
July 31, 2015	101.897	5.574	12.52	2119	158,176	0.7480	0.9465	0.6494	[0.0202, 0.0151, 0.0170, 0.0173, 0.0189, 0.0204]
June 30, 2015	99.486	5.754	12.45	2119	159,334	0.8875	0.9450	0.6539	[0.0209, 0.0157, 0.0178, 0.0182, 0.0197, 0.0214]
May 29, 2015	101.634	5.908	12.43	2117	160,880	0.5950	0.9434	0.6552	[0.0210, 0.0153, 0.0169, 0.0171, 0.0187, 0.0198]
April 30, 2015	102.255	6.076	12.42	2115	162,455	0.4250	0.9418	0.6551	[0.0214, 0.0154, 0.0175, 0.0177, 0.0183, 0.0196]
March 31, 2015	103.944	5.870	12.40	2112	163,385	0.2910	0.9438	0.6539	[0.0210, 0.0157, 0.0173, 0.0176, 0.0193, 0.0206]
February 27, 2015	103.178	5.374	12.10	2108	160,771	0.4330	0.9487	0.6564	[0.0196, 0.0148, 0.0156, 0.0158, 0.0180, 0.0196]

Notes: In February and March the ING CoCo was not yet listed. Therefore there are only seven pricing dates for the ING CoCo, whereas the Banco Popular CoCo has nine pricing dates. As for the risk-free rates r, we use the 10 year maturity points from Overnight Indexed Swap (OIS) curves. These curves denote the fixed rates for fixed-versus-floating swap contracts where the floating leg is the overnight rate. We use the Libor variant for the dollar-denominated ING CoCo, and the Euribor variant for the euro-denominated Banco Popular CoCo.

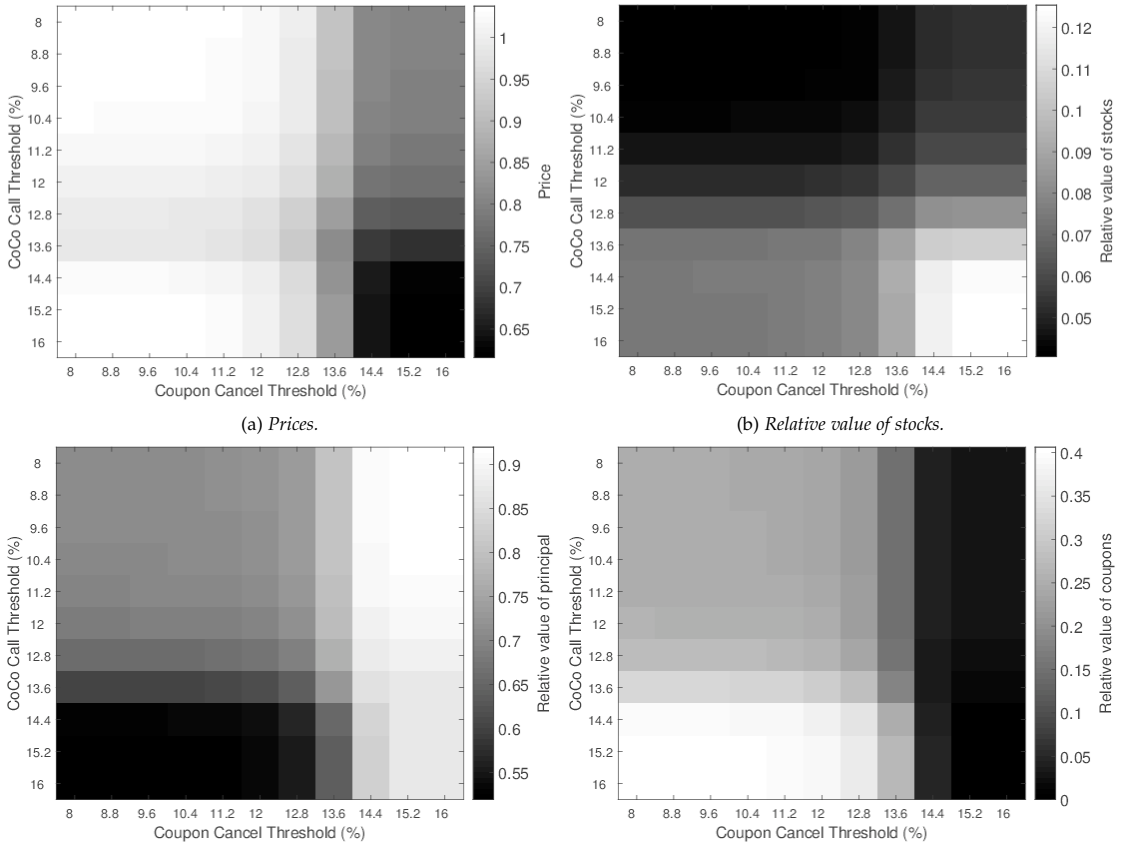

(a) *Prices.*

(b) *Relative value of stocks.*

(c) *Relative value of principal.*

(d) *Relative value of coupons.*

FIGURE 5.3: Results of the CoCo pricing procedure for the ING CoCo on June 30, 2015, using the results from the AT1P model from Table 5.3 and $G = 10,000$ simulation paths per combination of c_{cc} and c_{φ}. Pricing is done using a range of different values for the coupon cancel threshold c_{cc} and the CoCo call threshold c_{φ}. Panel (a) shows the resulting CoCo prices. Panel (b), (c), and (d) show the proportion of this price that can be attributed to the potential value of stocks received, principal received, and coupon payments, respectively.

Furthermore, as introduced in Section 4.3, the CET1 ratio cannot become consistently higher than 15.08% in the AT1P model. This implies that for $c_{cc} > 15\%$ the relative contribution of coupon payments is nearly zero, as almost no coupons will be payed out. For $c_{\varphi} > 15\%$, the CoCo will never be called. These two observations explain the quick convergence of the CoCo prices and contribution of the different components for high levels of the thresholds.

For intermediate levels of the thresholds (around 10-14%), the relative contribution charts Figure 5.3b, Figure 5.3c, and Figure 5.3d, show similar behavior as in the CET1 model. For smaller values of the thresholds, they again show very quick convergence. This is explained by noting that when the firm value A_t is relatively close to the default level $\widehat{H}_t$, E_t is small. When in this situation the difference $A_t - \widehat{H}_t$ decreases somewhat, E_t will decrease by approximately the same amount, but A_t/E_t will increase at a far higher rate. This implies that, in the AT1P model, when the CET1 ratio is at a level between 7 and 10% at some point, it is very likely to either quickly go up again towards an intermediate level, or fall towards conversion. This explains the small differences in the relative contributions when the thresholds are set low.

TABLE 5.4: Price variation of the ING CoCo for different values of the coupon cancel and call thresholds in the AT1P model. Pricing done on June 30, 2015, where we recall that the market price of the CoCo was 1.0025 per unit of notional.

c_{cc} (%)	c_{φ} (%)	Estimated price	95% confidence interval
9	9	1.0515	[1.0461; 1.0569]
	10	1.0488	[1.0434; 1.0543]
	11	1.0423	[1.0368; 1.0478]
	12	1.0317	[1.0261; 1.0374]
10	9	1.0503	[1.0449; 1.0558]
	10	1.0476	[1.0421; 1.0531]
	11	1.0411	[1.0355; 1.0466]
	12	1.0303	[1.0246; 1.0360]
11	9	1.0471	[1.0416; 1.0526]
	10	1.0444	[1.0388; 1.0499]
	11	1.0377	[1.0321; 1.0433]
	12	1.0266	[1.0208; 1.0323]
12	9	1.0374	[1.0318; 1.0431]
	10	1.0347	[1.0290; 1.0403]
	11	1.0277	[1.0219; 1.0335]
	12	1.0157	[1.0098; 1.0216]

These effects also have some economical intuition. Firstly, banks are indeed likely not to let their CET1 ratio become too high. Secondly, when the CET1 ratio decreases towards a dangerous level of about 7-9%, the bank management will attempt to quickly get it in the safe-zone again, as such a low CET1 ratio can have significant impact on the market's confidence in the bank's credit-worthiness. However, this deteriorating market confidence may very well reinforce the downward trend as well, indeed pushing the CET1 ratio more quickly towards conversion.

Now in Figure 5.3a and Table 5.4, apart from the effects described above, we see some differing behavior. Where in the direct CET1 model the CoCo price is stricly decreasing in c_{cc} and c_{φ}, this is not the case in the AT1P model. In the AT1P model the price is still strictly decreasing in c_{cc}, but it is decreasing in c_{φ} only up to 13.8%, and increasing for higher values of c_{φ}, when c_{cc} is not too high. This is explained as follows. For c_{φ} low, the CoCo is called very often, especially as the CET1 ratio does not float around a lot at low values, as explained above. This gives a high price. When c_{φ} is intermediate, the CoCo is extended regularly, and when it is extended, conversion happens relatively often as well, as the CET1 ratio can easily slip from intermediate to low values and through the conversion barrier. This drives down the price. When c_{φ} is high, the CoCo is redeemed very rarely. However, when the CET1 ratio is very high, it is unlikely that conversion will occur in the period after the call date, and the fact value is lost due to the time value of money, is compensated by the extra coupons received. This combination leads to the price increasing again.

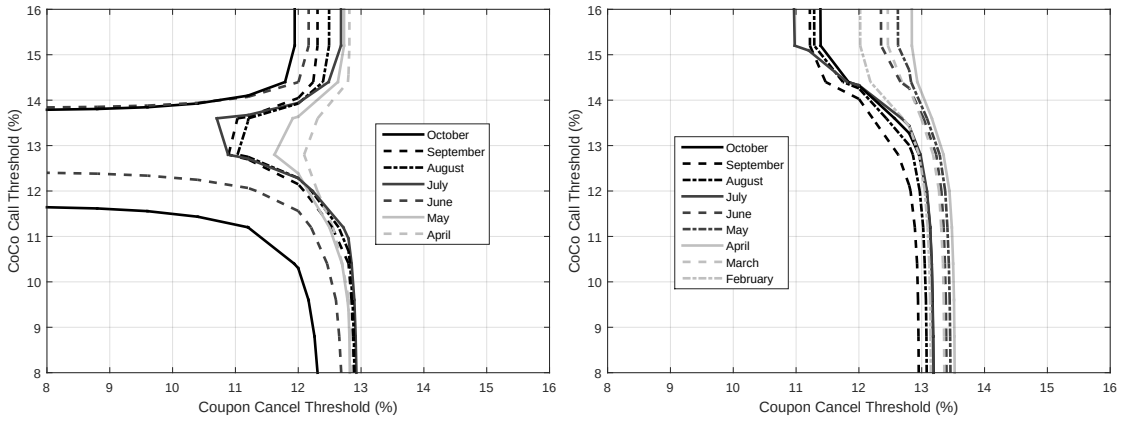

(a) *ING Group* (b) *Banco Popular Group*

FIGURE 5.4: Combinations of the coupon cancel threshold c_{cc} and the CoCo call threshold c_{φ} that make the AT1P model implied CoCo price equal to the market observed price. For the model parameters and the market observed prices we use the values from Table 5.3. The pricing dates are the last days of the months mentioned in the legends.

5.2.2 Comparison to observed market prices

Now we move on to comparing the results from our pricing algorithm to the market observed prices on the different pricing dates. Using the settings from Table 5.3, we perform the same analysis as in Section 5.1. Figure 5.4 shows the results of this analysis for both the ING and the Banco Popular CoCo.

The most obvious observation from Figure 5.4 is that for ING, for many values of c_{cc} there exist multiple possible values for c_{φ} that make the AT1P model price equal to the market price. This is explained by the observations made in Section 5.2.1. This effect is only limitedly visible for Banco Popular. The effect is smaller for Banco Popular because the asset value and thus the CET1 ratio has more variability for Banco Popular, which implies that the CET1 ratio roams around at low values more often. This in turn leads to differences in price for different low values of c_{φ}.

Overall, Figure 5.4 displays that the AT1P model shows more consistency than the CET1 model. The contour lines lie closer to each other, both for the ING and for the Banco Popular CoCo. Furthermore, we again observe that the CoCo price is not very sensitive to the amount of extension risk. However, for the AT1P model, this only holds for sufficiently small values of c_{φ}. In the region of small values for c_{φ}, we see again that the values for c_{cc} making the model price equal to the market price are very high. However, for higher c_{φ}, the coupon cancel threshold pricing the CoCo correctly are lower and more realistic.

5.3 Comparing the conversion behavior

In Section 5.1 and Section 5.2 we have seen that the pricing behavior of the direct CET1 and the AT1P model look rather similar at first sight. The effects of the thresholds on the CoCo price

are similar, and and the thresholds needed to arrive at the market price are also close to each other at levels of around 12-14%. We do see strong differences in the relative contribution of the different components to the CoCo price. To further analyze these differences, we take a closer look at the conversion behavior of both models. Figure 5.5 and Figure 5.6 display two empirical distributions extracted from simulation paths created with the direct CET1 model and the AT1P model, respectively. Figure 5.5a and Figure 5.6a show the distribution of the *conversion recovery rates*. That is, what percentage of the principal the stocks received at conversion are worth. A recovery rate of 1 hence means that conversion did not result in any extra loss of value, as the value of the stocks received at conversion is equal to the original claim. A recovery rate of 0 means that the claim is worthless after conversion.

Figure 5.5a shows that in the direct CET1 model conversion happens very often (68.1% in the paths considered), but does not lead to a high average loss of value. At the majority of conversions the stock price was above the floor price, resulting in a recovery rate of 1. This is somewhat surprising, as we use a correlation of $\rho = 0.9$ between the shocks in stock price and the shocks in the CET1 ratio, meaning they should move together rather tightly. Conversion happens so often, however, that there are a lot of paths where the stock price has not gone down enough to result in significant loss of value.

Figure 5.6a shows a completely different story for the AT1P model. While the overall conversion rate is much lower (18.3% in the paths considered), the average loss of value is much higher. This is explained by inspecting (3.3.10) combined with the regression results from (4.3.3). (3.3.10) tells that, while containing an idiosyncratic shock, the value of the CET1 ratio is very tightly linked to the assets-on-equity ratio. Especially for a high value of the correlation, such as the $\varrho = 0.9$ considered in this case. Furthermore, the idiosyncratic shocks on the CET1 ratio are not persistent due to the lack of an autoregressive component in (3.3.10). Now combining this insight with (4.3.3), we see that the CET1 ratio will cross the 7% conversion barrier for a rather specific range of values of the assets-on-equity-ratio. This specific range in turns leads to a specific range of stock prices at conversion, due to the direct link between E_t and A_t in the AT1P model (see (3.3.7)). This explains the variation in recovery rates for the AT1P model. We note that the recovery statistics for the AT1P model look a lot more realistic than those of the CET1 model: a rather low conversion rate, but a high average loss of value when conversion occurs.

Figure 5.5b and Figure 5.6b show that the distribution of conversion times is rather similar for both models. Due to the continuous nature of the models it takes some time before reaching conversion. And the longer conversion is avoided, the smaller the probability of conversion, as the CET1 ratio is then more likely to have drifted away from the conversion barrier. For both models we see a significant drop at $t = 5$ years. This is caused by the fact that $t = 5$ is a call date for the CoCo, and it is redeemed in a lot of the paths at this point, especially as the call threshold is set fairly low at $c_\varphi = 9\%$.

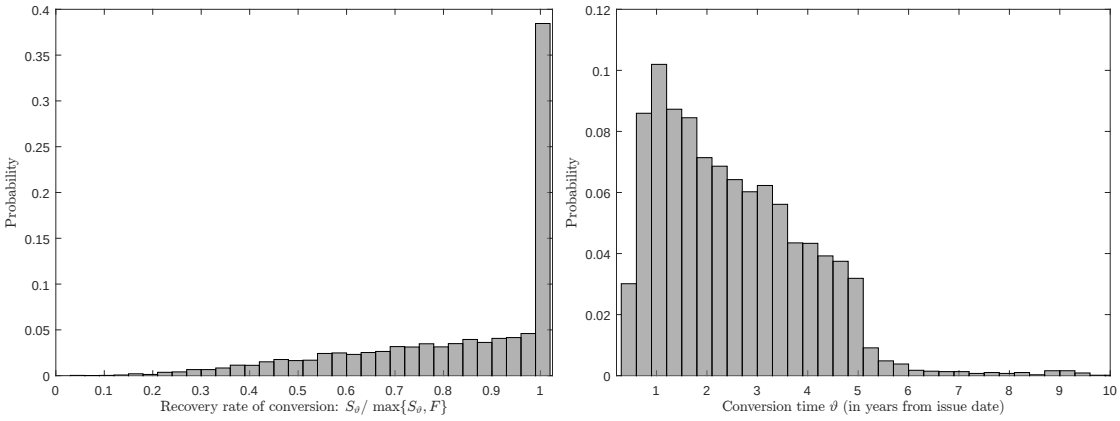

(a) *Histogram of conversion recovery rates: mean rate is 0.82.* (b) *Histogram of conversion times:* $\mathbb{E}_t\left[\vartheta | \vartheta < \min\{\varphi, \tau\}\right] = 2.51$.

FIGURE 5.5: Empirical distributions of the recovery rates of conversion, and the conversion times for the **direct CET1 model**. Paths built for the ING CoCo on June 30, 2015, using parameter settings from Table 5.1. The overall conversion rate on these paths is 68.1%. Both distributions and the reported means are conditional on conversion occurring before default and redemption. Thresholds are set at $c_{cc} = c_\varphi = 9\%$, and $d = 0$, $\rho = 0.9$. Estimated price using these settings on $G = 10,000$ simulation paths is 1.0690 with 95% confidence interval $[1.0660; 1.0712]$.

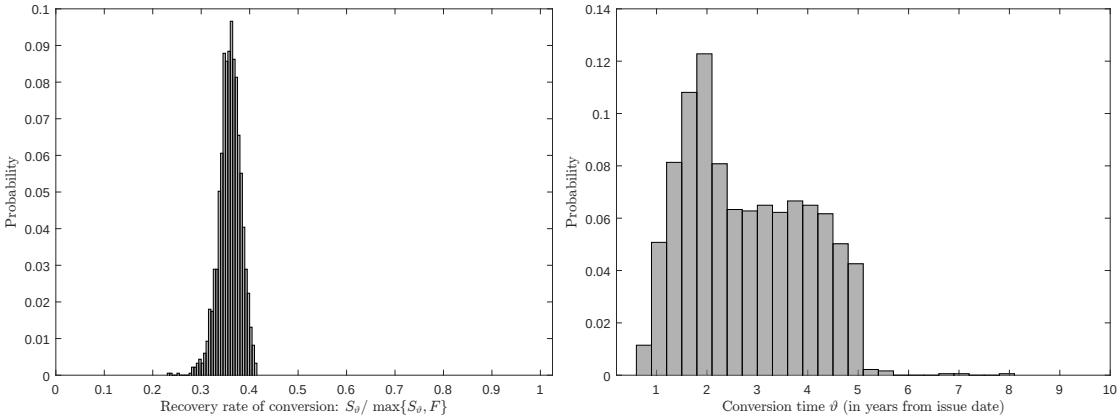

(a) *Histogram of conversion recovery rates: mean rate is 0.36.* (b) *Histogram of conversion times:* $\mathbb{E}_t\left[\vartheta | \vartheta < \min\{\varphi, \tau\}\right] = 2.78$.

FIGURE 5.6: Empirical distributions of the recovery rates of conversion, and the conversion times for the **AT1P model**. Paths built for the ING CoCo on June 30, 2015, using parameter settings from Table 5.3. The overall conversion rate on these paths is 18.3%. Both distributions and the reported means are conditional on conversion occurring before default and redemption. Thresholds are set at $c_{cc} = c_\varphi = 9\%$, and $q = 0$, $\varrho = 0.9$. Estimated price using these settings on $G = 10,000$ simulation paths is 1.0515 with 95% confidence interval $[1.0461; 1.0569]$.

5.4 Sensitivity analysis

In this section we investigate the sensitivity of the CoCo price for some of the parameters. To keep the analysis tractable, we focus solely on the ING CoCo on the pricing date June 30, 2015 in this section. We start by looking at different combinations of the pay-out rate q and 'correlation' parameter ϱ in the AT1P model, as well as different combinations of the pay-out rate d and

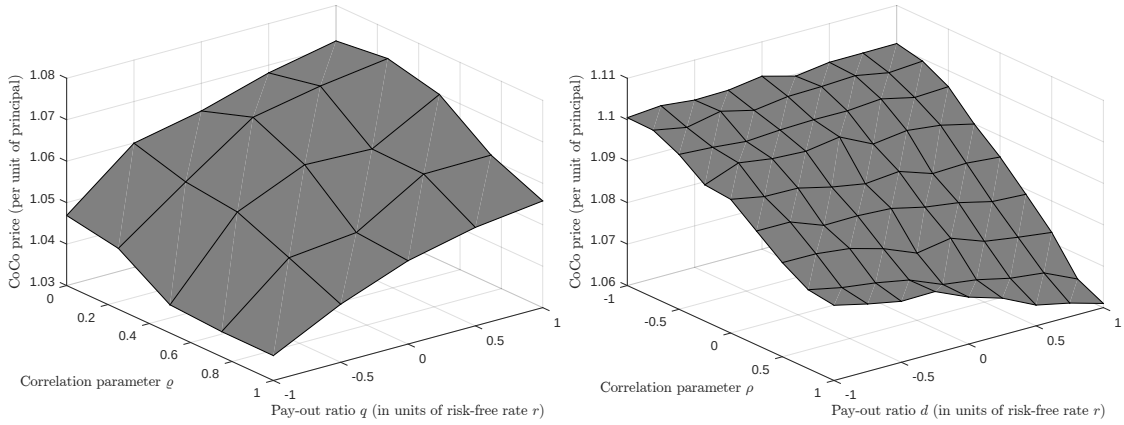

(a) *AT1P model* (b) *CET1 model*

FIGURE 5.7: Price variation of the ING CoCo for different values of the pay-out rate and correlation parameters in the AT1P and the CET1 model on $G = 10,000$ simulation paths for each combination of settings. Pricing done on June 30, 2015, where we recall that $r = 2.185\%$, and the market price of the CoCo was 1.0025 per unit of notional. For both models we set $c_{cc} = 9\%$ and $c_{\varphi} = 9\%$. These are values that we believe to be close to the actual point at which coupons and calls are canceled.

correlation parameter ρ in the CET1 model. We use a combination of the CoCo call and coupon cancel thresholds that we believe to lie close to the actual values at which coupons and calls will be canceled.

We set the coupon cancel threshold equal to 9%. We believe the bank will only cancel a coupon payment when its CET1 ratio moves dangerously close towards the conversion barrier, and when the regulator strongly advises the bank to do so. As canceling a coupon can have a strong signaling effect, banks will definitely have a very large incentive to postpone coupon cancellation as much as possible. As the regulator fears this signaling effect as well, it is not likely to intervene much earlier.

As for the call threshold, we believe this lies relatively close to the conversion threshold as well. Similarly to canceling a coupon, skipping a call may have a strong signaling effect, which makes both the bank and the regulator reticent in doing so. For this reason, we set $c_{\varphi} = 9\%$ as well.

In the AT1P model, we calibrate the parameters for different values of the pay-out rate q. Then, for the different solutions of these calibrations, we create simulation paths using different values of the 'correlation' parameter ϱ. Subsequently, we price the CoCo on these paths. Figure 5.7a displays the results of this analysis.

In the CET1 model, the pay-out rate d and the correlation parameter ρ do not influence the calibration. They only affect the simulation paths. We thus create simulation paths using different combinations of d and ρ, and price the ING CoCo on these paths. Figure 5.7b displays the results of this analysis.

From Figure 5.7b we see that the CoCo price is decreasing in the correlation parameter ρ in the direct CET1 model. This is logical, as higher ρ means lower stock price at conversion. When ρ is high, and the ratio decreases towards conversion, the stock price decreases as well, which

may lead to a stock price below the floor price at conversion, driving down the CoCo value. When ρ is low, the stock moves more independently of the CET1 ratio, and the stock price could very well be quite high at conversion, resulting in a limited loss of value for the CoCo holder. Thereby, ρ does not influence the probability of conversion. The CoCo price is decreasing in d as well, as a higher d in the direct CET1 model also simply results in a lower average stock price at conversion. Overall we note that even for highly stressed values of ρ and d, the direct CET1 model is not able to replicate the market observed CoCo price for realistic values of c_{cc} and c_{φ}.

In the AT1P model, the CoCo price is decreasing in ϱ as well, though this effect is somewhat more complicated than in the direct CET1 model. In the extreme case $\varrho = 0$, and when we take $\text{std}(A_t/E_t)$ constant, the CET1 ratio process does not depend on the assets-on-equity ratio. In this case it is rather likely that C_t does not cross the conversion, as it will take the form of white noise around the mean $\hat{\beta}_0 + \hat{\beta}_1 \cdot \text{std}(A_t/E_t)$. In this case conversion will almost only be triggered by the asset value crossing the default barrier. This implies that at conversion the stock price is always very low (most often zero). Then when ϱ increases, the bond duration will decrease, as conversions caused by the CET1 ratio hitting the barrier will start to occur as well. However, the average stock price at conversion will increase. From Figure 5.7a we see that for higher ϱ the effect of the decreasing duration (increasing probability of conversion) is counteracted more and more by the increasing average stock price at conversion.

As for the pay-out rate, the CoCo price increases for increasing q in the AT1P model. This is in contrast to what happens in the direct CET1 model. This is explained as follows. In the AT1P model, the pay-out rate influences every step of the process. In the calibration step, a high q implies higher volatilities and lower H. A high q implies a lower drift of the firm value and the default barrier. Then as we note that the volatilities are relative with respect to the height of the firm value, the volatility parameters are set higher. To match the market value of equity for these higher volatilities, H is set lower. In the pricing step, this results for low q, that the equity slips below the minimum from (3.3.9) more often, yielding a higher conversion rate and thus a lower price. Overall, we again note that even for highly stressed values of ϱ and q, the AT1P model is not able to replicate the market observed CoCo price for realistic values of c_{cc} and c_{φ}.

Next, we look at the appropriateness of our decision to set the effective maturity at 10 years. From Table 5.5 we see that this assumption is valid. Both in the AT1P and in the direct CET1 model, there is a small difference in CoCo price when the imposed maturity is set longer than 10 years. This implies indeed that there is not a lot of value added after the tenth year. The CoCo will be either converted or called after ten years the vast majority of the time, and the cash flows that do occur in the paths where the CoCo is still alive more than 10 years after issue are discounted heavily. We do see that imposing $T = 5$ years does yield a less accurate approximation of the price. Between the fifth and the tenth year there is still enough activity to contribute significantly to the price. This is also visible in Figure 5.5b and Figure 5.6b. We see that for the AT1P model, there is actually no difference at all between setting the maturity at 10 or longer. This implies that in the AT1P model the CoCo, in the paths considered, is always either converted or called after 10 years under these settings.

Finally, we assess the sensitivity of the CoCo prices in the AT1P model to the results of the

TABLE 5.5: Price variation of the ING CoCo for different values of the imposed maturity T in the AT1P and the CET1 model and $G = 10,000$ simulation paths. Pricing done on June 30, 2015, where we recall that the market price of the CoCo was 1.0025 per unit of notional. For both models we set $c_{cc} = 9\%$ and $c_{\varphi} = 9\%$. These are values that we believe to be close to the actual point at which coupons and calls are canceled.

	Direct CET1 model		**AT1P model**	
T	Est. price	95% conf.	Est. price	95% conf.
5	1.0725	[1.0704; 1.0746]	1.0534	[1.0481; 1.0588]
10	1.0689	[1.0667; 1.0711]	1.0515	[1.0461; 1.0569]
15	1.0685	[1.0663; 1.0706]	1.0515	[1.0461; 1.0569]
20	1.0682	[1.0660; 1.0704]	1.0515	[1.0461; 1.0569]
25	1.0689	[1.0667; 1.0711]	1.0515	[1.0461; 1.0569]

cross-sectional regression analysis from (4.3.3). Ideally, we would want to analyze the impact of our decision to run the regression on a single date by replicating the pricing approach while running the regression on different dates. However, as assembling the dataset we use for the regression is extremely time-consuming, we opt to run scenarios by applying shocks to the regression results. That is, we apply shocks to $\hat{\beta}_0$ and $\hat{\beta}_1$, calibrate the AT1P model using these shocked parameters, and assess what impact this has on the pricing results. Figure 5.8 shows the results of this analysis.

From Figure 5.8 we see that the CoCo price is not very sensitive to the value of $\hat{\beta}_0$. We do find gradually higher prices for higher $\hat{\beta}_0$. This is as expected, as a higher $\hat{\beta}_0$ implies generally higher CET1 ratios, and thus less conversions. Furthermore, we find decreasing prices for decreasing $\hat{\beta}_1$. This is again logical, as a lower (more negative) $\hat{\beta}_1$ implies that the CET1 ratio decreases faster when the assets-on-equity ratio increases. We find that the sensitivity to $\hat{\beta}_1$ is stronger. This is explained by the arguments set out in Section 5.2.1 on the behavior of the AT1P model. As the assets-on-equity ratio moves quite erratically when E_t is small, and $\hat{\beta}_1$ controls how the movements in A_t/E_t are translated into the CET1 ratio, the value of $\hat{\beta}_1$ has a significant impact on the amount of conversions. The intercept $\hat{\beta}_0$ has less impact, as the value of $\hat{\beta}_0$ only slightly shifts the critical region for the CET1 ratio, and does not have a strong impact when the CET1 ratio is in the *danger-zone* just above the conversion threshold. We again find that the model is not able to replicate the market observed price, even for stressed values of $\hat{\beta}_0$ and $\hat{\beta}_1$.

We conclude that both models are unable to replicate market observed CoCo price for realistic values of the thresholds, even for highly stressed values of the non-calibrated parameters. Section 5.5 outlines possible causes for this anomaly.

5.5 Discussion

This section provides possible explanations for the fact that both the AT1P and the direct CET1 model overprice AT1 CoCos for realistic values of the coupon cancel and call thresholds. The first cause is the fact that our models lack extra downward pressure or shocks on the CET1 ratio and/or the stock price following (the announcement of) a coupon cancellation, extension, or

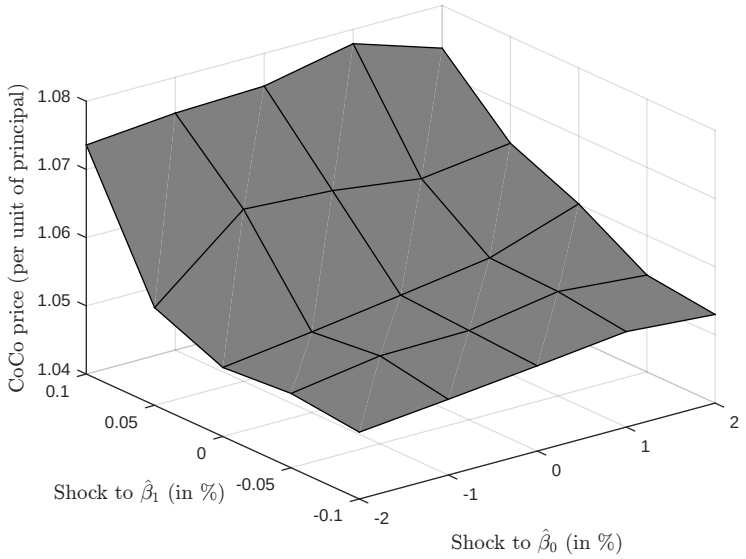

FIGURE 5.8: Price variation of the ING CoCo for different shocks to the cross-sectional regression results from (4.3.3) in the AT1P model on $G = 10,000$ simulation paths for each combination of settings. Pricing done on June 30, 2015, where we recall that the market price of the CoCo was 1.0025 per unit of notional. We set $c_{cc} = 9\%$ and $c_{\varphi} = 9\%$. These are values that we believe to be close to the actual point at which coupons and calls are canceled. We recall that in the base case we have $\hat{\beta}_0 = 15.2\%$ and $\hat{\beta}_1 = -0.1173\%$.

conversion. Our models assume the stock price and CET1 ratio to be continuous up to conversion. Thereby, the parameters of the processes are fixed over each simulation path, regardless of coupon cancellation, extension, or conversion occurring in that path. However, in reality, the announcement of a coupon cancellation or an extension will already be a clear signal to the market of deteriorating credit-worthiness, and may thus induce downward pressure on the stock price. Furthermore, it may indirectly put extra downward pressure on the CET1 ratio as well. Through a possible downgrade of the issuer, the risk weights on the bank's assets may increase, driving down the CET1 ratio. The announcement of conversion will be an even stronger signal, and will almost definitely imply a downward shock to the stock price.

Secondly, our models lack the uncertainty around the power of the regulator to force conversion. While we do include the power of the regulator to induce extension or coupon cancellation through the thresholds for the CET1 ratio, we omit the fact that the regulator also has the power to force conversion even when the CET1 ratio is still above the conversion threshold. The presence of this feature may have a scaring effect on the market, driving down CoCo prices.

Thirdly, we may consider a correction to the model CoCo prices that takes into account the Bond-CDS, or funding liquidity, basis, as suggested by Brigo et al. (2015). This is the difference between the credit spreads implied by the bond prices term structure, and the credit spreads implied by the CDS rates term structure. This can be interpreted as a funding liquidity basis, as bonds are funded instruments, while CDSs are not. A way to add this basis to the calibration procedure is to use *par-equivalent* CDS spreads (PECS) instead of regular CDS spreads. This is determined as the value of the CDS spread that makes the CDS-implied bond price equal to its

market price for the same maturity (see e.g. Elizalde, Doctor, and Saltuk (2009)). Using these shifted spreads would imply higher CDS rates, and thus calibrated parameters that would result in more conversion and lower CoCo prices.

To illustrate the implications of ignoring the Bond-CDS spread, we price a regular Tier 2 bond using the direct CET1 and the AT1P models, with the calibrated parameters from Table 5.1 and Table 5.3. We pick a bond issued by ING that has characteristics as close as possible to the CoCo bond analyzed in Chapter 5, apart from the conversion mechanism and the call and coupon cancel features. Table 5.6 gives the characteristics of this regular defaultable bond. Table 5.7 shows the results of the pricing analysis.

TABLE 5.6: Details of the regular defaultable bond by ING Group.

Issue date:	September 25, 2013
Name securities:	Subordinated notes
ISIN ID:	USN45780CT38
Maturity:	September 25, 2023 (10 years).
Coupons:	5.800% per annum, payable semi-annually in arrear.
Day count convention:	30/360.
Coupon cancel options:	None.
Callable?	No.
Seniority:	Unsecured, subordinated Tier 2.

TABLE 5.7: Price of the ING regular defaultable bond in both models for $G = 10,000$ simulation paths. Pricing done on June 30, 2015. Recovery rate is assumed to be 20%.

	Direct CET1 model		**AT1P model**	
Market price	Est. price	95% conf.	Est. price	95% conf.
1.0992	1.1185	[1.1116; 1.1253]	1.1139	[1.1074; 1.1203]

We indeed find the model prices to be 1.5-2% above the market observed price. This difference is explained by the Bond-CDS argument set out above. Now noting that this basis is likely to be present as well in CoCo prices, adding this to the CoCo pricing procedure will bring the model CoCo prices closer to market observed CoCo prices.

Fourthly, the market may have additional fear for regulatory changes. The CoCos we consider both contain clauses that state they may be redeemed for the principal amount once regulatory changes occur that alter the tax deductibility of coupon payments or the definition of AT1 capital. The market may fear that there is a significant probability that one of those events will occur, and may therefore be hesitant to pay above par for an AT1 CoCo.

Lastly, the AT1 CoCo bond market may contain an extra illiquidity spread. Due to the abundance of uncertain factors in AT1 CoCo contracts, a lot of investors are still prohibited or very reluctant to invest in CoCos. There is e.g. an overall prohibition to invest in CoCos for private investors in the EU, and many large institutional investors such as pension funds, may not invest in CoCos as well due to their strict mandates. This may have an additional downward effect on CoCo prices.

Chapter 6

Concluding remarks

This study assesses two pricing models for AT1 eligible non-dilutive conversion-to-equity CoCo bonds. These CoCos can be viewed as the sum of a perpetual, callable, defaultable bond for which the coupon payments can be canceled, and an option with as underlying the CET1 ratio, paying out a variable number of equity shares upon conversion. AT1 CoCos thus contain two important additional risk drivers compared to regular equity conversion CoCos: (i) coupon cancel risk, as coupon payments may be canceled on the discretion of the issuer or the regulator without consequences for the rest of the CoCo lifetime; and (ii) extension risk, as there may be no incentives to call, and the regulator may prohibit a call. We assume these risk factors are driven by the CET1 ratio: when the CET1 ratio is below a certain coupon cancel threshold at a payment date, the coupon payment is canceled, and when the CET1 ratio is below a certain call threshold at a call date, the CoCo is extended (the call date is skipped).

We model the CET1 ratio process and the stock price process to approximate CoCo prices using a Monte Carlo algorithm. We use two first passage-time approaches to do so: (i) the structural Analytically Tractable First-Passage Time (AT1P) model, based on Brigo and Tarenghi's 2004 extension of the Black-Cox model. We establish a link to the CET1 ratio in this framework using cross-sectional regression analysis; and (ii) an approach where we directly model the CET1 ratio as a mean reverting stochastic process, based on the framework of Cheridito and Xu (2015). In both approaches, we use expressions for the risk-neutral survival probabilities to calibrate the model parameters to market observed CDS spreads. For the calibration we further use data on CET1 ratios, market value of equity, and stock volatility.

As case studies, we test both models on AT1 CoCo issues by Banco Popular and ING, both from early 2015. We find that coupon cancel and extension risk have a significant impact on CoCo prices, both in the AT1P and in the direct CET1 model. When the coupon cancel threshold is set higher, coupons are canceled, significantly driving down CoCo prices. We find an effect of the extension risk as well, be it less large. When the call threshold is set higher, the CoCo is redeemed less often, which implies a larger probability of conversion, and stronger discounting of a potential principal redemption. This effect is counteracted by the value of potential extra coupon payments.

While both models show comparable prices for equal levels of the thresholds, they show large differences in the relative contribution of the three CoCo price components principal, coupons, and stocks. In the direct CET1 model the conversion rate is very high, but the average loss of value at conversion is low. In the AT1P model, the conversion rate is lower, but the average loss of value at conversion is much higher. The behavior of the AT1P model seems more realistic, as we expect conversion not to happen very often in reality, but with a large loss of value. Furthermore, the dispersion of CoCo prices for different values of the thresholds show more economical intuition in the AT1P model.

For both models, we need to set the call and coupon cancel thresholds unrealistically high to match market observed CoCo prices. In other words, when setting the thresholds at economically intuitive levels, both models overprice CoCos significantly. This may be caused by a number of reasons: (i) the lack of extra downward pressure or shocks following announcements of coupon cancellation, extension, or conversion; (ii) the lack of the uncertainty regarding the power of the regulator to force conversion; (iii) the absence of the Bond-CDS basis in the calibration procedure; (iv) the lack of an illiquidity premium.

6.1 Recommendations for further research

We outline here a number of recommendations for further research on AT1 CoCo prices. Firstly, as noted in Section 5.5, a weakness of our models is that they are Gaussian based and their parameters are fixed beforehand. An interesting extension would be to use more complex stochastic processes for the CET1 ratio and the stock price, including jumps and possible shifts of parameters following announcements of coupon cancellation, extension, and conversion. In the direct CET1 model, these more complex features may be added straight to the processes for the CET1 ratio and the stock price. In the AT1P model, these features may be added to the firm value process, and to the translation of the firm value to the CET1 ratio.

Furthermore, in the AT1P model, an interesting opportunity for further research would be to design a more dynamic link between the structural model and the CET1 ratio. A weakness of our method is that it establishes the link at one point in time, while this link is likely to be influenced strongly by the economic cycle. Making this link cyclical may result in better CoCo pricing strength.

It may also be interesting to add regulatory forced conversions to the framework, for example using a Parisian trigger feature as suggested by Leung and Kwok (2015). This Parisian trigger feature adds one extra path dependent state variable in the pricing model of a CoCo.

Fourthly, it would be interesting to perform pricing analyses over longer horizons, to be able to assess CoCo pricing strength during different economic circumstances and different corresponding CDS curves. As introduced in Section 4.2.2, the direct CET1 model proposes calibration problems when applied over a longer horizon. To overcome this issue, one may add the level and/or the slope of the CDS curve to the calibration procedure. This may remove the autocorrelation from the errors over long calibration horizons. Analysis of the exact implications of this addition is left for further research.

It may also be interesting to use term structures of bond prices or PECS for calibration and hedging, instead of regular CDS rates. This includes the Bond-CDS basis to the framework. Comparing both techniques in terms of their CoCo pricing strength can give important information regarding which products are most appropriate to hedge CoCo exposure.

In general, it would also be interesting for further research to analyze the hedging performance of both models. This hedging performance can be evaluated using the hedging portfolios from Section 3.3.2 and Section 3.4.2 and a time series of CoCo prices. Such an analysis can give important information on the effectiveness of using the proposed products, CDS contracts and stocks, for CoCo hedging, and thus on the validity of our models.

Finally, an interesting extension to our framework would be to add a stochastic model for the short rate. Our methods already provide the possibility to do so, and this may give some extra understanding in what drives AT1 CoCo prices.

Bibliography

Albul, B., D.M. Jaffee, and A. Tchistyi (2013, October). Contingent convertible bonds and capital structure decisions. Working paper.

Alili, L., P. Patie, and J.L. Pedersen (2005). Representations of the first hitting time density of an Ornstein-Uhlenbeck process. *Bernoulli 21(4)*, 967–980.

European Banking Authority (2014, November). Draft regulatory technical standards on criteria for determining the minimum requirement for own funds and eligible liabilities under Directive 2014/59/EU. Technical report, European Banking Authority.

Avdjiev, S., P. Bolton, W. Jiang, A. Kartasheva, and B. Bogdanova (2015, June). CoCo bond issuance and bank funding costs. Working paper of Bank of International Settlements (BIS) and Columbia Business School.

Barucci, E. and L. Del Viva (2013). Dynamic capital structure and the contingent capital option. *Annals of Finance 9(3)*, 337–364.

Berg, T. and C. Kaserer (2015, January). Does contingent capital induce excessive risk-taking? Journal of Financial Intermediation, Forthcoming. Available at SSRN: http://ssrn.com/abstract=1709341.

Bielecki, T. and M. Rutkowski (2002). *Credit Risk: Modeling, Valuation and Hedging*. Berlin: Springer Finance.

Black, F. and J.C. Cox (1976). Valuing corporate securities: Some effects of bond indenture provisions. *Journal of Finance 31(2)*, 351–367.

Bloomberg (2014, August). Equity implied volatility surface. Available at: Bloomberg (Accessed: 9 November 2015).

Bolton, P. and F. Samana (2012). Capital access bonds: contingent capital with an option to convert. *Economic Policy 27(70)*, 275–317.

Brandimarte, P. (2006). *Numerical Methods in Finance and Economics*. Hoboken, New Jersey: John Wiley and Sons.

Brigo, D., J. Garcia, and N. Pede (2015). CoCo bonds pricing with credit and equity calibrated first-passage firm value models. *International Journal of Theoretical and Applied Finance 18(3)*, 1550015 (31 pages).

Brigo, D., M. Morini, and A. Pallavicini (2013). *Counterparty Credit Risk, Collateral and Funding with cases from all asset classes*. Chichester: John Wiley and Sons.

Brigo, D., M. Morini, and M. Tarenghi (2010). Credit calibration with structural models and equity return swap valuation under counterparty risk. In T. Bielecki, D. Brigo, and F. Patras (Eds.), *Recent advancements in theory and practice of credit derivatives*. Bloomberg Press.

Brigo, D. and M. Tarenghi (2004, August). Credit default swap calibration and equity swap valuation under counterparty risk with a tractable structural model. Available at SSRN: http://ssrn.com/abstract=581302.

Buergi, M.P.H. (2012, March). A tough nut to crack: On the pricing of capital ratio triggered contingent convertibles. Available at SSRN: http://ssrn.com/abstract=2020571.

Calomiris, C.W. and R.J. Herring (2013). How to design a contingent convertible debt requirement that helps solve our too-big-to-fail problem. *Journal of Applied Corporate Finance 25(2)*, 21–44.

Chan, S. and S. Van Wijnbergen (2014). Cocos, contagion and systemic risk. *Duisenberg school of finance - Tinbergen Institute Discussion Paper 14-110/97*.

Cheridito, P. and Z. Xu (2014). A reduced-form contingent convertible bond model with deterministic conversion intensity. *Journal of Risk 17(3)*, 1–18.

Cheridito, P. and Z. Xu (2015, April). Pricing and hedging CoCos. Available at SSRN: http://ssrn.com/abstract=2201364.

Collin-Dufresne, P. and R. Goldstein (2001). Do credit spreads reflect stationary leverage ratios? *Journal of Finance 56*, 1929–1958.

Corcuera, J.M., J. De Spiegeleer, J. Fajardo, H. Jönsson, W. Schoutens, and A. Valdivia (2014). Close form pricing formulas for CoCa CoCos. Forthcoming in Journal of Banking & Finance.

Corcuera, J.M., J. De Spiegeleer, A. Ferreiro-Castilla, A.E. Kyprianou, D.B. Madan, and W. Schoutens (2013). Pricing of contingent convertibles under smile conform models. *Journal of Credit Risk 9(3)*, 121–140.

Crouhy, M., D. Galai, and R. Mark (2000). A comparative analysis of current credit risk models. *Journal of Banking & Finance 24*, 59–117.

De Spiegeleer, J. and W. Schoutens (2012). Pricing contingent convertibles: A derivatives approach. *Journal of Derivatives 20(2)*, 27–36.

De Spiegeleer, J. and W. Schoutens (2014). CoCo bonds with extension risk. *Wilmott Magazine 71*, 78–91.

Duffie, D. and K.J. Singleton (1999). Modeling term structures of defaultable bonds. *Review of Financial Studies 12(4)*, 687–720.

Elizalde, A., S. Doctor, and Y. Saltuk (2009). Bond-CDS basis handbook. J. P. Morgan Credit Derivative Research.

Flannery, M.J. (2005). 'No pain, no gain?' Effecting market discipline via reverse convertible debentures. In H.S. Scott (Ed.), *Capital Adequacy Beyond Basel: Banking, Securities, and Insurance*. Oxford University Press.

Flannery, M.J. (2009, October). Stabilizing large financial institutions with contingent capital certificates. Available at SSRN: http://ssrn.com/abstract=1485689.

Giesecke, K. (2004). Credit risk modeling and valuation: and introduction. In D. Shimko (Ed.), *Credit Risk: Model and Management* (2nd ed.). Oxford University Press.

Glasserman, P. and B. Nouri (2012). Contingent capital with a capital-ratio trigger. *Management Science 58(10)*, 1816–1833.

Göing-Jaeschke, A. and M. Yor (2003). A survey and some generalizations of bessel processes. *Bernoulli 9(2)*, 313–349.

Hilberink, B. and L.C.G. Rogers (2002). Optimal capital structure and endogenous default. *Finance and Stochastics 6*, 237–263.

Hilscher, J. and A. Raviv (2014, January). Bank stability and market discipline: The effect of contingent capital on risk taking and default probability. Available at SSRN: http://ssrn.com/abstract=575862.

Himmelberg, C.P. and S. Tsyplakov (2014, January). Incentive effects and pricing of contingent capital. Working paper.

Hull, J.C. (2011). *Options, Futures, and Other Derivatives* (8th ed.). New Jersey: Englewood Cliffs, Prentice-Hall.

Hyndman, R.J. and G. Athanasopoulos (2013). *Forecasting: principles and practice*. Available at: http://OTexts.org. Accessed on December 22, 2015.

Jung, H. (2012, April). Pricing of contingent convertibles. Working paper. Wharton Research Scholars Journal.

Kashyap, A.K., R.G. Rajan, and J.C. Stein (2008, August). Rethinking capital regulation. In *Proceedings - Economic Policy Symposium - Jackson Hole*, pp. 431–471. Federal Reserve Bank of Kansas City.

Koziol, C. and J. Lawrenz (2012). Contingent convertibles. solving or seeding the next banking crisis? *Journal of Banking and Finance 36*, 90–104.

Lando, D. (2004). *Credit Risk Modelling: Theory and Applications*. Princeton & Oxford: Princeton University Press.

Leland, H.E. (1994). Corporate debt value, bond covenants, and optimal capital structure. *Journal of Finance 49(4)*, 1213–1252.

Leung, C.M. and Y.K. Kwok (2015, September). Numerical pricing of Coco bonds with parisian trigger feature using the Fortet method. Available at SSRN: http://ssrn.com/abstract=2657991.

Ljung, G.M. and G.E.P. Box (1978). On a measure of a lack of fit in time series models. *Biometrika 65(2)*, 297–303.

Lo, C.F., H.C. Lee, and C.H. Hui (2003). A simple approach for pricing barrier options with time-dependent parameters. *Quantitative Finance 3*, 98–107.

McDonald, R.L. (2010, February). Contingent capital with a dual price trigger. Available at SSRN: http://ssrn.com/abstract=1553430.

Merton, R.C. (1974). On the pricing of corporate debt: the risk structure of interest rates. *Journal of Finance 29(2)*, 449–469.

Metzler, A. and R.M. Reesor (2015). Valuation and analysis of zero-coupon contingent capital bonds. *Mathematics and Financial Economics 9(2)*, 85–109.

O'Kane, D. and S. Turnbull (2003). Valuation of credit default swaps. Lehman Brothers, Fixed Income Quantitative Research.

Pennacchi, G. (2011, March). A structural model of contingent bank capital. FRB of Cleveland Working Paper No. 10-04. Available at SSRN: http://ssrn.com/abstract=1595080.

Rapisarda, F. (2005, March). Pricing barriers on underlyings with time-dependent parameters. Working paper. Available at SSRN: http://ssrn.com/abstract=2138100.

Richtmyer, R.D. and K.W. Morton (1967). *Difference Methods for Initial-Value Problems*. New York: Interscience Publishers (John Wiley).

Squam Lake Working Group (2009, April). An expedited resolution mechanism for distressed financial firms: Regulatory hybrid securities. Working paper. Council of Foreign Relations.

Strauss, W.A. (2008). *Partial Differential Equations: an Introduction* (2nd ed.). Hoboken, New Jersey: John Wiley and Sons.

Sundaresan, S. and Z. Wang (2010, April). Design of contingent capital with a stock price trigger for mandatory conversion.

The European Parliament and the Council of the European Union (2013a, June). *Directive 2013/36/EU: on access to the activity of credit institutions and the prudential supervision of credit institutions and investment firms, amending Directive 2002/87/EC and repealing Directives 2006/48/EC and 2006/49/EC*. Commonly known as the Capital Requirements Directive Part IV (CRDIV).

The European Parliament and the Council of the European Union (2013b, June). *Regulation (EU) No 575/2013: on prudential requirements for credit institutions and investment firms and amending Regulation (EU) No 648/2012*. Commonly known as the Capital Requirements Regulation (CRR).

The European Parliament and the Council of the European Union (2014, May). *Directive 2014/59/EU: establishing a framework for the recovery and resolution of credit institutions and investment firms and amending Council Directive 82/891/EEC, and Directives 2001/24/EC, 2002/47/EC, 2004/25/EC, 2005/56/EC, 2007/36/EC, 2011/35/EU, 2012/30/EU and 2013/36/EU, and Regulations (EU) No 1093/2010 and (EU) No 648/2012, of the European Parliament and of the Council*. Commonly known as the Banking Recovery and Resolution Directive (BRRD).

Thomas, L.H. (1949). Elliptic problems in linear differential equations over a network. Watson Sci. Comput. Lab Report, Columbia University, New York.

Whittall, C. (2014). Investors search for CoCo hedges. *International Financing Review 2018*.

Wilkens, S. and N. Bethke (2014). Contingent convertible (CoCo) bonds: A first empirical assessment of selected pricing models. *Financial Analysts Journal 70(2)*, 59–77.

Zeng, J. (2013, November). Contingent capital structure. Working paper.

Zhou, C. (2001). The term structure of credit spreads with jump risk. *Journal of Banking and Finance 25*, 2015–2040.

Appendices

Appendix A

List of banks used for cross-sectional regression analysis

Table A.1: This table shows the banks we use for the cross-sectional analysis on the link between asset/equity and CET1 ratio. All these banks are based in Europe and under supervision of the European Banking Authority.

Name:	Name:	Name:
ABN AMRO Bank N.V.	Commerzbank AG	Mediobanca S.p.A.
Allied Irish Banks plc	Rabobank B.A.	MPCA Ronda
Alpha Bank	Danske Bank	National Bank of Greece
BMPS S.p.A.	Deutsche Bank AG	NCG Banco
Banca Popolare Di Milano	DNB Bank Group	Nordea Bank AB (publ)
Banco Bilbao Vizcaya Argentaria	DZ Bank AG	Nykredit
Banco Comercial Português	Erste Group Bank AG	OP-Pohjola Group
Banco de Sabadell	Eurobank Ergasias	Piraeus Bank
Banco Financiero y de Ahorros	Groupe BPCE	Raiffeisen Zentralbank Österreich AG
Banco Popolare - Società Cooperativa	Groupe Crédit Agricole	Royal bank of Scotland Group plc
Banco Popular Español	Groupe Crédit Mutuel	Skandinaviska Enskilda Banken AB
Banco Santander	HSBC Holdings plc	SNS Bank N.V.
Barclays plc	ING Bank N.V.	Société Générale
Bayerische Landesbank	Intesa Sanpaolo S.p.A.	Svenska Handelsbanken AB
Belfius Banque SA	KBC Group NV	Swedbank AB
BNP Paribas	Kutxabank	Bank of Ireland
Caixa Geral de Depósitos	La Banque Postale	UniCredit S.p.A.
Caja de Ahorros y M.P. de Zaragoza	Landesbank Berlin Holding AG	UBI Banca
Caja de Ahorros y Pensiones de Barcelona	Lloyds Banking Group plc	WGZ Bank AG

Appendix B

Numerical solution survival probability direct CET1 model

We want to solve the PDE from (3.4.5), with boundary conditions from (3.4.6), for several maturities T. We use the Crank-Nicolson method to do so. The Crank-Nicolson method is an example of a finite difference method, and it is based on approximating the continuous derivatives in (3.4.5) using divided differences defined on a discrete grid (see Richtmyer and Morton (1967)).

Following Hull (2011) and Brandimarte (2006), where we adapt their methods to fit our Exponential Ornstein-Uhlenbeck CET1 underlying, we set up a discrete grid with respect to both time t and the logarithm of the CET1 ratio H. The maturity T is divided into P equally spaced intervals of length $\delta t = T/P$. Furthermore, we specify H_{max} to be the largest possible log-CET1 ratio value. We set this maximum at a level where we can safely assume it would never be reached in reality during the time to maturity. This is necessary, as for computational purposes we need to set some limit to the underlying process.

Then we divide the range of possible values for H into Q equally spaced intervals, to obtain $\delta H = H_{max}/Q$. Now in grid notation $g_{i,j} = g(i\delta t, j\delta H)$ denotes the value of the function g at the (i,j) point on the grid corresponding to time $i\delta t$ and log-CET1 ratio $j\delta H$, for $i = 0, 1, \ldots, P$, $j = 0, 1, \ldots, Q$. There are a total of $(P+1) \times (Q+1)$ points on this grid.

In order to construct the Crank-Nicolson method, we start by specifying the *explicit* method for solving the PDE. The explicit method is based on expressing the value $g_{i,j}$ explicitly in terms of the values for $g_{i+1,j+1}$, $g_{i+1,j}$, and $g_{i+1,j-1}$. Using approximations based on Taylor expansions, and noting that $H = j\delta H$, we can write the PDE from (3.4.5) explicitly as:

$$\frac{g_{i+1,j} - g_{i,j}}{\delta t} + \kappa\bar{h}\frac{g_{i+1,j+1} - g_{i+1,j-1}}{2\delta H} - \kappa j\frac{g_{i+1,j+1} - g_{i+1,j-1}}{2} + \frac{1}{2}\eta^2\frac{g_{i+1,j+1} - 2g_{i+1,j} + g_{i+1,j-1}}{(\delta H)^2} = 0, \tag{B.1}$$

for $i = 0, 1, \ldots, P-1$ and $j = 0, 1, \ldots, Q-1$. For details on how we arrive at this expression, see e.g. Brandimarte (2006, Chapter 5 and 9), where we adapt his techniques to an Ornstein-

Uhlenbeck underlying.

Contrary to the explicit method lies the *implicit* method, which is based on expressing the value $g_{i+1,j}$ implicitly in terms of the values for $g_{i,j+1}$, $g_{i,j}$, and $g_{i,j-1}$. Again using approximations based on Taylor expansions, and noting that $H = j\delta H$, we can write the PDE from (3.4.5) implicitly as:

$$\frac{g_{i+1,j} - g_{i,j}}{\delta t} + \kappa\bar{h}\frac{g_{i,j+1} - g_{i,j-1}}{2\delta H} - \kappa j\frac{g_{i,j+1} - g_{i,j-1}}{2} + \frac{1}{2}\eta^2\frac{g_{i,j+1} - 2g_{i,j} + g_{i,j-1}}{(\delta H)^2} = 0, \tag{B.2}$$

for $i = 0, 1, \ldots, P-1$ and $j = 0, 1, \ldots, Q-1$.

Finally, the Crank-Nicolson method is given by the average of the explicit and the implicit methods defined above. It has a higher accuracy and stability than the purely implicit or explicit methods, but requires a higher computation time (see Strauss (2008, Chapter 8)). However, for our purpose the computation time remains within reasonable bounds, making the Crank-Nicolson method the preferable alternative. When we take the average of (B.1) and (B.2) we obtain:

$$\begin{aligned}
&\frac{g_{i+1,j} - g_{i,j}}{\delta t} + \frac{\kappa\bar{h}}{4\delta H}(g_{i,j+1} - g_{i,j-1}) + \frac{\kappa\bar{h}}{4\delta H}(g_{i+1,j+1} - g_{i+1,j-1}) - \frac{\kappa j}{4}(g_{i,j+1} - g_{i,j-1}) \\
&\quad - \frac{\kappa j}{4}(g_{i+1,j+1} - g_{i+1,j-1}) + \frac{\eta^2}{4(\delta H)^2}(g_{i,j+1} - 2g_{i,j} + g_{i,j-1}) \\
&\quad + \frac{\eta^2}{4(\delta H)^2}(g_{i+1,j+1} - 2g_{i+1,j} + g_{i+1,j-1}) = 0 \iff \\
&\frac{g_{i,j-1}\delta t}{4}\left(\frac{\kappa\bar{h}}{\delta H} - \kappa j - \frac{\eta^2}{(\delta H)^2}\right) + g_{i,j}\left(1 + \frac{\delta t\eta^2}{2(\delta H)^2}\right) + \frac{g_{i,j+1}\delta t}{4}\left(-\frac{\kappa\bar{h}}{\delta H} + \kappa j - \frac{\eta^2}{(\delta H)^2}\right) = \\
&\frac{g_{i+1,j-1}\delta t}{4}\left(-\frac{\kappa\bar{h}}{\delta H} + \kappa j + \frac{\eta^2}{(\delta H)^2}\right) + g_{i+1,j}\left(1 - \frac{\delta t\eta^2}{2(\delta H)^2}\right) + \frac{g_{i+1,j+1}\delta t}{4}\left(\frac{\kappa\bar{h}}{\delta H} - \kappa j + \frac{\eta^2}{(\delta H)^2}\right) \iff \\
&-\alpha_j g_{i,j-1} + (1 - \beta_j)g_{i,j} - \gamma g_{i,j+1} = \alpha_j g_{i+1,j-1} + (1 + \beta_j)g_{i+1,j} + \gamma_j g_{i+1,j+1},
\end{aligned} \tag{B.3}$$

where:

$$\begin{aligned}
\alpha_j &= \frac{\delta t}{4}\left(\frac{\eta^2}{(\delta H)^2} + \kappa j - \frac{\kappa\bar{h}}{\delta H}\right), \\
\beta_j &= -\frac{\delta t}{2}\left(\frac{\eta^2}{(\delta H)^2}\right), \text{ and} \\
\gamma_j &= \frac{\delta t}{4}\left(\frac{\eta^2}{(\delta H)^2} - \kappa j + \frac{\kappa\bar{h}}{\delta H}\right),
\end{aligned}$$

for $i = 0, 1, \ldots, P-1$ and $j = 0, 1, \ldots, Q-1$.

Now, we note that we only need to consider values of the CET1 ratio larger than 4.5, as the survival probability is zero by definition for CET1 ratio values lower than or equal to 4.5 (see Section 4.2). We hence set H_{min} to be the minimum value of the log-CET1 ratio, which in this case is equal to the default barrier $\log(c_\tau) = h_\tau = \log(4.5)$. We only need to consider the domain $H_{min} \leq H \leq H_{max}$. Now on the boundaries of the grid we determine the corresponding

function values. We obtain, using the boundary conditions from (3.4.6):

$$g(t, H_{min}) = 0, \qquad \text{for } 0 \leq t \leq T, \tag{B.4}$$

$$g_{T,H} = \mathbb{I}_{\{H > h_\tau\}}, \qquad \text{for } H_{min} \leq H \leq H_{max}, \tag{B.5}$$

$$g_{t,H_{max}} = 1, \qquad \text{for } 0 \leq t \leq T. \tag{B.6}$$

The intuition behind these conditions is as follows: (B.4) for a CET1 ratio of 4.5, at any time point, the survival probability is 0, as the company is by assumption in default here; (B.5) at maturity, the survival probability is 1 when the CET1 ratio is larger than 4.5, and zero otherwise; and (B.6) at the largest log-CET1 ratio value H_{max}, the survival probability is 1 at any point in time, as we can say (almost) surely that the ratio will not drop to the default barrier once it has reached this high level.

Taking these boundary conditions into account, we can express the system of equations from (B.3) in matrix notation as a tridiagonal system:

$$\begin{pmatrix} 1-\beta_1 & -\gamma_1 & & & & \\ -\alpha_2 & 1-\beta_2 & -\gamma_2 & & 0 & \\ & -\alpha_3 & 1-\beta_3 & -\gamma_3 & & \\ & & \ddots & \ddots & \ddots & \\ & 0 & & -\alpha_{Q-2} & 1-\beta_{Q-2} & -\gamma_{Q-2} \\ & & & & -\alpha_{Q-1} & 1-\beta_{Q-1} \end{pmatrix} \begin{pmatrix} g_{i,1} \\ g_{i,2} \\ g_{i,3} \\ \vdots \\ g_{i,Q-2} \\ g_{i,Q-1} \end{pmatrix} =$$

$$\begin{pmatrix} 1+\beta_1 & \gamma_1 & & & & \\ \alpha_2 & 1+\beta_2 & \gamma_2 & & 0 & \\ & \alpha_3 & 1+\beta_3 & \gamma_3 & & \\ & & \ddots & \ddots & \ddots & \\ & 0 & & \alpha_{Q-2} & 1+\beta_{Q-2} & \gamma_{Q-2} \\ & & & & \alpha_{Q-1} & 1+\beta_{Q-1} \end{pmatrix} \begin{pmatrix} g_{i+1,1} \\ g_{i+1,2} \\ g_{i+1,3} \\ \vdots \\ g_{i+1,Q-2} \\ g_{i+1,Q-1} \end{pmatrix}. \tag{B.7}$$

This system, combined with the boundary conditions in (B.4)-(B.6), can be solved using the iterative Tridiagonal Matrix Algorithm (TDMA, Thomas (1949)). This enable us to fill in the values at every point in the grid. The risk-neutral survival probability $\mathbb{Q}_t^{CET1}(\tau > T)$ for a given starting value for the log-CET1 ratio can then be read from the grid at $i = 0$. For a starting value of the log-CET1 ratio that is not in the grid $H_{min}, H_{min} + \delta H, \ldots, Q\delta H \equiv H_{max}$, we use linear interpolation to determine the risk-neutral survival probability.

Appendix C

Stability calibration CET1 model

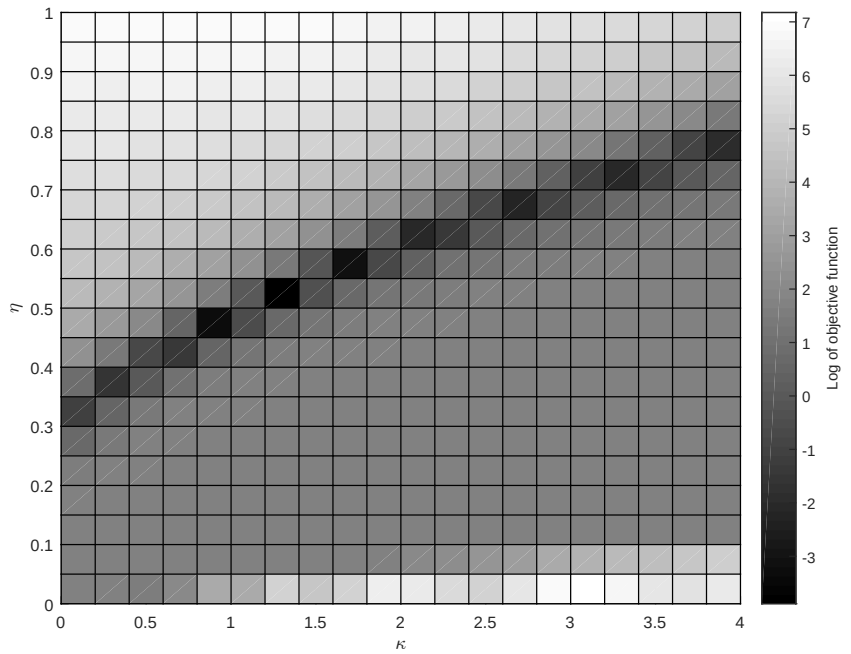

(a) *Stability of η and κ for fixed H_t and $\bar{h}$.*

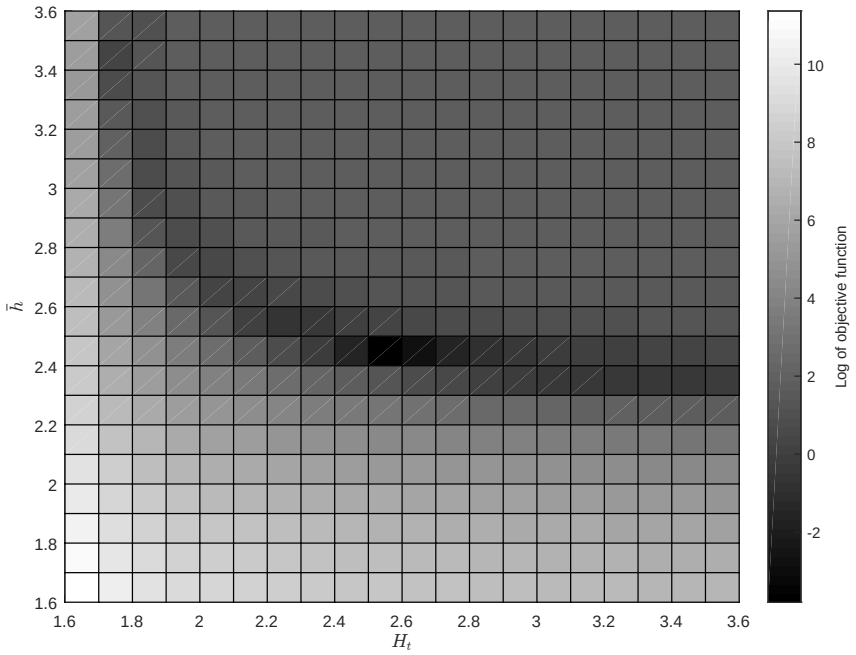

(b) *Stability of H_t and $\bar{h}$ for fixed η and κ.*

FIGURE C.1: Value of the logarithm of objective function (4.2.1) for varying values of pairs of parameters, keeping the parameters not considered equal to their optimal calibrated values. We use the calibration results for ING on June 30, 2015, where we have as calibrated optimal parameters $H_t = 2.5657$, $\kappa = 0.9430$, $\eta = 0.4666$, and $\bar{h} = 2.3893$.

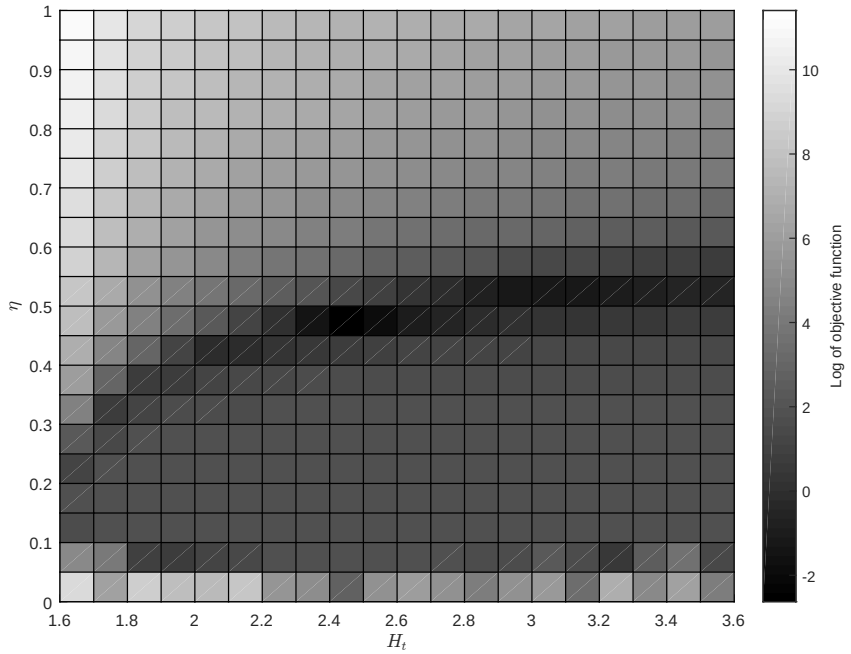

(a) *Stability of H_t and η for fixed $\bar{h}$ and κ.*

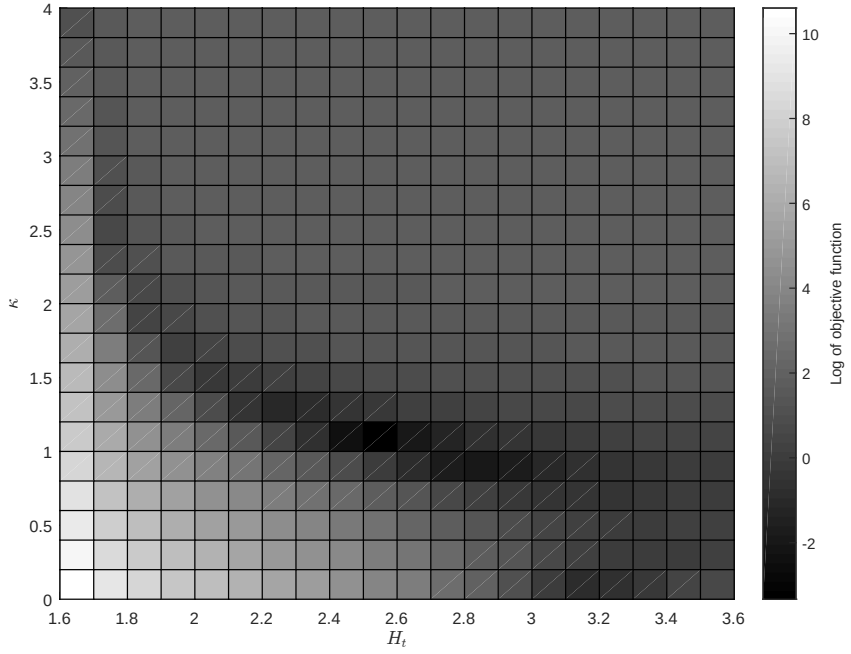

(b) *Stability of H_t and κ for fixed $\bar{h}$ and η.*

FIGURE C.2: Value of the logarithm of objective function (4.2.1) for varying values of pairs of parameters, keeping the parameters not considered equal to their optimal calibrated values. We use the calibration results for ING on June 30, 2015, where we have as calibrated optimal parameters $H_t = 2.5657$, $\kappa = 0.9430$, $\eta = 0.4666$, and $\bar{h} = 2.3893$.

Appendix D

Analytical expression survival probability AT1P model

We are proposed with the task of finding an expression for $\mathbb{Q}_t(\tau > T)$ under the model of (3.3.4) and (3.3.6), for different values for T. We note that the risk-neutral survival probability can be interpreted as a European down-and-out binary call option on an underlying with time-dependent parameters. That is, the pay-off is one if the underlying stays above the barrier level up to maturity (survival) and pay-off is zero when the underlying hits the barrier at any time before or at maturity (default). For this reason, we can adapt techniques from barrier option pricing as to arrive at our result. We note however that the presence of time-dependent parameters excludes us from using simple analytical expressions for pricing standard flat-barrier options. This is one of the reasons the AT1P model does not contain a flat barrier, but a specifically curved one, as in (3.3.6).

As put forward by Brigo and Tarenghi (2004), the default probabilities implied by the model of (3.3.4) and (3.3.6), are the same as the default probabilities implied by the 'shadow'-model specified as:

$$\text{'Firm value': } \mathrm{d}A_t^* = (r(t) - q^*(t))A_t^*\mathrm{d}t + \sigma_A(t)A_t^*\mathrm{d}W_t^{\mathbb{Q}} \tag{D.1}$$

$$\text{'Default barrier': } H_t^* = H\exp\left(-\int_t^T \left(r(u) - q^*(u) - L\sigma_A^2(u)\right)\mathrm{d}u\right), \tag{D.2}$$

when $q^*(t) = r(t) - L\sigma_A^2(t)$ and $A_0^* = A_0$. This can be seen by noting that:

$$\widehat{H}_t = H\exp\left(-\int_0^t (q(u) - q^*(u))\mathrm{d}u\right).$$

Now by integrating A^* and A we see that the first time A_t^* hits $H_t^* = H$ is the same as the first time A_t hits $\widehat{H}_t$. Hence it suffices to find the risk-neutral survival probabilities from the model of (D.1) and (D.2) for different values of T. This equivalence serves us nicely, as Rapisarda (2005) shows a way to derive the risk-neutral survival probability for this system.

Finding these survival probabilities starts at the famous Black-Scholes PDE that has to be satisfied for any derivative $\Pi(t, A^*)$ on an underlying A^* following a GBM:

$$\frac{\partial \Pi}{\partial t}(A^*, t) + (r(t) - q^*(t))A^* \frac{\partial \Pi}{\partial s}(A^*, t) + \frac{1}{2}\sigma_A^2(t)(A^*)^2 \frac{\partial^2 \Pi}{\partial (A^*)^2}(A^*, t) - r(t)\Pi(A^*, t) = 0. \quad \text{(D.3)}$$

Rapisarda (2005) attacks this PDE with tools stemming from physics, as he rewrites (D.3) to become a one-dimensional diffusion equation. This is a well-known PDE from physics describing a material undergoing diffusion. Rapisarda then writes the solution of the PDE as a so-called *Green's function*, and he shows that only for a barrier of the form of (D.2) it is possible to find the Green's function that solves the PDE with the relevant boundary conditions corresponding to a barrier option. His derivation makes use of the *method of images*, widely used in the world of physics.

Rapisarda (2005) then proceeds with specifying for what value of L the barrier becomes as flat as possible, as to be able to accurately approximate the price of barrier options with a fixed barrier using this method. This value L^* is shown to be:

$$L^* = \frac{1}{2} + \frac{\int_0^T \left[\int_t^T \left(r(u) - q^*(u) - \frac{1}{2}\sigma_A^2(u)\right) \mathrm{d}u\right] \left(\int_t^T \sigma_A^2(u) \mathrm{d}u\right) \mathrm{d}t}{\int_0^T \left(\int_t^T \sigma_A^2(u) \mathrm{d}u\right)^2 \mathrm{d}t},$$

which reduces to $L^* = \frac{1}{2} + (r - q^* - \frac{1}{2}\sigma_A^2)/(\sigma_A^2)$ for the easy case of constant parameters, where we correspondingly find $H_t^* = H$. Going back to the general case L, the risk-neutral survival probability using this methodology is derived to be:

$$\begin{aligned} \mathbb{Q}_t(\tau > T) = \Phi &\left(\frac{\log\left(\frac{V_t}{H}\right) + \int_t^T \left(r(u) - q^*(u) - \frac{1}{2}\sigma_A^2(u)\right) \mathrm{d}u}{\sqrt{\int_t^T \sigma_A^2(u) \mathrm{d}u}} \right) \\ &- \left(\frac{H_t^*}{V_t}\right)^{2L-1} \Phi \left(\frac{\log\left(\frac{(H_t^*)^2}{V_t H}\right) + \int_t^T \left(r(u) - q^*(u) - \frac{1}{2}\sigma_A^2(u)\right) \mathrm{d}u}{\sqrt{\int_t^T \sigma_A^2(u) \mathrm{d}u}} \right), \end{aligned} \quad \text{(D.4)}$$

where $\Phi(\cdot)$ denotes the cumulative distribution function of the standard Gaussian distribution. Now plugging in $q^*(t) = r(t) - L\sigma_A^2(t)$ in (D.4) we arrive at our final expression:

$$\mathbb{Q}_t^{AT1P}(\tau > T) = \Phi \left(\frac{\log\left(\frac{V_t}{H}\right) + \frac{2L-1}{2} \int_t^T \sigma_A^2(u) \mathrm{d}u}{\sqrt{\int_t^T \sigma_A^2(u) \mathrm{d}u}} \right) - \left(\frac{H}{V_t}\right)^{2L-1} \Phi \left(\frac{\log\left(\frac{H}{V_t}\right) + \frac{2L-1}{2} \int_t^T \sigma_A^2(u) \mathrm{d}u}{\sqrt{\int_t^T \sigma_A^2(u) \mathrm{d}u}} \right), \quad \text{(D.5)}$$

denoting the risk-neutral survival probability for maturity T within the model of (3.3.4) and (3.3.6).

Appendix E

Analytical expression equity value AT1P model

The expression for the equity value is found in a way remarkably similar to the derivation of the risk-neutral survival probabilities from Appendix D. As suggested in Section 3.3, the equity value can be interpreted as a European down-and-out call option on an underlying with time-dependent parameters, allowing us again to use techniques from barrier option pricing as to arrive at our result. This derivation is again based on the equivalence between the model of (3.3.4) and (3.3.6) and that of (D.1), (D.2) from Appendix D. We employ results of the latter model to infer the expression for the equity value in the former model.

In this framework we can again specify (D.3) as the relevant PDE that has to be satisfied by our solution. Note that the characteristics of the derivative that we want to price only occur in the boundary conditions and not in the PDE itself, making the PDE for both the survival probabilities and the equity value equal.

We again use the results from Rapisarda (2005) to derive the analytical expression for the equity value E_t at any $t < T$. He derives for the value of a European down-and-out call option at time t, DOC_t:

$$DOC_t = e^{-\int_t^T r(u)\mathrm{d}u}\Bigg\{A_t^* \exp\left[\int_t^T \left(v(u) + \frac{1}{2}\sigma_A^2(u)\right)\mathrm{d}u\right](1-\Phi(d_1)) - H_T^*(1-\Phi(d_2)) \\ - H_t^*\left(\frac{H_t^*}{A_t}\right)^{2L} \exp\left[\int_t^T \left(v(u) + \frac{1}{2}\sigma_A^2(u)\right)\mathrm{d}u\right](1-\Phi(d_3)) + H_T^*\left(\frac{H_t^*}{A_t}\right)^{2L-1}(1-\Phi(d_4))\Bigg\}, \tag{E.1}$$

where:

$$v(t) = r(t) - q^*(t) - \frac{1}{2}\sigma_A^2(t),$$

$$d_1 = \frac{\log\left[\frac{H_T^*}{H}\right] - \log\left[\frac{A_t^*}{H}\right] - \int_t^T \left(v(u) + \sigma_A^2(u)\right) \mathrm{d}u}{\sqrt{\int_t^T \sigma_A^2(u)\mathrm{d}u}},$$
$$d_2 = \frac{\log\left[\frac{H_T^*}{H}\right] - \log\left[\frac{A_t^*}{H}\right] - \int_t^T v(u)\mathrm{d}u}{\sqrt{\int_t^T \sigma_A^2(u)\mathrm{d}u}},$$
$$d_3 = \frac{\log\left[\frac{H_T^*}{H}\right] - \log\left[\frac{(H_t^*)^2}{HA_t^*}\right] - \int_t^T \left(v(u) + \sigma_A^2(u)\right) \mathrm{d}u}{\sqrt{\int_t^T \sigma_A^2(u)\mathrm{d}u}},$$
$$d_4 = \frac{\log\left[\frac{H_T^*}{H}\right] - \log\left[\frac{(H_t^*)^2}{HA_t^*}\right] - \int_t^T v(u)\mathrm{d}u}{\sqrt{\int_t^T \sigma_A^2(u)\mathrm{d}u}}.$$

Now plugging in $q^*(t) = r(t) - L\sigma_A^2(t)$ in (E.1) we arrive at an expression for the equity value E_t in the model of (3.3.4) and (3.3.6). As put forward in Brigo et al. (2013, Chapter 8), in the special case when $L = 0$, this expression remarkably reduces to that of a forward contract in the region where the 'option' is in the money. However, for $L \neq 0$, we still need the expression in (E.1) to evaluate the equity value.

As the expression above is cumbersome to implement in `MATLAB R2015a`, we opt to turn to the numerical method set out in Appendix B to approximate accurately the equity value in the model of (3.3.4) and (3.3.6). This again reduces to solving the PDE similar to the one from Appendix D:

$$\frac{\partial \Pi}{\partial t}(A,t) + (r(t) - q(t))A\frac{\partial \Pi}{\partial s}(A,t) + \frac{1}{2}\sigma_A^2(t)(A)^2\frac{\partial^2 \Pi}{\partial (A)^2}(A,t) - r(t)\Pi(A,t) = 0. \tag{E.2}$$

Along the lines of Appendix B, however with a GBM underlying instead of a Ornstein-Uhlenbeck underlying, and with time-dependent volatility, we find the Crank-Nicolson parameters:

$$\alpha_j = \frac{\delta t}{4}\left(\sigma_A^2(j)j^2 - rj\right),$$
$$\beta_j = -\frac{\delta t}{2}\left(\sigma_A^2(j)j^2 + r\right), \text{ and}$$
$$\gamma_j = \frac{\delta t}{4}\left(\sigma_A^2(j)j^2 + rj\right),$$

for $i = 0, 1, \ldots, P-1$ and $j = 0, 1, \ldots, Q-1$.

Now, we note that we only need to consider values of the asset value larger than the starting default barrier H, as the equity value is zero by definition for lower asset values. We hence set A_{min} to be the minimum value of the asset value, which in this case is equal to the starting default barrier H. We only need to consider the domain $A_{min} \leq A \leq A_{max}$. Now on the boundaries of the grid we determine the corresponding derivative values. We obtain, using the boundary conditions for a European down-and-out call option:

$$\Pi(t, A_{min}) = \max\left\{A_{min} - \widehat{H}_t e^{-rt}, 0\right\}, \qquad \text{for } 0 \leq t \leq T, \tag{E.3}$$

$$\Pi(T, A) = \max\{A_T - \widehat{H}_T, 0\}, \qquad \text{for } A_{min} \leq A \leq A_{max}, \tag{E.4}$$

$$\Pi(t, A_{max}) = A_{max} - \widehat{H}_t e^{-rt}, \qquad \text{for } 0 \leq t \leq T. \tag{E.5}$$

The intuition behind these conditions is as follows: (E.3) for an asset value of H, at any time point, the equity value is determined by the shape of the default barrier. For an upward sloping barrier, the equity value is zero, as the asset value will always be lower than the default barrier in this case. For a downward sloping barrier, the equity value can still be somewhat above zero; (E.4) at maturity, the equity value is $(A_T - \widehat{H}_T)$ when the asset value is higher than the default barrier, and zero otherwise; and (E.5) at the largest asset value A_{max}, the equity value is at any point in time is equal to the difference between the asset value and the discounted default barrier, as we can say (almost) surely that the asset value will not drop to the default barrier once it has reached this high level.

Now using the Crank-Nicolson parameters along with the boundary conditions (E.3), (E.4), and (E.5), we can determine the equity value E_t^{AT1P} as explained in Appendix B.